

## TECHNICAL REPORT STANDARD PAGE

---

1. Title and Subtitle  
**Assessment of Laboratory Friction Testing  
Equipment and Validation of Pavement Friction  
Characteristics with Field and Accelerated  
Friction Testing**
2. Author(s)  
Zhong Wu, Ph.D., P.E.; Ricardo Hungria, Ph.D.;  
Sudhir Bharati
3. Performing Organization Name and Address  
Louisiana Transportation Research Center  
4101 Gourrier Avenue  
Baton Rouge, LA 70808
4. Sponsoring Agency Name and Address  
Louisiana Department of Transportation and  
Development  
P.O. Box 94245  
Baton Rouge, LA 70804-9245
5. Report No.  
**FHWA/LA.25/707**
6. Report Date  
April 2025
7. Performing Organization Code  
LTRC Project Number: 20-4P  
SIO Number: DOTLT100340
8. Type of Report and Period Covered  
Final Report  
January 2021 – December 2024
9. No. of Pages  
121
10. Supplementary Notes  
Conducted in Cooperation with the U.S. Department of Transportation, Federal Highway  
Administration.
11. Distribution Statement  
Unrestricted. This document is available through the National Technical Information  
Service, Springfield, VA 21161.
12. Key Words  
Aggregate friction rating; three-wheel polishing; dynamic friction tester; polished stone  
value
13. Abstract

This report reviews the research and advancements in using the Three-Wheel Polishing Device (TWPD) for aggregate polishing and the Dynamic Friction Tester (DFT) to measure the polishing resistance of coarse aggregates in asphalt wearing course mixes. The Louisiana Department of Transportation and Development (DOTD) currently employs the British Polishing Wheel (BPW) test procedure to determine the polished stone value (PSV) of aggregates and specifies PSV-based aggregate friction rating requirements in asphalt

mixture design for wearing courses. However, due to significant variations in aggregate production and shipments, it is common for the same type of aggregate, delivered at different times, to yield substantially different PSV results.

In this project, seven coarse aggregate sources, including three sandstone types, three limestone types, and one rhyolite type, were selected, and eight field pavement sections were identified for laboratory and field friction testing. The primary objectives were: (1) to assess variations of PSV test results; (2) to evaluate a new TWPD-based aggregate friction testing procedure; (3) to validate and update the previously developed harmonization correlations for different field friction measurements; and (4) to determine threshold friction design values (i.e., DFT and mean profile/texture depth values) for commonly used wearing course mixtures in Louisiana.

The laboratory BWT/PSV test results indicated high variability among the tested aggregate samples, which can be attributed to factors such as differences in source material due to aggregate production processes and shipment timing, testing sample preparation, and the sensitivity of polishing and measurement devices, such as the BWT and British Pendulum Tester (BPT). By contrast, the TWPD polishing tests for the seven aggregates examined produced distinct polishing resistance results. An analysis of the variability in TWPD tests combined with DFT measurements considered factors such as aggregate type, DFT speed, 90° sample rotation, sample duplication, and operator differences. From these analyses, it was determined that DFT20 (i.e., DFT measurement at 20 km/hr) exhibited no significant statistical variation across different measurements. This indicates that DFT20 is a reliable aggregate polishing resistance metric unaffected by the aforementioned variables. Furthermore, the DFT20 @ 100,000 polishing values closely followed the chemical composition percentage order of the seven coarse aggregates tested. Aggregates with higher silica (SiO<sub>2</sub>) and lower calcium oxide (CaO) content demonstrated superior friction performance. However, the PSV results did not align with the friction resistance rankings observed in the TWPD tests, even when the same aggregate materials were used. This discrepancy highlights limitations in the PSV test compared to the TWPD procedure.

Additionally, DFT measurements provide a broader range of values than BPT-measured PSV values, suggesting that TWPD offers a more consistent and repeatable method for assessing laboratory aggregate polishing resistance. Based on these findings, it is recommended that DOTD adopt the TWPD/DFT testing procedure for initial aggregate source friction rating evaluations. Additionally, this project proposes a new aggregate friction rating table based on the DFT20 @ 100,000 polishing values for the aggregates tested.

The field friction measurements from this project, combined with data collected in LTRC Project 12-5P, were analyzed to perform comprehensive statistical evaluations of the effects of aggregate properties and mixture design on skid resistance values and their variability. Statistical correlation models were updated to capture relationships among different in-situ friction measurement devices, as well as various surface texture and frictional properties.

Finally, to establish threshold friction design values, a new F(60) prediction model was developed. This model incorporates DFT20, Mean Profile Depth (MPD), and polishing cycles, enabling the determination of threshold friction design values for aggregates based on their DFT20 results and the mixture's MPD. These values are aligned with the pavement's design average daily traffic (ADT) per design lane and expected service life.

This project offers actionable recommendations and improved tools for aggregate friction testing, field friction evaluation, and pavement friction design. The findings support the development of more reliable, accurate methods for assessing and designing pavement surfaces to enhance safety and performance.

## **Project Review Committee**

Each research project will have an advisory committee appointed by the LTRC Director. The Project Review Committee is responsible for assisting the LTRC Administrator or Manager in the development of acceptable research problem statements, requests for proposals, review of research proposals, oversight of approved research projects, and implementation of findings.

LTRC appreciates the dedication of the following Project Review Committee Members in guiding this research study to fruition.

### ***LTRC Administrator/Manager***

Zhongjie “Doc” Zhang, Ph.D., P.E.  
Pavement and Geotechnical Research Administrator

### ***Members***

Mark Ordogne  
Brandon Johnson  
Luanna Cambas  
Barry Moore  
Scott Nelson  
William Temple  
Chris Abadie

### ***Directorate Implementation Sponsor***

Chad Winchester, P.E.  
DOTD Chief Engineer

# **Assessment of Laboratory Friction Testing Equipment and Validation of Pavement Friction Characteristics with Field and Accelerated Friction Testing**

By  
Zhong Wu, Ph.D., P.E.  
Ricardo Hungria, Ph.D.  
Sudhir Bharati

DOTD Pavement Research Facility  
2865 North Line Rd  
70767 Port Allen, Louisiana

LTRC Project No. 20-4P  
SIO No. DOTLT100340

conducted for  
Louisiana Department of Transportation and Development  
Louisiana Transportation Research Center

The contents of this report reflect the views of the author/principal investigator, who is responsible for the facts and the accuracy of the data presented herein.

The contents do not necessarily reflect the views or policies of the Louisiana Department of Transportation and Development, the Federal Highway Administration, or the Louisiana Transportation Research Center. This report does not constitute a standard, specification, or regulation.

April 2025

## Abstract

This report reviews the research and advancements in using the three-wheel polishing device (TWPD) for aggregate polishing and the dynamic friction tester (DFT) to measure the polishing resistance of coarse aggregates in asphalt wearing course mixes. The Louisiana Department of Transportation and Development (DOTD) currently employs the British Polishing Wheel (BPW) test procedure to determine the polished stone value (PSV) of aggregates and specifies PSV-based aggregate friction rating requirements in asphalt mixture design for wearing courses. However, due to significant variations in aggregate production and shipments, it is common for the same type of aggregate, delivered at different times, to yield substantially different PSV results.

In this project, seven coarse aggregate sources, including three sandstone types, three limestone types, and one rhyolite type, were selected, and eight field pavement sections were identified for laboratory and field friction testing. The primary objectives were: (1) to assess variations of PSV test results; (2) to evaluate a new TWPD-based aggregate friction testing procedure; (3) to validate and update the previously-developed harmonization correlations for different field friction measurements; and (4) to determine threshold friction design values (i.e., DFT and mean profile/texture depth values) for commonly used wearing course mixtures in Louisiana.

The laboratory BWT/PSV test results indicated high variability among the tested aggregate samples, which can be attributed to factors such as differences in source material due to aggregate production processes and shipment timing, testing sample preparation, and the sensitivity of polishing and measurement devices, such as the BWT and British Pendulum Tester (BPT). By contrast, the TWPD polishing tests for the seven aggregates examined produced distinct polishing resistance results. An analysis of the variability in TWPD tests combined with DFT measurements considered factors such as aggregate type, DFT speed, 90° sample rotation, sample duplication, and operator differences. From these analyses, it was determined that DFT20 (i.e., DFT measurement at 20 km/hr) exhibited no significant statistical variation across different measurements. This indicates that DFT20 is a reliable aggregate polishing resistance metric unaffected by the aforementioned variables. Furthermore, the DFT20 @ 100,000 polishing values closely followed the chemical composition percentage order of the seven coarse aggregates tested. Aggregates with higher silica (SiO<sub>2</sub>) and lower calcium oxide (CaO) content demonstrated superior friction performance. However, the PSV results did not align with the friction resistance rankings observed in the TWPD tests, even

when the same aggregate materials were used. This discrepancy highlights limitations in the PSV test compared to the TWPD procedure.

Additionally, DFT measurements provide a broader range of values than BPT-measured PSV values, suggesting that TWPD offers a more consistent and repeatable method for assessing laboratory aggregate polishing resistance. Based on these findings, it is recommended that DOTD adopt the TWPD/DFT testing procedure for initial aggregate source friction rating evaluations. Additionally, this project proposes a new aggregate friction rating table based on the DFT20 @ 100,000 polishing values for the aggregates tested.

The field friction measurements from this project, combined with data collected in LTRC Project 12-5P, were analyzed to perform comprehensive statistical evaluations of the effects of aggregate properties and mixture design on skid resistance values and their variability. Statistical correlation models were updated to capture relationships among different in-situ friction measurement devices, as well as various surface textures and frictional properties.

Finally, to establish threshold friction design values, a new F(60) prediction model was developed. This model incorporates DFT20, Mean Profile Depth (MPD), and polishing cycles, enabling the determination of threshold friction design values for aggregates based on their DFT20 results and the mixture's MPD. These values are aligned with the pavement's design average daily traffic (ADT) per design lane and expected service life.

This project offers actionable recommendations and improved tools for aggregate friction testing, field friction evaluation, and pavement friction design. The findings support the development of more reliable, accurate methods for assessing and designing pavement surfaces to enhance safety and performance.

## **Acknowledgements**

This study was supported by the Louisiana Transportation Research Center (LTRC) and the Louisiana Department of Transportation and Development (DOTD) under LTRC Research Project Number 20-4P. The authors would like to express thanks to all those who provided valuable help on this study. Specially, the authors would like to express thanks to the DOTD Materials and Testing Laboratory (MATLAB) personnel, particularly Faren Spooner and the laboratory technicians. The authors would also like to acknowledge LTRC's Pavement Research testing crew of Terrell Gorham, Biyuan Zheng, and Ray Kimble, who carried out field testing for this study.

## **Implementation Statement**

Based on the results of the aggregate polishing tests, it is recommended that the Louisiana Department of Transportation and Development (DOTD) adopt the TWPD/DFT testing procedure, as outlined in AASHTO PP103, for initial evaluations of aggregate source friction ratings. Additionally, a new aggregate friction rating table, developed using DFT20 @ 100,000 polishing values, has been proposed for implementation.

# Table of Contents

Technical Report Standard Page .....	1
Project Review Committee .....	4
LTRC Administrator/Manager .....	4
Members .....	4
Directorate Implementation Sponsor .....	4
Assessment of Laboratory Friction Testing Equipment and Validation of Pavement Friction Characteristics with Field and Accelerated Friction Testing.....	5
Abstract .....	6
Acknowledgements .....	8
Implementation Statement .....	9
Table of Contents .....	10
List of Tables.....	12
List of Figures .....	13
Introduction.....	15
Literature Review.....	16
Friction Fundamentals .....	16
Current Research Implementing Three-Wheel Polisher Device (TWPD) and Dynamic Friction Testing (DFT).....	19
Correlations between Different Friction Measurements from Different Test Devices.....	22
Studies on Field Pavement Friction .....	27
Friction Design Guidelines .....	32
Objective .....	34
Scope.....	35
Methodology .....	36
Laboratory Evaluation of Aggregate Polishing Resistance .....	36
Field Friction Tests.....	42
Analysis Procedure .....	45
Discussion of Results.....	47
Results from BWP Polishing Tests .....	47
Results from Three-Wheel Polishing Tests.....	55
Results from In-Situ Pavement Friction Measurements .....	72
Correlation Analysis Among Field Measurements .....	80
Development of F(60) Prediction Model.....	85

Conclusions.....	91
Recommendations.....	94
Acronyms, Abbreviations, and Symbols.....	95
References.....	96
Appendix A.....	101
Laboratory Method of Polishing Aggregates Using the Three Wheel Polisher Machine along with Dynamic Friction Tester (DFT) and Circular Texture Meter (CTM).....	101
Appendix B.....	108
DFT Data Analysis.....	108

## List of Tables

Table 1. Factors affecting tire-pavement friction [3] .....	17
Table 2. Aggregate friction rating table [47].....	33
Table 3. Methods used to evaluate skid resistance properties .....	33
Table 4. Aggregates general information .....	37
Table 5. Aggregate chemical compositions .....	37
Table 6. Field testing projects .....	43
Table 7. Field testing projects job mix formulas (JMF).....	44
Table 8. Initial and final BPN results from samples polished by BWP .....	48
Table 9. Aggregate friction ratings of selected aggregates .....	50
Table 10. Standard deviations of PSV results .....	51
Table 11. Comparison of aggregate friction rating .....	52
Table 12. Initial and final microtexture results from samples polished by TWPD.....	56
Table 13. Initial and final macrotexture results of samples polished by TWPD .....	58
Table 14. Adjusted DFT20 values.....	60
Table 15. DFT at different test speeds .....	63
Table 16. Regression coefficients per aggregate type.....	66
Table 17. Ranking based on PSV vs polished DFT20 .....	67
Table 18. Ranking based on unpolished BPN vs unpolished DFT20 .....	68
Table 19. Range of DFT20 @ 100,000 vs PSV values .....	69
Table 20. Summary of DFT20 @ 100,000 polishing cycle results for all TWPD ring samples .....	70
Table 21. (a) First proposal and (b) second proposal for new aggregate friction rating based on DFT20.....	71
Table 22. Aggregates rated based on the new DFT20 based rating system .....	72
Table 23. Field DFT and MPD results .....	72
Table 24. LWST and Laser Profile test results.....	73
Table 25. F(60) prediction results .....	88
Table 26. Aggregate DFT20 requirement depending on ADT and mixture type.....	89
Table 27. Data collection format for MPD .....	105
Table 28. Data collection format for DFT .....	106
Table 29. 30 DFT20 measurements at same position with voltages .....	109
Table 30. DFT and CTM test results per tested aggregate ring sample .....	120

## List of Figures

Figure 1. Mechanisms of tire-pavement friction [3].....	17
Figure 2. Microscopic view of pavement surface showing microtexture and macrotexture [2] .....	18
Figure 3. Polished Stone Value (PSV) Test.....	39
Figure 4. Three-Wheel Polishing Device (TWPD).....	40
Figure 5. Three-Wheel Polishing Test (TWPT).....	41
Figure 6. Aggregate texture measurement devices with TWPT polishing .....	41
Figure 7. Field testing layout [2].....	42
Figure 8. Field testing crew and equipment.....	43
Figure 9. Locations of test sections.....	45
Figure 10. Polishing stone test results.....	49
Figure 11. PSV ranking.....	51
Figure 12. Variations of BWP test results due to shipments .....	54
Figure 13. Average DFT20 results per aggregate type.....	57
Figure 14. Average DFT20 results per aggregate type along with reduction percentage.....	57
Figure 15. MPD of polished and unpolished samples .....	59
Figure 16. $\Delta$ DFT20 vs $\Delta$ MPD prediction.....	60
Figure 17. Blended DFT20 vs polishing cycles.....	61
Figure 18. DFT20 Results per aggregate type .....	62
Figure 19. Relationship between BPN and DFT20 .....	66
Figure 20. SN40R field results.....	74
Figure 21. SN40S field results .....	75
Figure 22. LWST MPD field results .....	75
Figure 23. DFT20 field results.....	76
Figure 24. BPT field results .....	77
Figure 25. CTM MPD.....	77
Figure 26. F(60) field results .....	79
Figure 27. SN40R vs SN40S .....	80
Figure 28. DFT vs MPD .....	81
Figure 29. SN40R vs DFT20 .....	82
Figure 30. SN40S vs DFT20.....	82
Figure 31. SN40R vs MPD .....	83
Figure 32. SN40S vs MPD.....	83

Figure 33. Laser Profiler (MPD) vs CTM (MPD) .....	84
Figure 34. Cycles vs T.I. ....	87
Figure 35. F(60) prediction.....	88
Figure 36. Cycles vs F(60).....	90
Figure 37. Aggregate ring sample preparation process.....	103
Figure 38. Composition of Three-Wheel Polisher Device [53].....	104
Figure 39. DFT data at different speeds.....	109
Figure 40. Reliability analysis .....	109
Figure 41. DFT Results at 90° rotation.....	111
Figure 42. DFT20 results considering sample effect and 90° rotation .....	113
Figure 43. DFT40 results considering sample effect and 90° rotation .....	115
Figure 44. DFT60 results considering sample effect and 90° rotation .....	117
Figure 45. DFT difference based on time and operator .....	119

# Introduction

Crashes are complex events typically attributed to three primary factors: driver-related, vehicle-related, and highway condition-related causes. Transportation agencies have the ability to monitor these factors and improve highway conditions to mitigate crash risks. Within highway conditions, low pavement friction, particularly under wet conditions, is a major contributing factor to crashes [1]. Recognizing the critical role of surface friction in roadway safety, many state highway agencies have implemented specifications and friction design guidelines to ensure satisfactory surface friction is maintained throughout a pavement's service life.

The current DOTD aggregate friction rating system relies solely on the Polished Stone Value (PSV) of coarse aggregates. However, significant variability in PSV values is frequently observed between aggregate shipments from the same quarry. Even when tests are conducted on samples from the same batch, discrepancies in PSV values may arise due to actual variations in the produced aggregates or the type of testing equipment used.

This variability often leads to questions and concerns from aggregate suppliers, particularly when their aggregates fail to meet the PSV targets set by DOTD, resulting in a reduced Friction Rating and a lower classification. To address this issue, there is a need to formalize the use of aggregate polishing tests to optimize aggregate utilization and ensure a desirable skid resistance value over the pavement's service life.

Furthermore, it is necessary to evaluate whether the Dynamic Friction Tester (DFT) provides more reliable friction characteristics of aggregates than the British Pendulum Tester (BPT), which is currently used by DOTD. Implementing more accurate and consistent friction testing methods could enhance the reliability of aggregate friction ratings and improve pavement performance.

# Literature Review

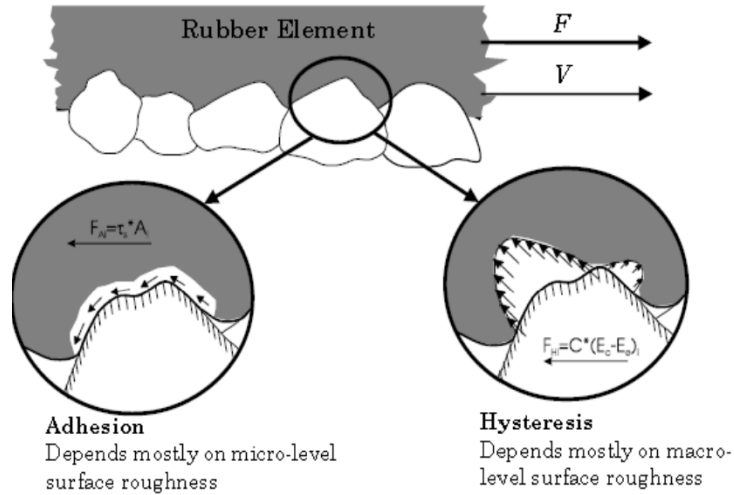
## Friction Fundamentals

The concept of pavement friction corresponds to the proportion of vertical and horizontal forces that arise as a tire traverses a pavement texture. It refers to a force that acts against the direction of movement at the contact surface [2]. Friction is the primary determinant that maintains automobiles on the roadway and provides the essential force to decelerate or halt them. Minimum stopping distance, minimum horizontal radius, minimum radius of vertical curves, and super-elevation are all crucial parameters in the geometric design of pavements. However, the primary determinant in mitigating collisions is the frictional interaction between a tire and the pavement [3] [4].

The likelihood of sliding is greatly heightened when the pavement surface is wet. A research study conducted in Kentucky demonstrated that the occurrence of collisions under wet weather conditions is directly proportional to the decrease in surface friction [5]. Hall et al. (2009) conducted a study in Texas, which indicated that there is a higher percentage of crashes when the friction surface is lower [3]. In a study conducted by Najafi et al., it was determined that friction has a substantial role in influencing the frequency of crashes, regardless of whether the pavement is wet or dry [6].

The friction experienced by tires on pavement is caused by two factors: adhesion and hysteresis. The adhesion process is a consequence of the bonding and interlocking that occurs between rubber and pavement particles. Conversely, hysteresis refers to the thermal energy generated as a result of the interaction between tires and pavement. When a tire makes contact with the gap between the aggregates of a pavement surface, it results in deformation of the tire. When this deformed tire relaxes, a portion of the stored energy will be reclaimed while another portion will be dissipated as heat energy. Hysteresis refers to the dissipation of energy in the form of heat [7]. The relationship between hysteresis and adhesion is significant in relation to surface qualities and tire properties. According to Hall et al., adhesion is primarily associated with microtexture, while hysteresis is primarily associated with macrotexture [3]. Figure 1 depicts the mechanism of friction on the tire surface.

**Figure 1. Mechanisms of tire-pavement friction [3]**



The friction on pavement surfaces is primarily influenced by four key factors: the features of the pavement surface, the operating parameters of the vehicle, the properties of the tires, and environmental factors. These are outlined below in Table 1 [3]. Of the four categories highlighted in Table 1, highway agencies are able to exclusively manage the features of the pavement surface. This project also examined the friction resulting from the properties of the pavement surface.

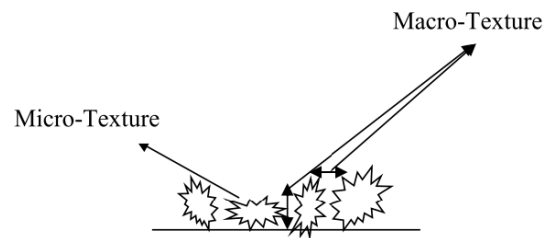
**Table 1. Factors affecting tire-pavement friction [3]**

Pavement Surface Characteristics	Vehicle Operating Parameters	Tire Properties	Environment
Microtexture	Slip Speed	Foot Print	Climate
Macrottexture	Vehicle Speed	Tread Design and Condition	Wind
Megattexture	Bracking Action	Rubber Composition and Hardness	Temperature
Unevenness	Driving	Inflation Pressure	Water (e.g., rainfall, condensation)
Material Properties	Maneuver	Load	Snow and Ice
Temperature	Turning	Temperature	Contamination (i.e., fluid)
	Overtaking		Anti-skid material (e.g., salt, sand)
			Dirt, mud, and debris

In accordance with the guidelines provided by the American Association of State Highway and Transportation Officials (AASHTO), pavement friction is defined as the extent to which the pavement surface deviates from a perfectly flat and level surface. The texture features associated with friction are commonly referred to as macrotexture and microtexture, as described by Kummer and Meyer in 1960 [8]. The criteria set by the Permanent International Association of Road Congress (PIARC) in 1987 to differentiate different textures based on wavelength ( $\lambda$ ) and amplitude (A) correspond as follows:

Microtexture refers to the surface roughness quality at the sub-visible or microscopic level, with a range of  $\lambda < 0.02$  in. and  $A = 0.04$  to 20 mils. The surface characteristics of the aggregate particles in the asphalt mixture determine this aspect. The macrotexture, with a range of  $\lambda = 0.02$  to 2 in. and  $A = 0.005$  to 0.8 in., refers to the surface roughness quality of an asphalt mixture. This quality is determined by the mixture parameters, including the shape, size, and gradation of the aggregate. The megatexture ranges from  $\lambda = 2$  to 20 in. and  $A = 0.005$  to 2 in. Megatexture has wavelengths of the same magnitude as the interface between the pavement and the tire. The pavement surface is primarily characterized by the presence of distress, flaws, or "waviness." The key features for pavement surface friction, which are depicted in Figure 2, are microtextures and macrotextures, as described earlier [9]. Numerous studies have been conducted to examine the impact of microtexture and macrotexture on pavement surface friction. Notable contributions in this area include the works of Davis (2001), McDaniel and Coree (2003), Hanson and Prowell (2004), Wilson and Dunn (2005), and Goodman et al. (2006) [2] [10] [11] [12] [13] [14].

**Figure 2. Microscopic view of pavement surface showing microtexture and macrotexture [2]**



The influence of microtexture and macrotexture on pavement surface friction is widely recognized [2]. The magnitude of pavement friction is most influenced by microtexture, while the friction-speed gradient (i.e., the rate at which friction changes with slip speeds) is primarily affected by the macrotexture [3]. The surface texture of the coarse aggregate mostly influences the microtexture of flexible pavements, whereas the macrotexture is primarily influenced by

the gradation of the aggregate and the volumetric parameters of the hot mix asphalt (HMA) mixture. Furthermore, the mean texture depth (MTD) and mean profile depth (MPD) are commonly used to characterize the macrotexture of pavement. There is a wide array of instruments that can be utilized to characterize pavement friction and texture. Certain devices are primarily utilized in the field, while others can be employed in both laboratory and field settings. The following section provides a description of four frequently employed instruments for friction and texture testing, which are also utilized in this study. These devices include the Locked Wheel Skid Trailer (LWST), British Pendulum Tester (BPT), Dynamic Friction Tester (DFT), and Circular Track Meter (CTM). Other studies, such as those by Henry (2000), Wallman et al. (2001), Hall et al. (2009), and Choi (2011), have conducted more extensive evaluations of friction and texture testing devices [3] [15].

### **Current Research Implementing Three-Wheel Polisher Device (TWPD) and Dynamic Friction Testing (DFT)**

The Three Wheel Polishing Device (TWPD) has been used in various kinds of research projects. One investigation focused on the effect of the aggregate type and polishing level on the long-term skid resistance of a thin friction course. This research explored the effect of the aggregate type and the polishing level on the long-term skid resistance of a thin friction course built with calcined bauxite [16]. The friction performance of this project was assessed using the PSV test, TWPD, and DFT device. The mineral hardness of the aggregate was linked with the skid resistance of the aggregate and the thin friction course by regression analysis. The grey correlation and t-test were utilized to examine the parameters that affect the skid resistance of the thin friction course.

After analyzing the data, it was found that the 88# calcined bauxite outperformed the limestone, basalt, and 75# calcined bauxite in terms of skid resistance. One of the findings of this research was that the PSV attenuation rate of aggregate has a strong correlation with the attenuation rate at DFT60. The PSV attenuation rate has a direct relationship with the attenuation rate at DFT40. Furthermore, the aggregate hardness parameter (AHP) presents the ability of the aggregate and asphalt mixture to maintain long-term skid resistance. This parameter is composed of the summation of the average hardness of the aggregate and the contrast of its hardness. In this project, the PSV and the DFT results (at speeds of 20, 40, 60, and 80 km/hr) were plotted against the AHP. From this analysis, it was found that the polishing resistance is directly related to the mineral composition of the aggregate.

Another study focused on correlating the friction test results under accelerated laboratory polishing and aggregate crushing [17]. This study investigated the frictional properties and crushing resistance of coarse aggregates used in asphalt concrete to ensure optimal performance under traffic loads [17]. Testing was conducted on 25 aggregate sources using the Dynamic Friction Test (DFT), British Pendulum Test (BPT), and Aggregate Crushing Value (ACV) tests. The DFT and BPT assessed frictional performance, while the ACV test evaluated crushing resistance. Accelerated polishing was performed using the Three-Wheel Polishing Device (TWPD). The results showed that aggregates with high crushing resistance and low friction loss performed better under traffic loads. Strong correlations were identified between friction loss and ACV parameters, as well as between final friction life and BPT parameters. The findings suggest that TWPD/BPT and ACV tests can serve as substitutes for the DFT when it is unavailable, although with reduced sensitivity in marginal materials. This highlights the potential for integrating friction and crushing evaluations in aggregate testing to better characterize pavement performance.

A different investigation focused on the usage of DFT and BPT to assess the effect of aggregate microtexture losses on skid resistance on chip seals [18]. This study investigated the impact of aggregate microtexture on the skid resistance of pavement surfaces, with a focus on chip seals. Laboratory experiments were conducted using different aggregate types, grain sizes, and polishing levels. A Micro-Deval (MD) apparatus was used to polish aggregates at controlled levels. Skid resistance and texture measurements were performed using the Dynamic Friction Tester (DFT) and British Pendulum Tester (BPT), while texture depth was evaluated with an outflow meter test. Additional visual assessments were made using scanning electron microscopy (SEM) and optical microscopy (OPM). Among the key findings of this research is that slag aggregates exhibited superior skid resistance compared to natural aggregates across all polishing levels. Furthermore, the skid resistance decreased with higher polishing levels for all aggregate types and grain sizes. Additionally, strong correlations were observed between the DFT and BPT results, validating the usage of both methods in assessing skid resistance. Finally, SEM and OPM images highlighted the significant loss of aggregate microtexture due to polishing.

Another investigation utilized the TWPD device to study the influence of alternative friction aggregates on the texture and friction characteristics of high friction surface treatment [19]. This study evaluated the friction and texture properties of high-friction surface treatments (HFST) using 12 types of friction aggregates, including alternative options to calcined bauxite, a common but expensive aggregate. The research utilized both laboratory tests and field applications. Laboratory experiments employed the Three-Wheel Polishing Device (TWPD)

for simulated traffic polishing and the Dynamic Friction Tester (DFT) to measure friction coefficients at varying speeds. Field tests at the NCAT Test Track involved monitoring friction and texture under real-world conditions using DFT and other methods. Among the key findings is that calcined bauxite exhibited the best friction performance and durability, making it superior for HFST applications. Taconite emerged as a promising alternative due to its strong abrasion resistance and friction properties. Furthermore, slag, silica, and quartz aggregates showed poor friction and texture characteristics, making them unsuitable for HFST. Additionally, laboratory tests identified 70,000 polishing cycles with TWPD as sufficient to reach a terminal friction stage. Strong linear correlations were observed between laboratory and field DFT results, validating the reliability of lab simulations. Finally, aggregate properties, such as particle size and angularity, significantly influenced macrotexture (MPD) but showed limited correlation with friction (DFT60).

Another effort was made utilizing the TWPD to develop a practical specimen preparation and testing protocol for the evaluation of the friction performance of asphalt pavement aggregates [20]. This study evaluated a practical specimen preparation and testing protocol for assessing the friction performance of aggregates in asphalt pavement using the Three-Wheel Polishing Device (TWPD) and the Dynamic Friction Tester (DFT). A key goal was to reduce the time and cost of preparing samples compared to the AASHTO PP103 method. The research focused on optimizing specimen preparation, addressing operational variability, and evaluating the reproducibility of the TWPD/DFT test protocol. Among the key findings, the proposed preparation method reduced time from over 15 hours to under five hours and costs from approximately \$30 to \$10 per specimen while achieving similar results. Furthermore, the reproducibility of the friction tests using three identical TWPDs was confirmed, with no statistically significant variability in friction results across different devices. Additionally, friction outcomes were unaffected by slight gaps of up to 16% between aggregates in the specimen, indicating flexibility in preparation rigor. The study validated that solid tires could replace pneumatic tires for polishing without compromising test accuracy, offering cost and safety advantages. The method was robust against operational factors such as tire tread depth and rubber pad usage, showing minimal impact on friction measurement results.

A different study utilized the TWPD device to develop empirical prediction models to determine the coefficient of friction of various surface treatments using different aggregate characteristics [21]. This study investigated the friction and polishing resistance of high-friction surface treatment (HFST) aggregates. A combination of calcined bauxite and five local aggregates was tested to predict the dynamic friction coefficient (DFC) based on aggregate characteristics such as angularity and surface texture. The research incorporated both

laboratory and field testing to assess skid resistance, emphasizing the role of HFST in enhancing pavement safety and reducing crash rates. Among the key findings of this research, calcined bauxite displayed superior friction and polishing resistance, confirming its suitability for HFST. Flint chat, steel slag, and rhyolite trap rock were identified as potential alternatives to calcined bauxite. Friction losses stabilized after 70,000 polishing cycles, suggesting a terminal performance point for HFST materials. Empirical models were developed to correlate DFC with aggregate characteristics, achieving high predictive accuracy. Surface texture and angularity were critical parameters influencing friction performance, with microtexture dominating low-speed friction.

Finally, a recent study proposed alternative methods to the AASHTO PP103 standard, which uses TWPD, for evaluating the frictional resistance of aggregates [22]. The goal of this study was to streamline the polishing process, reducing time and resources while maintaining reliable results. Two alternative approaches were tested. The first was Micro-Deval abrasion and DFT combination, in which aggregates were abraded using the Micro-Deval apparatus, and their frictional resistance was evaluated with the Dynamic Friction Tester (DFT). This method reduced testing time significantly while maintaining a high correlation ( $R^2 > 0.75$ ) with the AASHTO PP103 standard.

The second approach was the development of a regression model prediction. A regression model was developed using conventional aggregate tests (e.g., Micro-Deval Abrasion Loss, Los Angeles Abrasion Loss, and Acid Insoluble Residue) to predict friction values. This approach demonstrated high predictive accuracy and was suitable for the rapid screening of aggregate frictional properties. In this investigation, the DFT device was used to measure the friction of the aggregates at speeds of 20 km/hr under wet conditions. Furthermore, it was fundamental in validating the friction performance after polishing cycles and correlating with other mechanical tests.

### **Correlations between Different Friction Measurements from Different Test Devices**

The phenomenon of friction between rubber and road surface is complex. Friction is influenced by various factors, including slip speed, pavement texture, road surface contaminants (i.e., water, snow, dust), and rubber properties, which are influenced by temperature and slip speed [23]. As a result, it is common for various test equipment to have disparate measured frictions, even when situated at an identical place on the same pavement. Previous research has examined

the relationship between friction data obtained from various testing systems. This section examines two correlations: (1) the correlation associated with the LWST skid numbers obtained from smooth and ribbed tires, and (2) the correlation between the LWST skid number and the friction number obtained from portable friction devices.

The original LWST has a pair of ribbed test tires positioned bilaterally on the trailer. The ribbed test tire exhibits less sensitivity to the flow rate of the water delivery system, resulting in a higher level of reproducibility in the recorded skid number across various devices [24]. Nevertheless, the ribbed test tire exhibits insensitivity toward the macrotexture of the pavement surface, specifically within the range of 0.02 to 2 in. The reason for this is that the grooves present on the ribbed tire possess the capability to effectively facilitate water drainage, irrespective of the overall texture of the pavement. Early researchers observed this constraint while assessing the impact of surface grooving on the skid resistance of the pavement using the Large-Wave Surface Test [25]. The justification for the benefit of surface grooving on wet pavement friction is contingent upon the utilization of LWST in conjunction with smooth test tires. The skid number recorded with a smooth tire is influenced by both the microtexture and macrotexture of the pavement, as it depends on the macrotexture of the pavement to decrease the thickness of the water film between the tire and pavement.

Numerous experts have conducted investigations into the quantitative correlation between the smooth and ribbed test tires. Henry and Saito (1983) conducted a comparative analysis of the LWST test results in Pennsylvania, utilizing tires from 22 different field sections and varying aggregate and mix types [26]. The study revealed a strong correlation between the ratio of skid numbers obtained from ribbed and smooth test tires and the macrotexture of the pavement, as indicated by Equation 1.

$$\frac{SN_{40R}}{SN_{40S}} = 0.887 * MTD^{0.36} \quad (1)$$

Where,

SN<sub>40R</sub> = Skid number measured by LWST with a ribbed tire at the speed of 40 mph;

SN<sub>40S</sub> = Skid number measured by LWST with a smooth tire at the speed of 40 mph; and

MTD = Mean texture depth.

Prior to the availability of DFT, the polished stone value (PSV), or BPN on the polished aggregate surface, was frequently associated with the LWST skid number of the pavement. This kind of correlation facilitated the anticipation of the field skid number from laboratory

results because BPN could be used in both the field and the laboratory. Based on 25 field test data from two types of dense graded wearing course mixtures in Kansas, Parcell et al. found linear correlations between BPN and LWST skid numbers at different speeds [27]. Additionally, Diringer and Barros compared field and laboratory test data for 26 sites in New Jersey to establish a non-linear link between the terminal skid number and the PSV of the aggregate [28]:

$$SN_{40R_{Terminal}} = 12.4 * (1 - e^{-0.023*PSV}) + 1.15 * PSV - 8 \quad (2)$$

Where,

$SN_{40R_{terminal}}$  = terminal skid number measured by ribbed tire at the speed of 40 mph; and

PSV = polishing stone value.

As previously mentioned, both PSV and BPN serve as indicators of the pavement's microtexture. Thus, the impact of macrotexture is disregarded in the relationships stated above. As a matter of fact, microtexture and macrotexture work together to produce pavement friction [8]. Many researchers believed that taking into account both the pavement's macrotexture and microtexture could result in a stronger association with LWST skid number [29] [30] [31] [32]. Additionally, skid resistance data gathered from 20 test sections in West Virginia was examined by Leu and Henry, who created a ribbed-tire skid number prediction model that took into account both macrotexture and microtexture [30]. In this model, the pavement's macrotexture, measured by sand-patch MTD, influences the speed gradient of the recorded LWST skid number, whereas the pavement's microtexture, measured by BPN, influences the intercept skid number at zero speed ( $SN_0$ ). In Equation 3, the generated model is displayed. Balmer and Hegmon also posted an approximation equation, Equation 4, for computing  $SN_{40R}$  [31].

$$SN(S)R = (-31 + 1.38 * BPN)e^{-0.041*S*MTD^{-0.47}} \quad (3)$$

$$SN_{40R} = (-31 + 1.38 * BPN)e^{-0.29*\sqrt{MTD}} \quad (4)$$

Where,

$SN(S)R$  = ribbed-tire LWST skid number at test speed S;

BPN = British Pendulum number; and

MTD = Sand-patch mean texture depth (mm).

Equations 5 and 6 illustrate Henry's subsequent proposal of a straightforward linear regression model between the skid number, BPN, and sand-patch MTD [32]. Using test data gathered from 22 Pennsylvania test sections, he calculated the regression constants. Different pavement

surface types, such as standard mix, open-graded mix, and customized surface treatments, were used in these test sections. Henry also compared the test data obtained in the fall of 1978 with data obtained in the spring of 1979 and saw a seasonal fluctuation in the regression constants.

$$SN40R = a_0 + a_1 * BPN + a_2 * MTD \quad (5)$$

$$SN40R = b_0 + b_1 * BPN + b_2 * MTD \quad (6)$$

Where,

SN40R, SN40S = skid number measured by LWST at 40 mph with the ribbed tire and the smooth tire respectively;

BPN = British Pendulum friction number;

MTD = Sand-patch mean texture depth (mm); and

$a_0, a_1, a_2, b_0, b_1, b_2$  = Regression constants.

The International Friction Index (IFI) model, created by the Permanent International Association of Road Congress (PIARC), is one of the most widely used harmonization models. The PIARC study used 41 distinct devices from 16 different nations, including 27 friction devices and 14 texture devices. The average stopping speed of cars on the route was determined to be 60 km/hr. Since smooth test tires are known to be sensitive to both the microtexture and macrotexture of the pavement, it was decided to use them to measure pavement friction, which is more influenced by macrotexture at higher sliding speeds.

The friction number and texture (MPD or MTD) measured in two steps at any slide speed S by any device can be used to calculate F(60). First, use Equations 7 and 8 to convert the friction number  $FR_S$ , measured at slip speed S, to the friction number  $FR_{60}$ , measured at 60 km/hr using the same device. Next, use Equation 9 to convert  $FR_{60}$  to the IFI reference friction number F(60).

$$Sp = a + b * Tx \quad (7)$$

$$FR_{60} = FR_S * e^{\frac{S-60}{Sp}} \quad (8)$$

$$F(60) = A + B * FR_{60} + C * Tx \quad (9)$$

Where,

Sp = IFI speed number;

a, b, A, B, and C = calibration constants, C = 0 for smooth-tire devices;

Tx = pavement macrotexture in either MPD or MTD;

$FR_S$  = friction number measured at slip speed S by any device;  
 $FR_{60}$  = friction number measured at slip speed 60 km/hr; and  
 $F(60)$  =IFI reference friction number.

The American Society of Testing and Materials (ASTM) has approved the PIARC model for use in ASTM E1960 standards. ASTM E1960 recommends measuring macrotexture using MPD (ASTM E 1845) and microtexture using DFT20 (ASTM E 1911) to compute  $F(60)$  [2]. This can then be used to calibrate the calibration constants (A, B, and C) for additional devices. ASTM E 1960 uses a single set of calibration constants ( $a=14.2$  and  $b=89.7$ ) to determine the speed number from MPD [33].

Correlations between these friction measurements can be made since the IFI model can translate both the skid number measured by LWST and the friction number reported by DFT or BPT to  $F(60)$ . Nonetheless, a subsequent harmonization model analysis conducted in Europe by Descronet et al. revealed that the relationship between pavement texture and speed number varies depending on the device. It has been discovered by other studies that the PIARC model's factors (a, b, A, B, and C) need to be recalibrated [34].

In 2016, Wu et al. conducted a comprehensive study to evaluate the current DOTD coarse aggregate friction rating table and provide recommendations for the frictional mix design guidelines. For this purpose, the wearing course mixtures of different pavements containing eight commonly used aggregates were evaluated, along with four typical mixes. The mixes were 12.5 mm Superpave, 19 mm Superpave, Stone Matrix Asphalt (SMA), and Open Grade Friction Course (OGFC). Multiple field tests were conducted to gather surface friction information and texture data, including LWST skid numbers at different speeds (30, 40, and 50 mph) utilizing both ribbed and smooth tire, laser profiler, DFT and CTM. These tests were conducted at the beginning, mid-point, and end of a 1000 ft. stretch of pavement. The data gathered from these tests was used to perform a comprehensive statistical analysis of the influence of the aggregate properties and mixture design on skid resistance. Different statistical correlation models were developed using the information from the different measuring devices. This analysis led to the development of a procedure that could predict the end-of-life skid resistance of the pavement based on traffic information and blend PSV results and gradation parameters.

## Studies on Field Pavement Friction

Several recent studies on the frictional characterizations of pavement are highlighted in this section. The ASTM standard E1960 and the IFI model form the basis of most of these investigations [35] [36].

Based on the aggregate texture property and gradation, Sullivan (2005) created a prediction model to determine the IFI friction number  $F(60)$  and the stopping distance of a vehicle [37]. The previously discussed PIARC model serves as the foundation for this prediction model. According to the suggested model, the aggregate gradation and mix binder content are used to forecast the pavement's macrotexture (MPD). Information from 17 NCAT test sections was used to create the MPD prediction model. In order to calculate  $F(60)$  from PSV and MPD, Sullivan used the IFI model with the original calibration coefficients. It is important to state that the model does not account for the deterioration of pavement friction brought on by traffic cleaning.

Jackson (2008) conducted a field test investigation to compare several pieces of test equipment for texture and friction [34]. At the National Center of Asphalt Technology (NCAT), ten road test sections were used for the initial field tests (LWST, DFT, and CTM). The NCAT test consists of 200 ft. for each segment. Each section's friction was tested using LWST at 40 mph using test tires that were both smooth and ribbed. In every part, five distinct locations were used to conduct CTM and DFT. Based on the IFI model found in Equation 9, researchers recalculated constants (A and B) for the LWST. Subsequently, in order to confirm the calibrated IFI speed number model, comparable field friction and texture experiments were carried out on ten Florida DOT road sections, including three open graded, five dense graded, and two concrete pavement sections. The team discovered that the calibration parameters from the NCAT parts and the Florida test sections differed significantly.

Liang (2009) gathered a variety of pavement texture (MPD from CTM) and friction (DFT and LWST) data from eight road sections in Ohio [38]. To establish correlations between the skid resistance of field pavements and the laboratory test results from accelerated polishing equipment created by the researcher, field data had to be gathered. The team decided to include low, medium, and high friction aggregates in the eight test portions. Every test segment is approximately 500 ft. in length. Every test was conducted using the left wheel route. The test data was analyzed using single- and multi-variable regressions rather than the IFI model, and a number of correlations between the pavement's friction and texture measurements (MPD, DFT20, and DFT64) and the skid number SN40R were established. Equations 10 through 12

display the multi-variable regression correlations. It is important to note that the HMA samples were made using the same job mix formula (JMF) of the road sections and were subjected to laboratory polishing tests.

$$SN40R = 26.762 + 1.726 * MPD + 0.429 * DFT_{20} \quad (10)$$

$$SN40R = 15.104 + 1.921 * MPD + 0.709 * DFT_{64} \quad (11)$$

$$SN40R = 14.517 - 0.075 * DFT_{20} + 0.828 * DFT_{64} \quad (12)$$

Where,

SN40R = Skid number measured by LWST with a ribbed tire at the speed of 40 mph;

SN40S = Skid number measured by LWST with a smooth tire at the speed of 40 mph; and

DFT<sub>20</sub> = Friction number measured by DFT at the speed of 20 km/hr.

DFT<sub>64</sub> = Friction number measured by DFT at the speed of 64 km/hr.

A collaborative field test study performed by six state DOTs was done to reevaluate the IFI model by Flintsch et al. (2009). This field investigation was performed using five distinct friction testers on 24 test sections of Virginia Smart Road with different mixture types. The IFI friction number F(60) was determined by the DFT20 and MPD and compared with F(60) acquired using other high-speed friction testers. It was discovered that the surfaces evaluated in the Virginia Smart Road Rodeo, the IFI model did not yield harmonized findings among the devices employed by the consortium members. Regardless of whether a power or linear model was applied, the speed number Sp obtained from each of the five friction testers showed a weak correlation with the MPD. This weak correlation was displayed, despite applying a linear or power model. Nevertheless, the power model displayed a slightly better fit to the test data. The calibration constants (a, b, A, B, and C) in the IFI model for the various devices under investigation were ultimately recalculated by the study team.

Fuentes and Gunaratne (2010) examined the Wallops Runway Friction Workshop data from 2007–2008, which was gathered from 14 distinct pavement surfaces utilizing various test apparatuses [39]. These researchers verified that the pavement's macrotexture and the test device both affected the IFI's speed number Sp. To calibrate the IFI model's calibration constants, the team proposed a revised process.

Kowalsaki et al. (2010) studied the friction of flexible pavements [40]. The study's goals were to: (1) determine a laboratory accelerated polishing method for the HMA samples; (2) investigate ways to improve pavement skid resistance by blending different aggregates and using high-friction mix types; (3) develop a preliminary procedure for determining IFI-based flag value as a baseline indicator for laboratory friction measurements; and (4) investigate the relationship between traffic volume and the change in skid resistance in the pavement. Tests were performed in the field as well as the laboratory. 50 laboratory-prepared HMA slabs, including two stone matrix asphalt (SMA) slabs, two porous friction course (PFC) slabs, and 40 Superpave slabs, were examined under DFT and CTM in the lab tests. The Superpave samples were prepared using a partial factorial test design, allowing for the investigation of the following effects: (1) aggregate type, (2) aggregate size, (3) aggregate gradation, and (4) high-friction aggregate content. A unique compaction process was created to replicate the field compaction of the HMA. Based on the NCAT TWPD, a unique Circular Track Polishing Machine (CTPM) was developed. Furthermore, a predictive model was built for the terminal F(60) based on aggregate type, size, and gradation. This model was also based on the laboratory test results from 46 Superpave slabs. An additional 22 sections of public roads were tested for this field investigation. Moreover, historical test data from three Indiana test track portions were examined. A restricted number of BPT, DFT, CTM, and LWST were all part of the field testing program. Furthermore, regardless of the type of test tire utilized, the researchers discovered that the F(60) from the field test data was lower than the F(60) computed from the LWST data. The IFI model, however, was not further recalibrated by the researcher.

There are several features of this study that were less than ideal, and as a result, the aims of the investigation were not entirely fulfilled. For example, only the Superpave slabs were used as the basis for the laboratory-developed terminal F(60) prediction model. Additionally, other states provided field data, and these states' mix designs differed from those of the laboratory slabs. The field test data gathering included multiple operators and four LWSTs. For this reason, the data from field tests were not sufficient to validate the polishing model produced in the laboratory.

The National Center for Asphalt Technology (NCAT) carried out research to discover how the skid number recorded in the field and the frictional properties of the polished HMA samples in the lab were related [41]. The study's first phase involved developing an optimal laboratory test procedure for the Three-Wheel Polishing Device (TWPD) used at NCAT [42]. In the second phase of the investigation, following a number of TWPD polishing runs, DFT was performed on four distinct wearing course mixes, including two stone matrix asphalt mixes and two dense graded asphalt mixes. The identical aggregate source and mix design used in

the appropriate NCAT test sections were used to prepare these wearing course mixes. LWST measured the skid number on the test section using a ribbed tire at 40 mph after a particular number of ESALs. In this investigation, it was found that there was a linear correlation between the number of ESALs in the field and the number of laboratory polishing passes. Due to the loss of the binder and the consequent exposure of the aggregate in its initial polishing stage, researchers noticed that the friction characteristics recorded in both the laboratory and the field initially increased with the number of polishing cycles. In the laboratory, the friction typically peaks at 16,000 polishing passes, and in the field at 1.2 million ESALs. Thus, 32,000 polishing passes in the lab should have the same impact as approximately 2.4 million ESALs in the field, and so on. Equation 13 shows that the DFT60 recorded from the laboratory samples was connected to the matching SN40R measured in the field by linear regression after the number of ESALs in the field and the laboratory polishing passes were parsed. With an  $R^2$  of 0.935, it was discovered that the SN40R and DFT60 had a very strong linear equation correlation.

$$SN40R = -19.43 + 136 * DFT_{60} \quad (13)$$

Where,

SN40R = Skid number measured by LWST with a ribbed tire at the speed of 40 mph; and

DFT<sub>60</sub> = Friction number measured by DFT at the speed of 60 km/hr.

For the Texas Department of Transportation, Masad et al. carried out a thorough investigation of the skid resistance of flexible pavement [43] [44]. A prediction model was created in Phase 1 of the project to forecast the friction recorded in the lab as a function of mix gradation and material attributes. The Aggregate Imaging System and the Micro-Deval device were used in the proposed model to calculate the aggregate texture parameters ( $a_{agg}$ ,  $b_{agg}$ , and  $c_{agg}$ ). The gradation curve, which measures the macrottexture of the mixture, was used to calculate the aggregate gradation parameters ( $k$  and  $\lambda$ ). The mixture friction parameters ( $a_{mix}$ ,  $b_{mix}$ , and  $c_{mix}$ ) were then able to be calculated using the aggregate texture and gradation parameters. These parameters were utilized to forecast the F(60) value of the laboratory-prepared mixture at various laboratory polishing passes under NCAT TWPD. This is shown below in Equation 14.

$$F(60) = a_{mix} + b_{mix} * e^{(-c_{mix}*N)} \quad (14)$$

Where,

F(60) = IFI reference friction number;

$a_{mix}$ ,  $b_{mix}$ , and  $c_{mix}$  = friction parameters of the wearing course mixture; and

N = number of polishing cycles under NCAT TWPD.

Phase 2 of the study established a correlation between the field skid number (SN50S) at a given number of traffic passes and the F(60) of the laboratory mixture at a particular polishing cycle N. It was discovered that the measured SN50S utilizing the LWST is lower than the computed SN50S from the DFT20 and MPD based on the PIARC model. Equation 15 illustrates the revised relationship that was created between the SN50S and the F(60) as a result.

$$SN50S = 5.135 + 128.486 * (F(60) - 0.045) * e^{\frac{-20}{Sp}} \quad (15)$$

Where,

SN50S = skid number measured by LWST with a smooth tire at the speed of 50 mph;

F(60) = IFI reference friction number; and

Sp = IFI speed number.

The traffic multiplication factor (TMF) was established in order to determine the relationship between the field traffic and the laboratory polishing cycle. TMF is calculated by dividing the estimated total number of cars that have been driven throughout the course of their service life by 1000, as shown in Equation 16. Equation 17 illustrates the suggested link between TMF and the laboratory polishing cycle N.

$$TMF = \frac{AADT * Years\ in\ Service * 365}{1000} \quad (16)$$

$$N = TMF * 10^{\frac{1}{A+B*\frac{C}{c_{mix}}}} \quad (17)$$

Where,

N = polishing cycle of the NCAT TWPD;

AADT = annual average daily traffic; and

A, B, and C = regression coefficients,

A = -0.452, B = 58.95, and C = 5.834×10-6.

Equations 14 through 17 can be combined to determine a pavement's skid number based on basic aggregate parameters (e.g.,  $a_{agg}$ ,  $b_{agg}$ ,  $c_{agg}$ ,  $k$  and  $\lambda$ ) after a certain number of traffic passes. Guidelines for Louisiana's friction mix design were created by Wu and King (2012) at the Louisiana Transportation Research Center (LTRC) using a laboratory approach. 36 laboratory slabs were made using four distinct mix types (12.5 mm Superpave, 19 mm Superpave, Stone Matrix Asphalt (SMA), and Open Graded Friction Course (OGFC)) and three different aggregates (Limestone, Sandstone, and Limestone (70%) + Sandstone (30%)) [9]. Using a Three Wheel Polishing Device (TWPD) built by NCAT, all slabs were polished

up to 100,000 polishing cycles. CTM and DFT were used to measure the friction values. Both the mixture and aggregate properties have been integrated into the established friction design approach. Additionally, Wu and King's report suggested that low-friction aggregate and high-friction performance aggregate might be blended together without lowering the mixture's final friction rating.

Recently, the Texas A&M Transportation Institute developed a surface aggregate classification of reclaimed asphalt pavements [45]. This report addressed the need to improve pavement skid resistance in wet conditions using Surface Aggregate Classification A (SAC-A) materials and explored the role of reclaimed asphalt pavement (RAP) in conserving SAC-A resources while maintaining safety. The primary objectives of this study were to assess RAP's potential to conserve resources, to develop SAC ratings for RAP materials, and to establish guidelines for using RAP in surface mixes to meet skid resistance standards. The research approach was to conduct field evaluations to assess the skid resistance, to characterize RAP and virgin aggregates, and to design and test RAP mixture slabs in the laboratory. Findings indicated that moderate RAP use between 15% and 25% can assist in maintaining adequate friction levels, but higher contents can negatively affect performance. Furthermore, RAP mixtures were tested for skid resistance, texture, and durability under controlled conditions, indicating that RAP can contribute to enhance the friction performance when appropriately incorporated into mixes.

### **Friction Design Guidelines**

Currently, Louisiana DOTD uses Table 2, the aggregate friction rating chart, to guarantee that the pavement has enough skid resistance based on PSV. In order to document the precise techniques that various states employ to manage field skid resistance, DOTD carried out a survey in 2006 [46]. Table 3 lists the friction practices of Washington, D.C., and 27 other states from the survey. The majority of states, including Louisiana, have specifications that restrict the use of low-quality aggregates in course mix from a frictional standpoint. This limits the use of aggregates that are readily available locally and also contributes to the depletion of high-quality aggregates, raising the price of pavement construction. Therefore, it is necessary to assess current friction design processes and make necessary modifications.

**Table 2. Aggregate friction rating table [47]**

Friction Rating	Allowable Usage
I <sup>(a)</sup>	All mixtures
II <sup>(b)</sup>	All mixtures
III <sup>(c)</sup>	All mixtures, except travel lane wearing courses with plan ADT greater than 7000
IV <sup>(d)</sup>	All mixtures, except travel lane wearing courses

Note: (a)  $PSV > 37$ , (b)  $35 \leq PSV \leq 37$ , (c)  $30 \leq PSV \leq 34$ , (d)  $20 \leq PSV \leq 29$

**Table 3. Methods used to evaluate skid resistance properties**

Method	Agencies
British Pendulum	New Jersey, Alabama
Acid Insoluble Residue (AIR)	Arkansas, Oklahoma, Wyoming, Washington D.C.
Other Chemical Tests	Indiana (Soundness)
Skid Trailer	California, Florida, Georgia, Iowa, Mississippi, Montana, Nevada
Multiple Methods	Tennessee (BPN, AIR, Percent Lime, Soundness, Skid Trailer)
	New York (AIR, Skid Trailer)
	Pennsylvania (Petrographic, BPN, AIR)
	Virginia (Geology, Skid Trailer, Local Experience)
West Virginia (AIR, Skid Trailer)	
Other	Maryland (Test Track)
No Method (Restriction)	Delaware (use only Maryland approval quarries)
	Kansas (based on historical performance)
	Minnesota (no carbonate aggregate in wearing course)
No Method	Connecticut, Maine, New Hampshire, North Carolina, Oregon

# Objective

The primary objectives of this project were:

- To assess the PSV test variation by varying the coarse aggregate quarry source, shipment time, and test operator.
- To propose a new aggregate friction testing procedure for DOTD, which can be used for initial source approval as well as for predicting the field friction performance of aggregates used in a wearing course mixture.
- To validate and update the harmonization correlations obtained in LTRC Projects 09-2B and 12-5P between field and laboratory frictional characteristics, different pavement friction and texture testing devices, different types of test tires (e.g., ribbed and smooth), and different testing speeds for typical Louisiana asphalt pavements.
- To determine threshold friction design values (i.e., DFT and mean profile/texture depth values) for commonly used wearing course mixtures in Louisiana.

## Scope

The surface friction and polishing resistance characteristics of coarse aggregate materials used in asphalt wearing course mixes were evaluated using two laboratory polishing test methods. The first method involved the Polished Stone Value (PSV) test, utilizing a British Wheel Polisher (BWP) for polishing and a British Pendulum Tester (BPT) for measurements. The second method, referred to as the Three-Wheel Polishing Test (TWPT), used a Dynamic Friction Tester (DFT) for measurements.

To assess variations in the PSV test, seven coarse aggregates were selected and tested at the Materials and Testing Laboratory. The obtained polishing resistance measurements and the chemical composition of the aggregates were analyzed to evaluate the test's variability in terms of shipment timing, operator handling, and internal quarry source differences.

To achieve the objective of identifying a more reliable aggregate friction testing method, a series of TWPT tests were performed on duplicate ring samples of the selected coarse aggregates. Due to the lower variation observed in the TWPT results, this method was recommended as a replacement for the BWP-based PSV test for initial aggregate source approval, accompanied by a proposed new friction rating table.

To update and refine the harmonization correlations between field friction measurement devices, in-situ field friction tests were conducted on eight selected asphalt pavement sections using devices such as DFT, BPT, CTM, and LWST. The field friction measurement results, including both the current and previous test sections, were analyzed to update and improve the corresponding harmonization correlations.

To establish threshold friction design values, a new F(60) prediction model was developed, incorporating DFT20, Mean Profile Depth (MPD), and polishing cycles. This model can be utilized to determine the threshold friction design values of aggregates based on their DFT20 and mixture's MPD, aligned with the pavement's design Average Daily Traffic (ADT) and expected service life.

# Methodology

## Laboratory Evaluation of Aggregate Polishing Resistance

### Aggregate Materials

Seven coarse aggregate sources were selected for this study, including three sandstone types, three limestone types, and one rhyolite type. Only aggregates passing through a 1/2-in. sieve and retained on a 3/8-in. sieve were used for laboratory testing. These aggregates were chosen based on the following considerations:

1. They are currently used in wearing course mixtures for DOTD roadway projects.
2. They are directly sourced from project asphalt plants, ensuring relevance to real-world applications.
3. They represent a diverse range of friction ratings on DOTD's Approved Materials List (AML).
4. Their performance can be continuously monitored in ongoing local roadway projects.

The general information and characteristics of these aggregates are summarized in Table 4. According to DOTD's current AML friction ratings [48], the three sandstone aggregates are classified as Friction Rating I (FR I), the rhyolite aggregate as FR II, and the three limestone aggregates as FR III.

**Table 4. Aggregates general information**

Number	Aggregate Name	Aggregate Source Code	Aggregate Type	Bulk Specific Gravity	Absorption %	LA Wt. Loss, %	MD Wt. Loss, %
1	Agg Source 1	APS00006880	Sandstone	2.570	1.24	24.2	9.4
2	Agg Source 2	APS00006370	Sandstone	2.600	1.24	31.6	29.3
3	Agg Source 3	APS00007520	Sandstone	2.560	1.50	20.5	12.3
4	Agg Source 4	APS00006710	Rhyolite	2.640	0.7	14.4	18.5
5	Agg Source 5	APS00012880	Silicious Limestone	2.670	0.8	22.1	19.1
6	Agg Source 6	APS00007380	Silicious Limestone	2.670	0.2	19.2	6.8
7	Agg Source 7	APS00007480	Silicious Limestone	2.670	0.38	19.9	10.5

Note: LA—Los Angeles Abrasion; MD—Micro-Deval; Wt.—weight

X-ray diffraction (XRD) tests were also conducted to determine the chemical compositions for each of the coarse aggregates in this study.

Table 5 presents the chemical composition percentage results of the seven aggregates. Three minerals had a prominent presence among the aggregates: Silicon Dioxide ( $\text{SiO}_2$ ), Calcium Oxide ( $\text{CaO}$ ), and Iron Oxide ( $\text{Fe}_2\text{O}_3$ ).  $\text{SiO}_2$  and  $\text{Fe}_2\text{O}_3$ , known for their higher hardness, were found in greater proportions in the sandstones, while  $\text{CaO}$ , which is softer, was more prevalent in the limestones. All of these properties may be used as indicators of the overall friction performance throughout the service life of the pavement [21].

**Table 5. Aggregate chemical compositions**

Aggregate	Silicon Dioxide	Aluminum Oxide	Iron Oxide	Calcium Oxide	Magnesium Oxide	Sulfur Trioxide	Sodium Oxide	Potassium Oxide	Zinc Oxide
Agg Source 1 (SS)	86.8	3.4	7.5	0.6	0.9	0	0	0.1	0.1
Agg Source 2 (SS)	57.8	2.4	13.4	24	0.8	0.1	0.1	0.7	0
Agg Source 3 (SS)	48.5	5.9	5.4	18.5	1.2	0.2	0.4	4.2	0
Agg Source 4 (RH)	55.7	9.1	30.1	0.6	0.6	0.1	1.2	1.7	0

Aggregate	Silicon Dioxide	Aluminum Oxide	Iron Oxide	Calcium Oxide	Magnesium Oxide	Sulfur Trioxide	Sodium Oxide	Potassium Oxide	Zinc Oxide
Agg Source 5 (LS)	15.5	1.1	5.3	70.9	6	0.4	0.2	0	0
Agg Source 6 (LS)	30.2	8	14.7	43.1	2	0.4	0.2	0.2	0.1
Agg Source 5 (LS)	19.1	1.2	8.1	67.3	2.7	0.5	0.1	0.3	0

Note: SS – Sandstone; LS – Limestone

### Aggregate Polishing Test Methods

As highlighted in the literature review, the friction resistance of an asphalt surface is directly influenced by its microtexture and macrotexture. Microtexture is primarily determined by the micro-asperities of the coarse aggregates used and their ability to resist polishing under traffic loading. Macrotexture depends on the aggregate size and mixture gradation, varying significantly based on the type of asphalt mix.

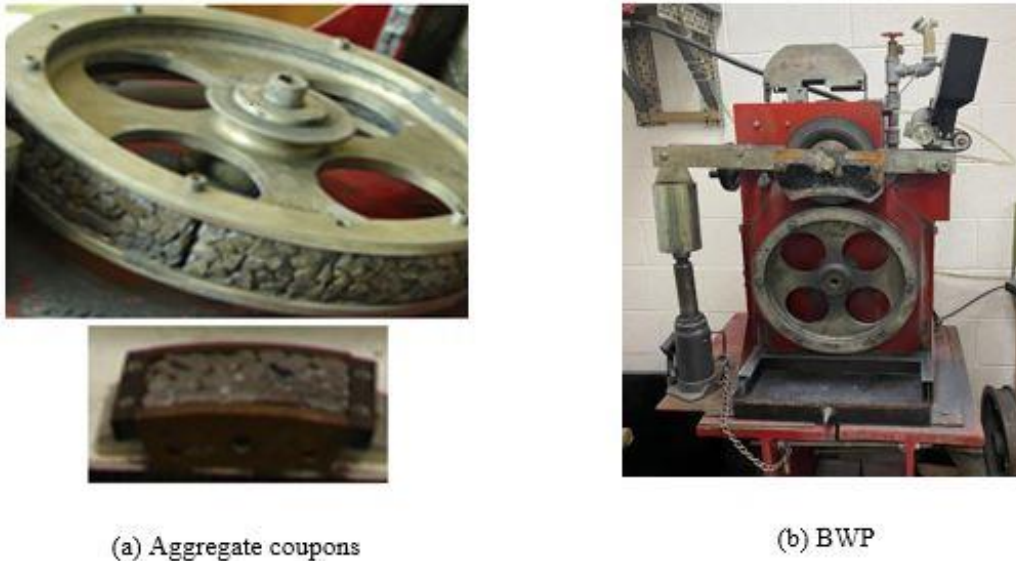
In this study, two laboratory aggregate polishing methods, the Polished Stone Value (PSV) Test and Three-Wheel Polishing Test (TWPT), were employed to evaluate the polishing resistance of the seven selected coarse aggregates. These methods aimed to assess the durability of the aggregates' microtexture under simulated traffic conditions.

### Polished Stone Value (PSV) Test

This test followed both AASHTO T 278 & T 279, along with ASTM D3319 & ASTM E1911 testing procedures, and was performed in two stages [49] [50] [51] [52]. First, aggregate coupon samples were made by fixing coarse aggregates into slightly curved coupon molds by applying an epoxy binder to the flat surface of selected aggregates. The selected aggregates passed the 1/2 in. (12.5 mm) sieve, retained on a 3/8 in. (9.5 mm) sieve, and later molded into seven curved coupon segments, as shown in Figure 3a. Next, these coupon samples were installed around a testing wheel and subjected to an accelerated polishing action in a special polishing machine called the British Wheel Polisher (BWP) for 10 hours, as shown in Figure 3b. These coupons were subjected to abrasive polishing under a loaded rubber tire, which rotates at  $320 \pm 5$  rpm, to simulate real-world conditions. The state of polish reached by each coupon sample was then tested with a British Pendulum Tester (BPT) by swinging the pendulum with a specific normal load and standard rubber pad over the aggregate surface. The average numbers of the BPT results (i.e., British Pendulum Numbers, or BPNs) both before

and after polishing (i.e., Polished Stone Value, or PSV) were reported for the tested aggregate. The higher the BPN and PSV values, the better initial surface roughness and more skid polish resistance for the evaluated aggregate.

**Figure 3. Polished Stone Value (PSV) Test**



### **Three-Wheel Polishing Test (TWPT)**

This test followed AASHTO PP103, “Standard Practice for Sample Preparation and Polishing of Unbound Aggregates for Dynamic Friction Testing” [53], to evaluate the frictional resistance of aggregates using the DFT after polishing with a three-wheel polishing device (TWPD).

For this experiment, a Troxler TWPD was utilized, as shown in Figure 4. This device consists of three tires, each having a designation of 2.80/2.50, which were applied with a load of 68 kg to the specimen’s surface. These tires rotated at a frequency of 180 wheel passes per minute. This frequency indicated that in approximately 27.78 hours, the ring would reach 100,000 cycles. This systematic approach ensures consistent preparation and testing of aggregates, aligning with guidelines outlined in AASHTO PP103 developed by Maryland DOT [53].

**Figure 4. Three-Wheel Polishing Device (TWPD)**



The TWPD testing samples used in this study, as shown in Figure 5a, were hand-made ring samples according to AASHTO PP103 [53]. The aggregates utilized in the study were sized at 3/8 in. (9.5 mm). Initially, the aggregates were sieved to attain the desired size, then thoroughly washed to remove debris and dust. Subsequently, the aggregate was subjected to oven drying for a duration of 24 hours at a temperature of 50°C to ensure moisture elimination. Selecting appropriately shaped samples was a critical step, ensuring their placement in the mold with the flat side facing downwards. Angularity was not measured, but eye judgment was used to avoid flat and angular aggregates.

The resin formula was determined through a trial-and-error process to identify the optimal composition. Initially, 1,332 grams (approximately 2.94 lbs.) of resin were poured into a container, followed by the addition of 49.5 grams of aerosol, which was blended thoroughly. Subsequently, 540 grams (approximately 1.19 lbs.) of Wollastonite were added and mixed again. The process concluded with the addition of 18 grams of Ketone to finalize the resin preparation.

Once each sample was ready, it was subjected to the Three-Wheel Polishing Test (TWPT), as shown in Figure 5b. This test consisted of three rotating wheels that travel a circumference of 208 mm at a speed of  $6.28 \pm 0.5$  rad/s ( $60 \pm 5$  rpm) [53].

**Figure 5. Three-Wheel Polishing Test (TWPT)**



(a) Aggregate ring sample



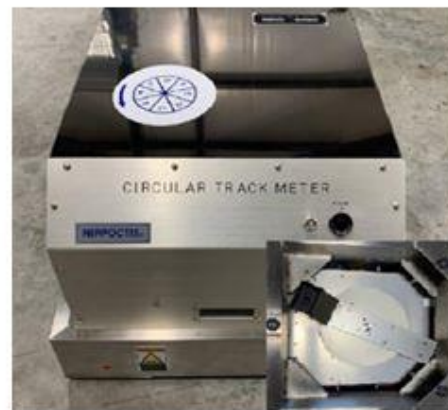
(b) Three wheels polishing

During the TWPT testing, both DFT and CTM devices were used to measure the aggregate sample's microtexture and macrotexture changes at 0, 50,000, and 100,000 cycles of TWPD wheel rotations. Figure 6 presents the DFT and CTM devices used in this study.

**Figure 6. Aggregate texture measurement devices with TWPT polishing**



(a) DFT



(b) CTM

## Field Friction Tests

Once all of the samples were evaluated, the research team assessed the field performance of the aggregates. The majority of the aggregates have been used in different routes across Louisiana. For the field testing, the skid number was determined by a lock wheel skid tester (LWST) vehicle. This vehicle utilized ribbed and smooth tires to characterize the skid number (SN) of the road. Furthermore, DFT and CTM analysis were performed to characterize the friction properties of the road and update a correlation between these values and the skid number. Figure 7 provides a layout of the testing conditions in which the experiments took place. Furthermore, Figure 8 presents an image of the field testing crew and equipment used for this part of the project. It is important to add that several of the field projects required traffic control, and only those in which the traffic data and the job mix formula (JMF) were available were selected. Figure 9 presents an image with the field project locations. Furthermore, Table 6 presents a list of the projects where field testing was conducted, while Table 7 presents the job mix formula (JMF) of the field projects. Additionally, a traffic indicator called traffic index (T.I.) was calculated for each road by applying Equation 18 [54]:

$$\text{Traffic Index (T.I.)} = \frac{\text{ADT@design lane} \times \text{years of service} \times 365}{10^6} \quad (18)$$

Where,

ADT@design lane = starting design period ADT at design lane.

**Figure 7. Field testing layout [2]**

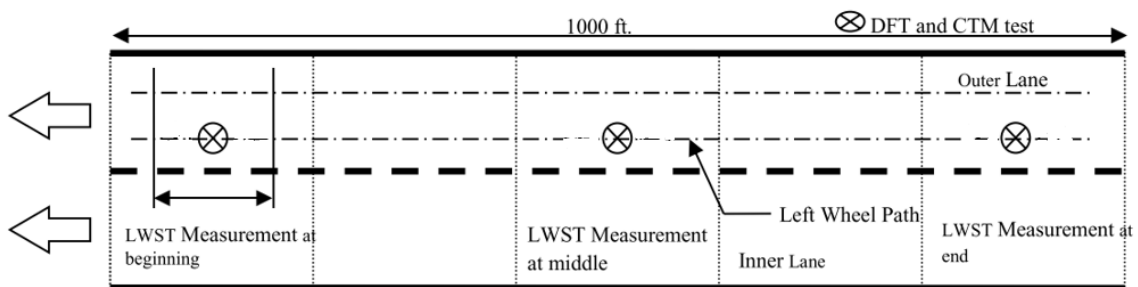


**Figure 8. Field testing crew and equipment**



**Table 6. Field testing projects**

Project	Road	Mixture Type	Coarse Aggregate (%)	Years in Service	Annual Growth Rate (%)	Growth Factor	ADT (Two ways)	Number of Lanes in One Direction	T.I.
H.014478	LA1107	12.5 mm Super Pave 100% Limestone	AGG SOURCE 6(74.51%)+RAP(25.49%)	2	2.3	2.023	1100	1	0.40
H.009628	LA92	12.5 mm Super Pave 100% Limestone	AGG SOURCE 7 (77.77%)+RAP(22.23%)	4	1	4.06	475	1	0.35
H.013250	US90	12.5 mm Super Pave 70% Limestone 30% Sandstone	AGG SOURCE 2(37.3%)+AGG SOURCE 7(18.66%)+AB26 (26.12%)+RAP (17.91%)	2	1.6	2.016	33100	2	6.04
H.010244	LA113	12.5 mm Super Pave 100% Limestone	AGG SOURCE 6 (76.28%)+RAP(23.72%)	2	1	2.01	900	1	0.33
H.012395	LA 415	12.5 SMA 30% Sandstone + 70% Limestone	AGG SOURCE 1(53.83%)+ABBS (46.17%)	2	1	3.03	25370	2	6.95
H.003003	I-10	12.5 OGFC 30% Sandstone + 70% Limestone	AGG SOURCE 1(31%)+ ABBS (69%)	1	2	1	45800	3	2.79

Project	Road	Mixture Type	Coarse Aggregate (%)	Years in Service	Annual Growth Rate (%)	Growth Factor	ADT (Two ways)	Number of Lanes in One Direction	T.I.
H.012649	LA 959	12.5 Super Pave 100% Limestone	AGG SOURCE 6 (100%)	3	1	3.03	1400	1	0.77
H.011495	LA88	12.5 Super Pave 100% Limestone	AGG SOURCE 7 (73.49%)+RAP(26.51%)	1	2	1	22750	1	4.15

**Table 7. Field testing projects job mix formulas (JMF)**

Road	LA 1107	LA92	US90	LA113	LA415	I-10	LA959	LA88
<b>Mixture Type</b>	SuperPave 12.5 mm	SuperPave 12.5 mm	SuperPave 12.5 mm	SuperPave 12.5 mm	SMA	OGFC	SuperPave 12.5 mm	SuperPave 12.5 mm
<b>Aggregate</b>	100% Limestone	100% Limestone	70% Limestone 30% Sandstone	100% Limestone	70% Limestone 30% Sandstone	70% Limestone 30% Sandstone	100% Limestone	100% Limestone
<b>VMA %</b>	13.9	14.2	13.7	14	16.8		14.8	14.2
<b>VFA %</b>	74	72	74	75	79		75	72
<b>Voids %</b>	3.6	4	3.5	3.5	3.6		3.7	4
<b>Binder Type</b>	PG 67-22	PG 70-22m	PG 76-22	PG70-22	PG 76-22		PG67-22	PG70-22
<b>Binder Content %</b>	4.6	4.7	5	4.6	6		4.9	4.7
<b>Metric (U.S.) Sieve</b>								
<b>37.5 mm (1 1/2 in.)</b>	100	100	100	100	100		100	100
<b>25.0 mm (1 in.)</b>	100	100	100	100	100		100	100
<b>19.0 mm (3/4 in.)</b>	100	100	100	100	100		100	100
<b>12.5 mm (1/2 in.)</b>	98	98	97	98	90		97	98
<b>9.5 mm (3/8 in.)</b>	88	88	86	88	72		88	88
<b>4.75 mm (No 4.)</b>	62	60	55	59	32		66	60
<b>2.36 mm (No. 8)</b>	44	40	36	43	21		45	40
<b>1.18 mm (No.16)</b>	32	30	26	30	18		32	30
<b>0.6 mm (No.30)</b>	23	27	20	22	14		24	27
<b>0.3 mm (No.50)</b>	14	18	14	12	12		15	18
<b>0.15 mm (No. 100)</b>	8	7	9	7	10		8	7
<b>0.075 mm (No. 200)</b>	6	4.2	6.8	4.7	7.6		6.5	4.2

Note: JMF regarding I-10 was not found.



This information was used to create models (DFT20 vs Polishing Cycles (N)) for every tested aggregate. Furthermore, the position of the DFT device was rotated 90° during testing in order to determine if there were variations due to rotation. The statistical differences were determined by Tukey tests to see if the measurements were statistically similar. Moreover, the variation due to the sample was also determined. Since duplicates were made for every tested aggregate ring sample, the statistical variation due to the sample effect was also determined by means of Tukey tests. The variation due to different operators was also assessed. Additionally, aggregate ring samples composed of more than one aggregate type were tested to determine the combined effect of different aggregates on the friction. The experimental data were compared to the predicted values from a previous study in order to validate the prediction results [55]. Finally, based on the DFT aggregate results, a new rating system was developed to replace the current DOTD aggregate friction system. This new friction rating system was developed using confidence intervals at an  $\alpha$  level of 0.05 and maximum and minimum ranges of data.

The ring sample macrotecture (MPD) was also collected by CTM at 0 and 100,000 polishing cycles on the two aggregate ring samples. The variation of the DFT measurements, along with the variations in MPD, were determined and plotted against each other to find a relationship between the variation in microtexture due to the variation in the macrotecture. Furthermore, an adjustment factor was developed based on this relationship.

### **Link Between Field and Laboratory Analysis Procedures**

As for the field evaluation, correlations were made to link the laboratory results with the field test results. For this analysis, information from a previous project (LTRC 09-2B) was utilized. First, a relationship between the laboratory polishing cycles and F(60) was developed. For this purpose, based on the slab information from Project 09-2B, a new F(60) model was developed. This model takes into account the effect of the mixture macrotecture (predicted through  $\lambda$  and  $k$  parameters, obtained after fitting a Weibull distribution on the slab aggregate gradation), the blended DFT20 of the aggregate ring sample, and the laboratory cycles of the TWPD test. Later, the information gathered from the field tests, including aggregate gradation, field DFT20, and field MPD, were used to predict the field F(60). Finally, the results of the prediction model were compared with the actual F(60) field results in order to validate them.

## Discussion of Results

This section presents the results of various laboratory and field measurements conducted on the aggregates and asphalt mixtures. The laboratory results from two polishing stone tests performed using a British Wheel Polisher (BWP) and a Three-Wheel Polisher Device (TWPD) are discussed first, focusing on the seven coarse aggregates included in this study. Following this, field friction measurement results are provided for eight selected asphalt pavement sections, obtained using in-situ devices such as the LWST, BPT, DFT, and CTM. Correlations among the different field friction measurement devices and the measured properties are also developed. Finally, the lab and field friction measurement results are utilized to create a friction prediction model for F(60), which accounts for the effects of both microtexture and macrotexture on mixture friction resistance during the asphalt mixture design phase.

### Results from BWP Polishing Tests

As outlined in the previous section, the current DOTD polishing stone test adheres to the procedures specified in AASHTO T278 and T279. These include sample preparation, polishing using a British Wheel Polisher (BWP), and friction measurements using a British Pendulum Tester (BPT) device. In this project, duplicate aggregate samples, each consisting of seven aggregate coupons, were prepared and polished for each of the eight selected aggregate materials.

#### BPT Results

The average results of the BWP polishing stone test for the seven aggregates, both before and after polishing, are summarized in Table 8 and Figure 10. The BPT-measured number (BPN) prior to polishing represents the aggregate's initial skid resistance, or initial surface roughness, while the BPN value after polishing with the BWP is referred to as the Polished Stone Value (PSV). The measured PSV values are currently utilized by DOTD to evaluate the friction rating of aggregates, as shown in Table 8.

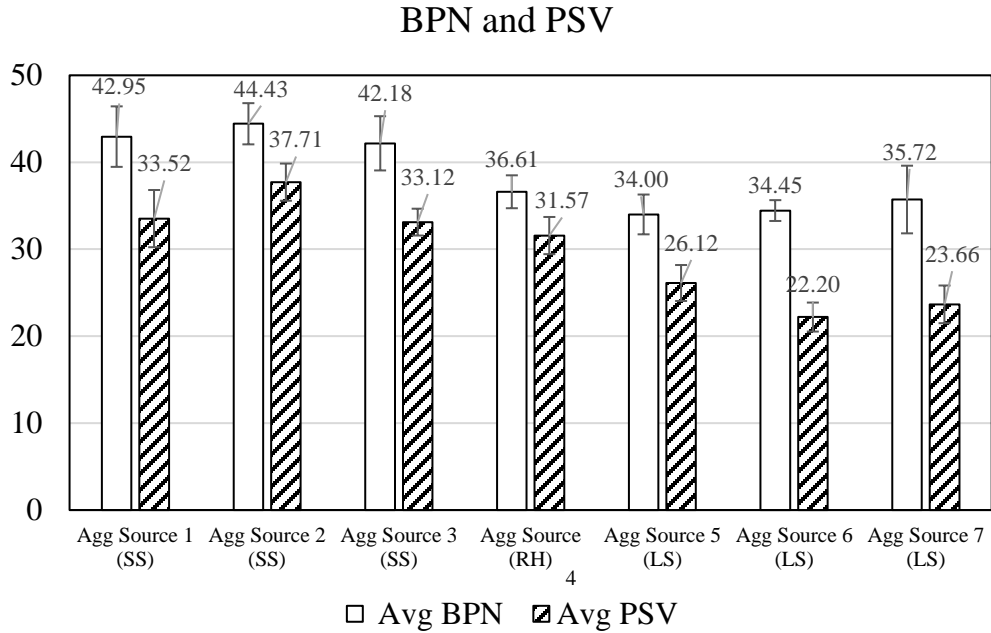
The results indicate that the average BPN (British Pendulum Number) values before polishing ranged from 33.4 to 44.4, while the average PSV (Polished Stone Value) values after polishing ranged from 22.0 to 37.8. As expected, the results confirm that sandstones demonstrated higher initial skid resistance and greater polishing resistance compared to limestones. The overall average standard deviation for the unpolished BPN values of the seven aggregates was 1.48,

and for the polished PSV values, it was 0.83. According to polishing stone test standards, the acceptable standard deviation limit for BPN measurements is 1.0 [56]. This indicates that the majority of the BWP test results in this study exceed the specified standard deviation limit, suggesting potential variability in the test measurements, primarily attributed to inconsistencies in sample coupon preparation.

**Table 8. Initial and final BPN results from samples polished by BWP**

Aggregate	Sample	Unpolished BPNs				Polished BPNs (PSV)			
		BPN	AVE	STD	CV %	PSV	AVE	STD	CV %
<b>Agg Source 1 (SS)</b>	1	41.40	42.6	1.697	4.0	33.00	33.2	0.318	8.5
	2	43.80				33.45			
<b>Agg Source 2 (SS)</b>	1	44.40	44.4	1.517	3.4	37.80	37.8	1.924	5.1
	2	n/a				n/a			
<b>Agg Source 3 (SS)</b>	1	42.85	42.9	1.585	3.7	34.20	33.1	1.556	3.9
	2	n/a				32.00			
<b>Agg Source 4 (RH)</b>	1	37.40	37.0	0.636	1.7	32.60	31.7	1.273	5.3
	2	36.50				30.80			
<b>Agg Source 5 (LS)</b>	1	32.80	33.4	0.849	2.5	25.86	26.3	0.665	6.4
	2	34.00				26.80			
<b>Agg Source 6 (LS)</b>	1	34.80	34.3	0.778	2.3	22.00	22.0	0.071	8.5
	2	33.70				21.90			
<b>Agg Source 7 (LS)</b>	1	33.35	35.7	3.288	9.2	23.65	23.6	0.035	8.9
	2	38.00				23.60			
<b>Overall Average</b>			<b>38.6</b>	<b>1.48</b>	<b>4.0</b>		<b>29.7</b>	<b>0.83</b>	<b>2.1</b>

**Figure 10. Polishing stone test results**



According to the current friction rating table shown in Table 9, the obtained PSV results were used to evaluate the aggregate friction ratings (FR). The table also includes friction rating results from DOTD’s current Approved Materials List and previous BWP test results, conducted in 2020 for the same seven aggregates tested in this study.

Ideally, the friction rating for a specific aggregate should remain consistent across tests conducted at different times. However, as shown in Table 9, the FR ratings for the aggregates tested in this study (e.g., AGG SOURCE 1, AGG SOURCE 2, AGG SOURCE 3, AGG SOURCE 4, AGG SOURCE 5, AGG SOURCE 6, and AGG SOURCE 7) were found to be FR-III, I, III, III, III, IV, IV, and IV, respectively. These ratings differ significantly from the results obtained in the other two sets of tests. This discrepancy further underscores the potential variability in the BWP-measured PSV values, raising questions about the consistency and reliability of these measurements for friction rating evaluations.

**Table 9. Aggregate friction ratings of selected aggregates**

No.	Aggregate	Type	Aggregate Friction Rating (FR)		
			AML Results	Results in 2020	Results from this study
1	Agg Source 1	Sandstone	FR I (PSV>37)	FR III (PSV=31)	FR III (PSV=33.2)
2	Agg Source 2	Sandstone	FR I (PSV>37)	FR I (PSV=39.1)	FR I (PSV=37.8)
3	Agg Source 3	Sandstone	FR I (PSV>37)	FR III (PSV=34.7)	FR III (PSV=33.1)
4	Agg Source 4	Rhyolite	FR II (35<PSV<37)	FR II (PSV=36.1)	FR III (PSV=31.7)
5	Agg Source 5	Silicious Limestone	FR III (30<PSV<34)	FR III (PSV=30.5)	FR IV (PSV=26.3)
6	Agg Source 6	Silicious Limestone	FR III (30<PSV<34)	FR IV (PSV=25)	FR IV (PSV=22)
7	Agg Source 7	Silicious Limestone	FR III (30<PSV<34)	FR IV (PSV=25.8)	FR IV (PSV=23.6)

**Evaluation of PSV-Based DOTD Aggregate Friction Rating Table**

**BWP Polishing Test Variation Assessment**

The variations in the BWP polishing test may arise from differences in coarse aggregate sources, sample coupon preparation, testing equipment, and operator handling. Among these factors, the primary contributors to variability are likely the coarse aggregate sources and the sample coupon preparation process during the test. In this project, duplicate testing samples, each consisting of seven aggregate coupons, were prepared using materials from the same sources for the seven aggregates evaluated.

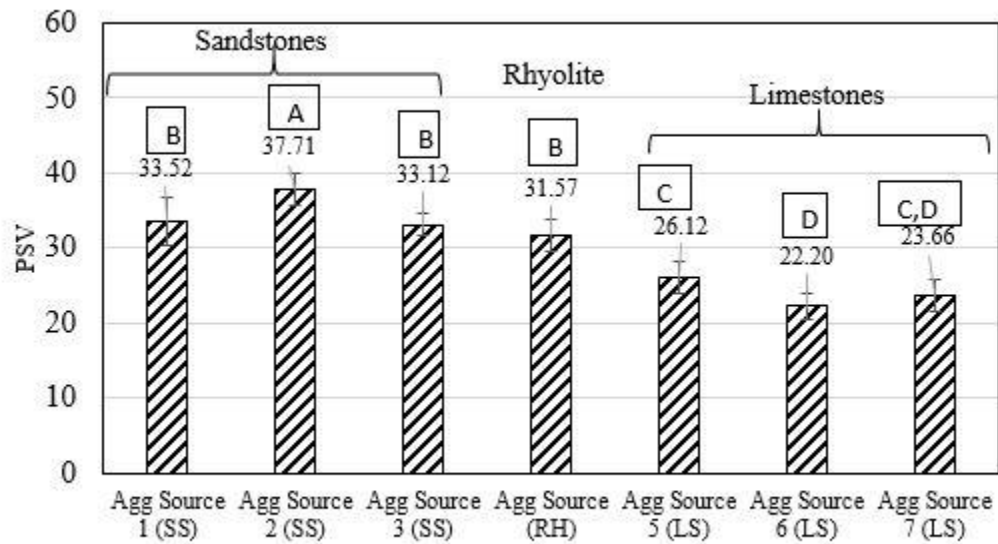
Table 10 presents the standard deviations of the Polished Stone Value (PSV) results for individual duplicate testing samples. As the table shows, the standard deviations of PSV values for the seven polished coupons ranged from 0.815 to 2.887, with an overall average of 2.058. This high variability in PSV results among duplicate samples can influence the aggregate friction rating, potentially shifting it from one level to another (e.g., from Level I to Level II), primarily due to inconsistencies in sample coupon preparation.

**Table 10. Standard deviations of PSV results**

Aggregates	Duplicate Sample 1		Duplicate Sample 2	
	Average PSV	STD	Average PSV	STD
Agg Source 1	33.00	2.887	33.18	2.749
Agg Source 2	37.71	2.138	n/a	n/a
Agg Source 3	33.86	2.116	32.11	0.815
Agg Source 4	32.43	2.225	30.71	1.799
Agg Source 5	25.83	2.106	26.50	2.074
Agg Source 6	22.14	2.116	22.25	1.242
Agg Source 7	23.75	2.441	23.57	2.050
<b>Overall Average Standard Deviation (STD)</b>			<b>2.058</b>	

Figure 11 illustrates the rankings of the seven aggregates based on their average PSV results. When comparing the rankings in Figure 11 to the corresponding friction ratings of the seven aggregates listed in Table 9, several differences are apparent. These discrepancies suggest that the PSV threshold values used in DOTD’s friction rating table may require re-evaluation and re-verification to ensure consistency and accuracy in assessing aggregate polishing resistance.

**Figure 11. PSV ranking**



## Aggregate Source Shipment Variation

Due to significant variations in aggregate production and shipments, different PSV test results are often observed for aggregates sourced from the same quarry but shipped at different times. In June 2021, DOTD’s Materials Laboratory (MATLAB) performed the polishing stone test on 42 different aggregate sources and rated them accordingly. The resulting PSV values were then used to evaluate the friction ratings of the tested aggregates and compare them to their existing friction ratings (FR). Table 11 summarizes the comparison of friction ratings from this study. Furthermore, Table 11 indicates the following key findings:

1. A significant portion of the tested aggregates (20 out of 42, or approximately 47.6%) exhibited decreases in their friction ratings based on the PSV results.
2. The majority of these decreases occurred in aggregate groups that were previously rated as FR I, II, and III.
3. Notably, only one tested aggregate (#41) showed an improvement in friction rating, moving from FR IV to FR III.

These results highlight the variability in PSV test outcomes, which may be attributed to differences in the source material due to aggregate production processes and shipment timing. Such findings underscore the need for further investigation into the factors influencing PSV test consistency and the impact of aggregate production variations on friction ratings.

**Table 11. Comparison of aggregate friction rating**

Aggregate No	APS Code	Aggregate Type	Ex. FR Value	Recent. FR Value	FR Changes
1	APS00006750	Granite	I	IV	-3
2	APS00007520	Sandstone	I	III	-2
3	APS00006370	Sandstone	I	I	0
4	APS00006560	Sandstone	I	I	0
5	APS00006760	Sandstone	I	III	-2
6	APS00006880	Sandstone	I	III	-2
7	APS00006250	Granite	II	IV	-2
8	APS00006710	Rhyolite	II	II	0
9	APS00006080	Sandstone	II	III	-1
10	APS00006730	Sandstone	II	III	-1
11	APS00007380	Siliceous Limestone	II	IV	-2
12	APS00007480	Siliceous Limestone	II	IV	-2
13	APS00006740	Granite	III	IV	-1
14	APS00005770	Limestone	III	IV	-1

Aggregate No	APS Code	Aggregate Type	Ex. FR Value	Recent. FR Value	FR Changes
15	APS00007180	Limestone	III	IV	-1
16	APS00007350	Limestone	III	IV	-1
17	APS00007190	Limestone	III	IV	-1
18	APS00006690	Limestone (Porous)	III	IV	-1
19	APS00006820	Siliceous Limestone	III	III	0
20	APS00006570	Siliceous Limestone	III	IV	-1
21	APS00011870	Siliceous Limestone	III	IV	-1
22	APS00012880	Siliceous Limestone	III	III	0
23	APS00006580	Siliceous Limestone	III	IV	-1
24	APS00006890	Siliceous Limestone	III	IV	-1
25	APS00011620	Granite	IV	IV	0
26	APS00012300	Granite	IV	IV	0
27	APS00005710	Limestone	IV	IV	0
28	APS00011430	Limestone	IV	IV	0
29	APS00006340	Limestone	IV	IV	0
30	APS00012600	Limestone	IV	IV	0
31	APS00005970	Limestone	IV	IV	0
32	APS00014110	Limestone	IV	IV	0
33	APS00007160	Limestone	IV	IV	0
34	APS00012130	Limestone	IV	IV	0
35	APS00007260	Limestone	IV	IV	0
36	APS00007340	Limestone	IV	IV	0
37	APS00007390	Limestone	IV	IV	0
38	APS00007430	Limestone	IV	IV	0
39	APS00012680	Limestone	IV	IV	0
40	APS00007500	Siliceous Limestone	IV	IV	0
41	APS00005960	Siliceous Limestone	IV	III	1
42	APS00012320	Siliceous Limestone	IV	IV	0

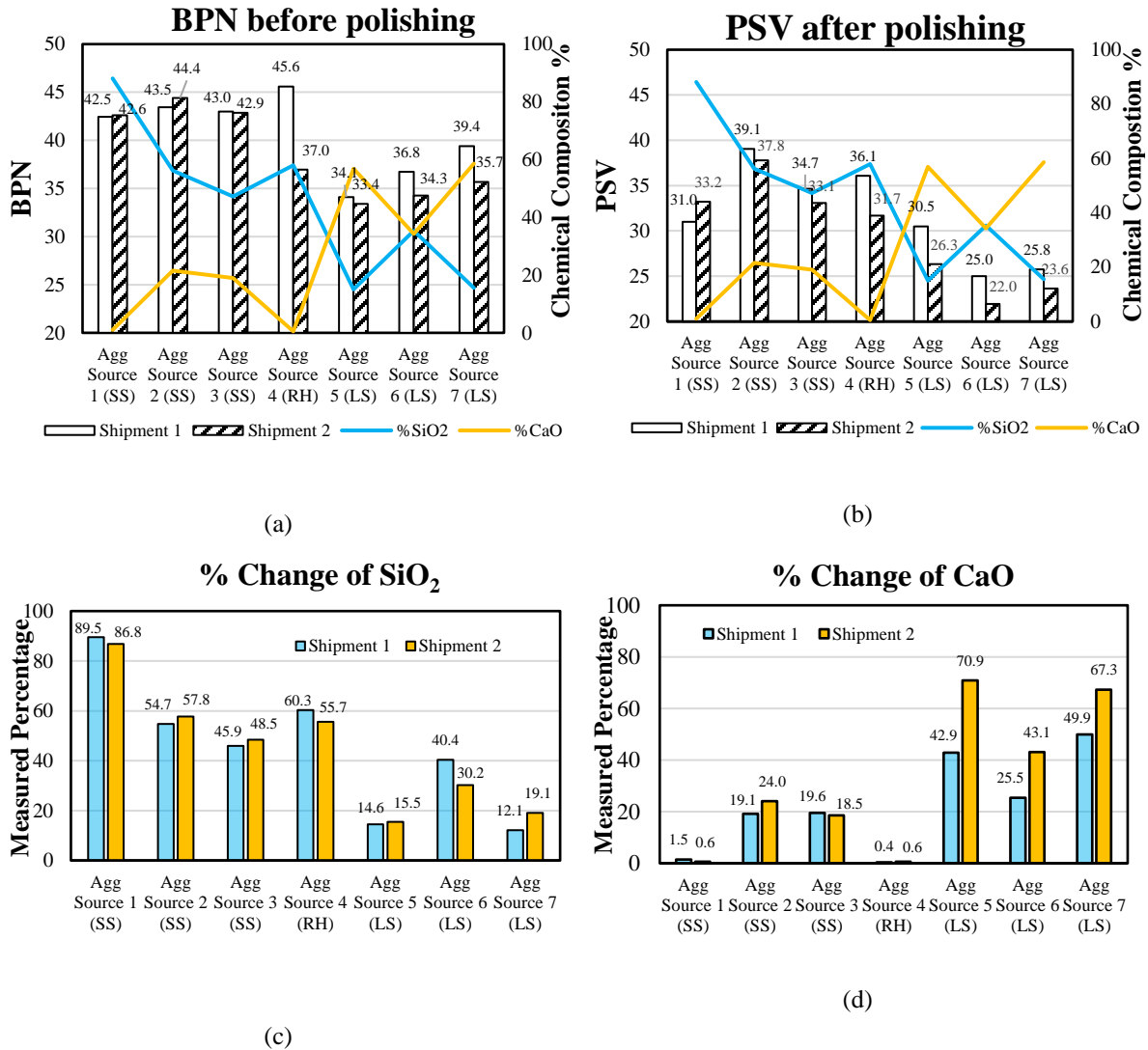
### Chemical Composition Variation

It is known that the petrological and morphological properties of aggregates significantly influence their hardness and overall polishing resistance. Even at the same quarry location, the chemical composition of aggregates may vary depending on the time and the specific area from which the material is mined and processed. This indicates that an aggregate material obtained from the same quarry but produced at different times may contain different chemical compositions, which can lead to different polishing resistance results from the PSV test.

Figure 12 illustrates the BWP test results for seven aggregates obtained from two different shipments, along with the variations in the chemical compositions of Silicon Dioxide (SiO<sub>2</sub>) and Calcium Oxide (CaO). The test results for Shipment 1 were taken from a previous study, while those for Shipment 2 were obtained in the current project.

As shown in Figure 12, there is a general trend indicating that higher SiO<sub>2</sub> content is associated with higher BPN and PSV values, suggesting better polishing resistance. Conversely, higher CaO content tends to correspond to lower aggregate polishing resistance values. While no single physical property shows a direct correlation with friction performance, the chemical composition properties collectively act as indicators of changes in PSV results, providing valuable insights into the variability of aggregate polishing resistance.

Figure 12. Variations of BWP test results due to shipments



## Results from Three-Wheel Polishing Tests

The three-wheel polishing test results in this study evaluated the frictional performance of seven selected coarse aggregates, as shown in Table 4, using the AASHTO PP103 testing method and a specialized three-wheel polisher device (TWPD), as shown in Figure 4. The micro- and macro-surface textures of the aggregate ring samples were assessed using DFT and CTM devices both before and after polishing. The following section provides a detailed analysis of these test measurement results. Furthermore, based on the statistical analysis of the obtained aggregate polishing resistance measurements, a new aggregate friction rating table was proposed for aggregate polishing resistance certification by DOTD.

### DFT20 Results—Aggregate Polishing Resistance

According to AASHTO PP103 [53], the DFT measurement at 20 km/hr (DFT20) is deemed as the indicator for the microtexture of tested aggregate's friction value during polishing. Table 12 presents the results at the unpolished (i.e., 0 polishing cycles) and polished state (i.e., 100,000 polishing cycles), while Figure 13 presents the DFT20 results for the different aggregates at 0, 50,000, and 100,000 polishing cycles per sample duplicate.

The DFT20 results, as shown in Figure 13, displayed a decay trend as the polishing cycles increased. The curve was the steepest between 0 and 50,000 polishing cycles, displaying an initial higher rate of polishing, which tends to slow down from 50,000 to 100,000 polishing cycles. Furthermore, it is relevant to add that the sandstones and the rhyolite exhibited superior performance at all stages compared to the limestones.

As shown in Figure 13, the DFT20 results at 0 polishing cycles yielded the highest results for sandstones. These results are indicators that the skid resistance potential of sandstones is higher than that of limestones. Furthermore, Figure 14 presents the average DFT20 results of the different aggregate ring samples as bar graphs at 0, 50,000, and 100,000 polishing cycles. Moreover, the percentage reduction of the average DFT20 is also presented in this figure on the second axis of the graph. This percentage DFT20 reduction results show that the polishing resistance of sandstones was lower than that of limestones. This finding was consistent with the findings of the BWP procedure. Nevertheless, it is important to clarify that within individual stone types, the ranking (i.e., the order of best friction-performing stone to worst) of the aggregates differed between the two procedures (i.e., TWPD with DFT20 and BWP with BPT).

According to the DFT20 ranking, AGG SOURCE 1 was the best-performing aggregate in terms of both skid resistance potential and polishing resistance, while AGG SOURCE 2 was considered the best by the PSV ranking. Additionally, AGG SOURCE 6 was considered as the worst-performing aggregate as per PSV ranking. On the other hand, AGG SOURCE 7 was deemed as the worst by the DFT20 ranking. Furthermore, the absolute loss in DFT20 values was higher for the sandstones (0.135) in comparison with the limestones (0.087). This result contrasted with those displayed by the BWP results.

**Table 12. Initial and final microtexture results from samples polished by TWPD**

Aggregate	Sample	Unpolished Samples				Polished Samples			
		DFT20	Avg	Std	CV %	DFT20	Avg	Std	CV %
Agg Source 7	1	0.310	0.299	0.013	4.5	0.220	0.231	0.010	4.5
	2	0.288				0.243			
Agg Source 2	1	0.603	0.590	0.021	3.6	0.455	0.435	0.016	3.7
	2	0.578				0.415			
Agg Source 3	1	0.550	0.559	0.024	4.3	0.423	0.430	0.011	2.6
	2	0.568				0.438			
Agg Source 6	1	0.388	0.371	0.014	3.6	0.268	0.270	0.005	1.9
	2	0.355				0.273			
Agg Source 1	1	0.625	0.628	0.010	1.6	0.525	0.508	0.017	3.4
	2	0.630				0.490			
Agg Source 4	1	0.548	0.523	0.019	3.6	0.473	0.456	0.009	1.9
	2	0.498				0.440			
Agg Source 5	1	0.390	0.418	0.014	3.5	0.335	0.325	0.013	3.9
	2	0.445				0.315			

Figure 13. Average DFT20 results per aggregate type

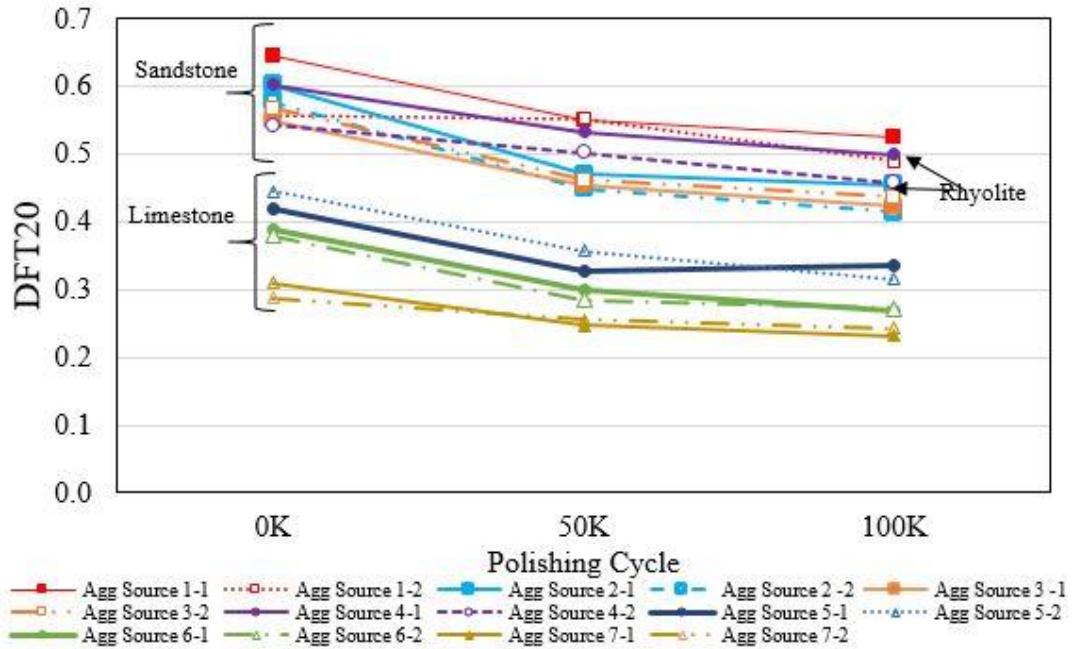
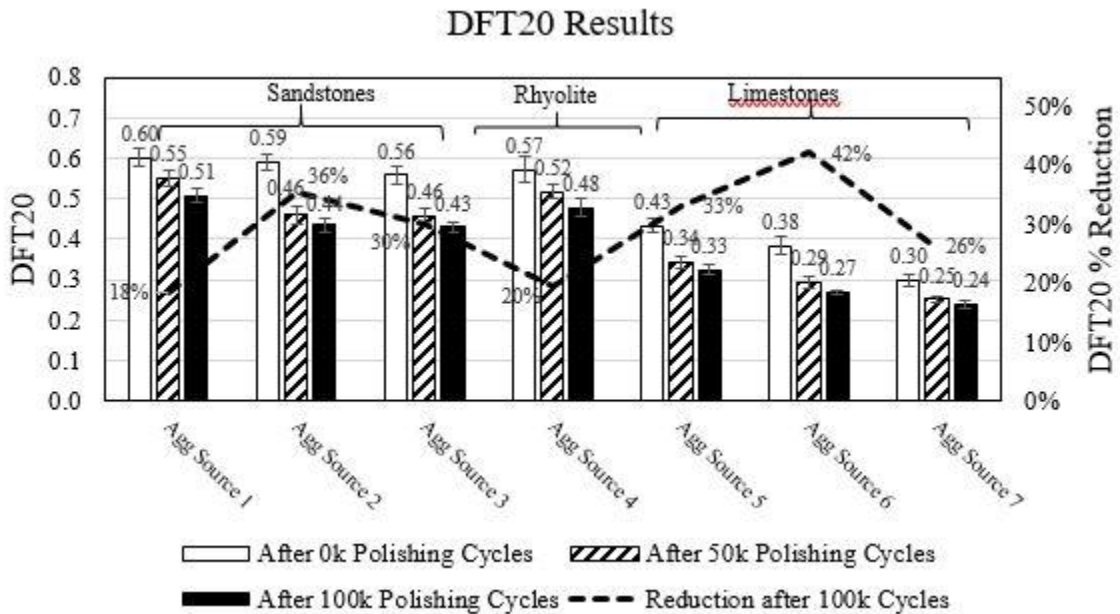


Figure 14. Average DFT20 results per aggregate type along with reduction percentage



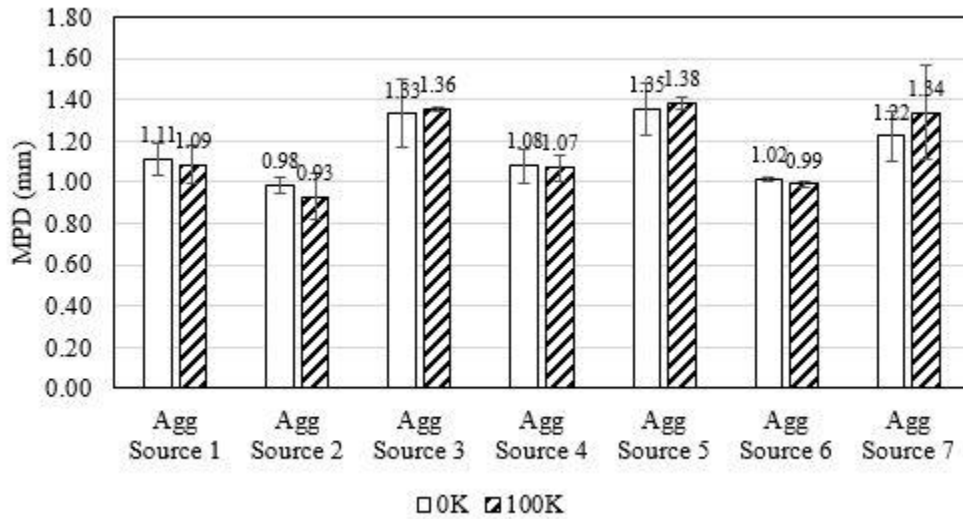
## Aggregate Macrotexture Results

The aggregate macrotexture of the ring sample was measured at the unpolished and polished stages, with the assistance of a circular texture meter (CTM) device, as shown in Table 13. As shown in Figure 15, the average macrotexture, presented in terms of mean profile depth (MPD), is slightly different among the aggregate types, with an overall average of 1.12 mm and a standard deviation of 0.25 mm. It is important to add that although similar-sized aggregates were used during the fabrication of the ring samples, the surface macrotexture varied based on the sample preparation. This indicates the presence of a difference in the macrotexture despite the uniform aggregate size. Furthermore, Figure 15 does not show a particular trend of increment or decrement in the macrotexture results. Only minimal changes were observed before and after polishing by the TWPD. Additionally, some samples developed cracks while being subjected to TWPD testing, which can contribute to higher surface roughness, leading to higher MPD values.

**Table 13. Initial and final macrotexture results of samples polished by TWPD**

Aggregate	Sample	Unpolished Samples				Polished Samples			
		MPD (mm)	Avg	Std	CV %	MPD (mm)	Avg	Std	CV %
Agg Source 7	1	1.313	1.224	0.087	7.1	1.500	1.339	0.061	4.5
	2	1.135				1.178			
Agg Source 2	1	1.010	0.983	0.096	9.8	1.008	0.931	0.034	3.7
	2	0.955				0.855			
Agg Source 3	1	1.448	1.331	0.167	12.5	1.350	1.355	0.064	4.7
	2	1.215				1.360			
Agg Source 6	1	1.008	1.015	0.030	3.0	1.003	0.990	0.043	4.4
	2	1.023				0.978			
Agg Source 1	1	1.168	1.114	0.073	6.5	1.150	1.086	0.068	6.2
	2	1.060				1.023			
Agg Source 4	1	1.140	1.080	0.037	3.4	1.115	1.070	0.060	5.6
	2	1.020				1.025			
Agg Source 5	1	1.443	1.353	0.036	2.6	1.420	1.393	0.104	7.5
	2	1.263				1.365			

Figure 15. MPD of polished and unpolished samples



### Adjustment for Macrotexture

A t-test was conducted on MPD results. The results from this test indicated that statistically significant differences in MPD were related to statistically significant differences in DFT20. This finding indicates that MPD can be used as a surrogate for aggregate ring sample variation. Figure 16 displays the direct relationship between the change in DFT20 based on the MPD variation. Based on this data, an adjustment factor was developed. Through regression analysis, an adjusted  $\Delta DFT20$  equation was found and is shown as Equation 21. This adjustment was performed on the tested aggregates, which is shown in Table 14.

$$\Delta DFT20 = 0.2 * \Delta MPD + 0.01 \quad (21)$$

Where,

$\Delta DFT20$ : Change in DFT20 measurements, and

$\Delta MPD$ : Change in MPD (mm).

**Figure 16.  $\Delta$ DFT20 vs  $\Delta$ MPD prediction**

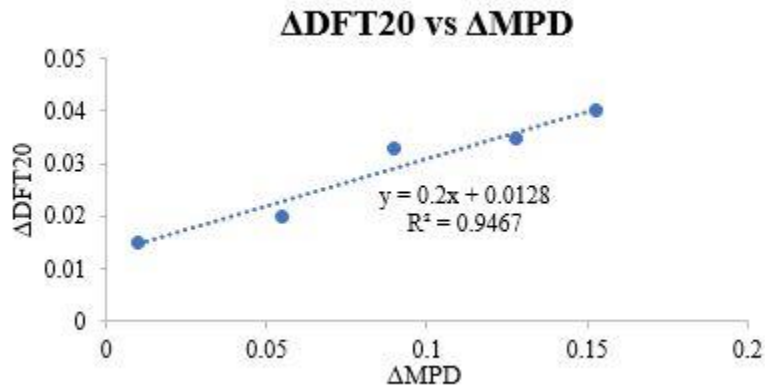


**Table 14. Adjusted DFT20 values**

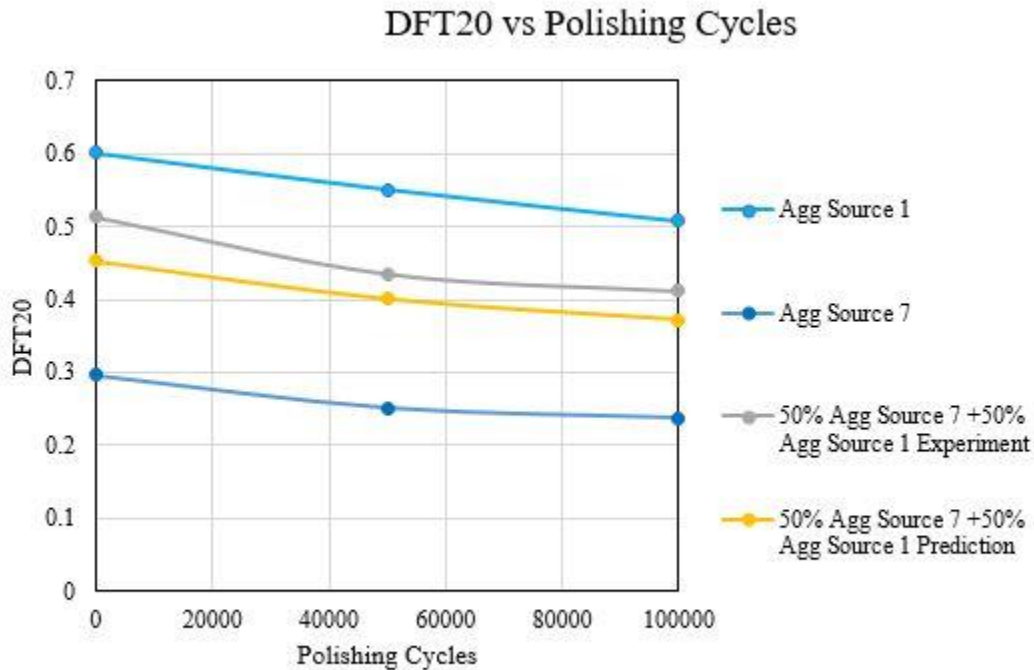
Aggregates	Average DFT20	Adj. DFT20
Agg Source 2	0.435	0.453
Agg Source 1	0.508	0.523
Agg Source 3	0.431	0.436
Agg Source 4	0.457	0.469
Agg Source 5	0.325	0.335
Agg Source 7	0.232	0.264
Agg Source 6	0.271	0.278

### **Blended DFT20 Results**

As shown in Table 6, the majority of the field projects have more than one aggregate in their wearing course. In order to account for this situation, the three-wheel polishing test and DFT20 analysis were conducted on a blended aggregate ring sample. For this sample, the aggregates utilized were AGG SOURCE 1 and AGG SOURCE 7, which were the aggregates with the best and worst friction performance to this point. The blend was conducted utilizing 50% by weight

of each aggregate. The purpose of this test was to determine if applying a percentage of each aggregate would have the same effect on its overall DFT20. Figure 17 presents both the results of the prediction and the experiment. From this analysis, it was found that the results from both the prediction and the experiment are very proximate to one another. Note that the slight DFT20 differences may be attributed to the individual aggregate selection variations during a ring sample preparation. Therefore, it is safe to expect that the combined percentage of each aggregate will have the same effect on its combined DFT20. This assumption is similar to the one in a previous study by Ashby regarding different aggregates of PSV combinations [55].

**Figure 17. Blended DFT20 vs polishing cycles**



### Difference Based on Repeatability

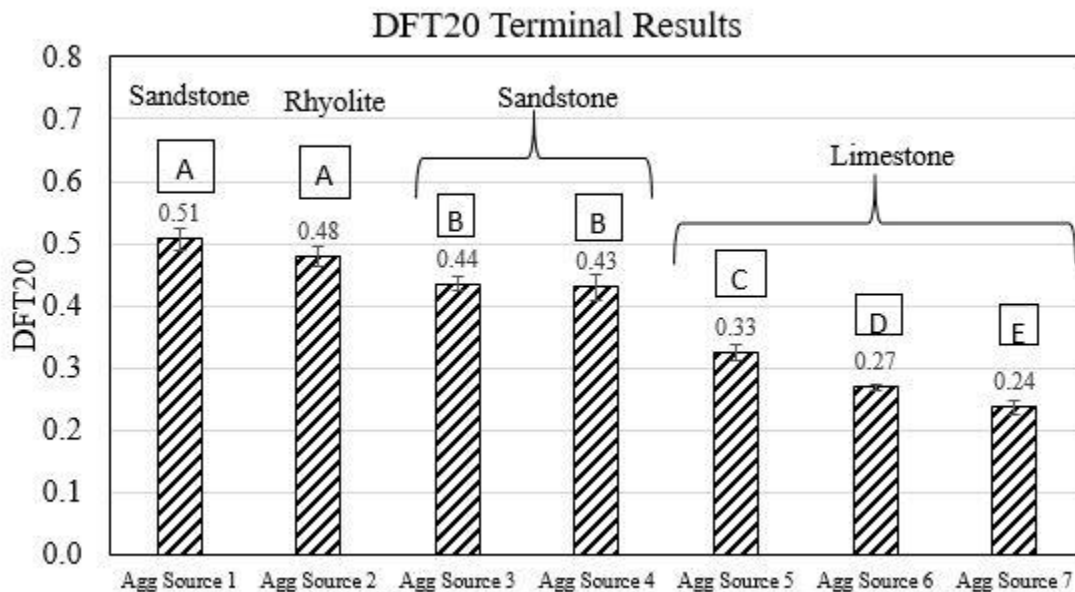
The DFT20 values at both the unpolished and polished stages between the duplicate samples were below the ASTM E1911's allowable standard deviation of 0.03 for DFT20 measurements for every aggregate ring sample. In fact, the average standard deviation for every test was 0.021 at 0 polishing cycles, 0.015 at 50,000 polishing cycles, and 0.013 at 100,000 polishing cycles. By contrast, the standard deviation from the BPT test procedure was not beyond the standard

deviation limit established for this kind of test. [57]. This is another finding that implies that DFT20 is a superior microtexture measurement indicator compared to the BPT.

### Difference Based on Aggregate

A post hoc Tukey test at an  $\alpha$  level of 0.05 was conducted per aggregate type with the purpose of determining which aggregate types are similar to one another. Figure 18 shows the different DFT20 terminal results by aggregate type. Furthermore, aggregates sharing the same letters on the graph are not statistically different. According to this test, AGG SOURCE 1 has the highest terminal friction results and is statistically superior to the rest of the samples, with the exception of AGG SOURCE 4. By contrast, AGG SOURCE 2 and AGG SOURCE 3 are not statistically different since they share letter B. Moreover, AGG SOURCE 5, AGG SOURCE 6, and AGG SOURCE 7, which were all limestones, were statistically different.

Figure 18. DFT20 Results per aggregate type



### Difference Based on DFT Device Speed

30 measurements were taken from the DFT device at different speeds (i.e., 20, 40, and 60 km/hr) on a single aggregate ring sample without any rotation; see Table 29 in Appendix B. A single-factor ANOVA was conducted on the DFT20, DFT40, and DFT60 results, as shown in Table 15. The result from the ANOVA analysis (P value < 0.05) rejects the null hypothesis in

favor of the alternative hypothesis. This analysis indicates that measurements taken by this device at different speeds do not yield statistically similar results when used at different speeds, and they must be used with care. Furthermore, previous research has shown that DFT60 can be used as a surrogate for a combination of macrotexture and microtexture. By contrast, DFT20 is only a surrogate for microtexture.

*Null Hypothesis:*

*Ho : The DFT results at different speeds are not statistically different from one another.*

*Alternative Hypothesis:*

*H1 : The DFT results at different speeds are statistically different from one another.*

**Table 15. DFT at different test speeds**

Groups	Count	Sum	Average	Variance	
DFT60	30	13.24	0.441	0.0001	
DFT40	30	13.76	0.459	0.0001	
DFT20	30	14.02	0.467	0.0002	
Source of Variation	SS	df	MS	F	P-value
Between Groups	0.0105	2	0.0053	37.8664	<0.001
Within Groups	0.0121	87	0.0001		
<b>Total</b>	0.0226	89			

### **Difference Based on 90° Rotation**

The next step in the analysis was to determine if the DFT20 displayed a substantial difference if 90° degree rotations occurred. For this purpose, three out of the seven studied aggregates were utilized (e.g., AGG SOURCE 1, AGG SOURCE 4, AGG SOURCE 5) and tested at speeds of 20, 40, and 60 km/hr. Furthermore, a Tukey HSD test at a confidence level of 0.05 was performed at each speed at 90° rotations (i.e., 0°, 90°, 180°, 270°) on the selected aggregate ring sample surfaces. This analysis indicated that there was no statistical difference among the samples for every 90° rotation and speed group. The corresponding graphs for this analysis can be found in Figure 41 in Appendix B. Figure 41 displays the DFT results at different rotation angles and different speeds. Since no Tukey letters are presented, no significant difference between each rotation at different speeds (i.e., 20, 40, and 60 km/hr) was found.

### **Difference Based on Sample Duplicate**

The next step in the project was to determine if the aggregate ring sample duplicates had an effect on the DFT results at different speeds. For this purpose, two different samples were studied per sample at three different speed groups (i.e., 20, 40 and 60 km/hr). It is important to note that this analysis was conducted at zero polishing cycles to minimize the effect of the aggregate polishing rate. Figure 42 in Appendix B presents the DFT20 results considering both the sample effect and 90° rotation. A Tukey HSD test at a confidence level of 0.05 was conducted on these data. No statistical difference was found for the DFT results of the different aggregates at a speed of 20 km/hr. Furthermore, a Tukey HSD test was conducted for the DFT results at 40 km/hr, as shown in Figure 43 in Appendix B. The DFT results among each sample revealed that there was no statistical difference within each sample, except for sample AGG SOURCE 4, which contains the Tukey letters on the graph. Finally, Figure 44 in Appendix B presents the DFT60 results of the different aggregate ring samples. A Tukey HSD test was also conducted at this speed, and it was found that two samples (e.g., AGG SOURCE 1 and AGG SOURCE 4) showed significant statistical differences. From the overall analysis at different speeds, it was concluded that only DFT20 did not display any type of statistical difference, including variations due to the sample effect and 90° rotation.

### **Difference Based on Operator**

The effect of the operator was also studied. For this purpose, different samples were made at different times and tested by a different operator. The samples that were remade and tested were AGG SOURCE 6, AGG SOURCE 4, AGG SOURCE 1, and AGG SOURCE 5. Figure 45 in Appendix B presents the corresponding results for the DFT measurements at different speed groups (i.e., 20, 40, and 60 km/hr). A Tukey HSD test at an  $\alpha$  level of 0.05 was performed for each DFT measurement of each aggregate. This analysis showed that there was no statistical difference among the different measurements, considering a different sample and different operator, for all the tested aggregates except AGG SOURCE 1. Nevertheless, no statistical difference was found for the DFT20 value of the AGG SOURCE 1 samples. There was only a difference in the results at 40 and 60 km/hr. This finding is relevant since it shows that the DFT20 value is reliable, even when considering the difference in operator.

### **Effects of Chemical Composition on Microtexture**

The general trend was observed, indicating that sandstones had a higher percentage of SiO<sub>2</sub> and a lower percentage of CaO, while limestones had a higher percentage of CaO and a low

percentage of CaO. AGG SOURCE 1 displayed the highest percentage of SiO<sub>2</sub> and showed the best skid resistance and polishing potential. Nevertheless, the BPT results did not show this behavior. In general, the outcomes from the BPT and the TWPD displayed variations in performance order. Based on the DFT20 measurements, AGG SOURCE 1 was the best friction-performing aggregate with the highest DFT20 value at 100,000 cycles of polishing, followed by rhyolite AGG SOURCE 4 and the rest of the sandstones, AGG SOURCE 2 and AGG SOURCE 3.

This DFT20 results sequence is directly correlated with high SiO<sub>2</sub> and low CaO content. According to Xu et al., SiO<sub>2</sub> enhances the friction performance of the different composites since the mechanical properties act primarily on the asperities of the SiO<sub>2</sub> particles [58]. Therefore, the friction resistance force is highly determined by the strength of the SiO<sub>2</sub> particles present in the component. Moreover, a previous study has shown that a high percentage of calcium particles can generate a large aggregate loss under abrasion. This situation explains why the aggregates with more CaO tend to wear off more during polishing [59]. The only aggregate that did not follow the chemical trend in this study was AGG SOURCE 5; this was due to the fact that it had the largest MgO content. Previous research has proven that MgO contributes to the reduction of the friction wear rate of the materials [60]. Furthermore, the BPT results display a different ranking within the same group of sandstones, indicating a less direct correlation with their chemical composition. This analysis also shows that the DFT20, in combination with TWPD, is a more reliable test procedure than the BPT in combination with BWP.

### **DFT20 Polishing Rate**

The polishing rate for each tested aggregate was determined by implementing the general decay model, as presented in a previous study [54].

$$DFT_{20} = a + b * e^{(-c*N)} \quad (19)$$

Where,

a,b,c are regression coefficients, “a” representing terminal DFT20, “a+b” representing initial DFT20, and “c” representing the polishing rate; and N is the number of polishing cycles.

The different aggregate DFT20 values are presented in Figure 13, and the decay model was applied to them in order to obtain a regression equation per aggregate type. Table 16 presents the corresponding coefficients and R<sup>2</sup>.

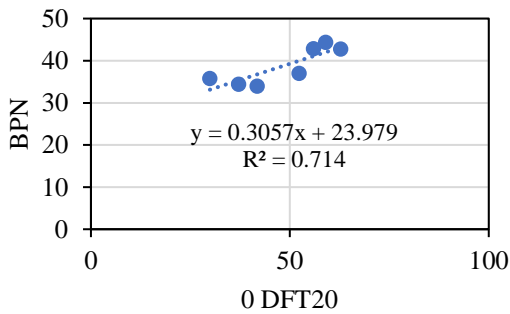
**Table 16. Regression coefficients per aggregate type**

Aggregate	a	b	c	R <sup>2</sup>
Agg Source 7	0.2375	0.05875	2.90*10 <sup>-05</sup>	1
Agg Source 2	0.435	0.155	3.65*10 <sup>-05</sup>	1
Agg Source 3	0.43	0.12875	3.00*10 <sup>-05</sup>	1
Agg Source 6	0.27	0.11375	3.24*10 <sup>-05</sup>	1
Agg Source 1	0.5075	0.09375	1.52*10 <sup>-05</sup>	1
Agg Source 4	0.4787	0.0938	1.77*10 <sup>-05</sup>	1
Agg Source 5	0.325	0.1075	3.63*10 <sup>-05</sup>	1

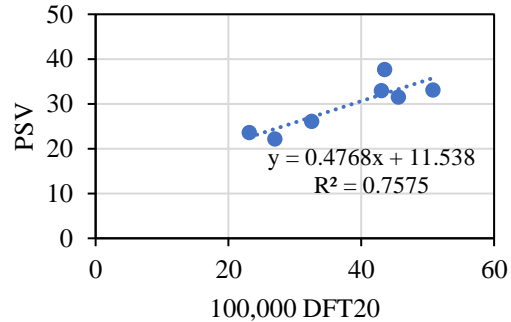
### Comparison Between TWPT and BWT Aggregate Polishing Results

Figure 19 illustrates the relationship between BPN and DFT20 (x100) for the seven aggregate sources both before and after polishing. The correlation between BPN and initial DFT measurements ( $R^2 = 0.71$ ) and between PSV and final DFT measurements ( $R^2 = 0.76$ ) indicates a moderate level of agreement. While both devices provide reasonably consistent microtexture readings, discrepancies are evident.

**Figure 19. Relationship between BPN and DFT20**



(a) DFT20 vs BPN before polishing



(b) 100,000 DFT20 vs PSV

In this study, aggregate materials from the same shipment were used to prepare samples for both the BWT and TWPT, ensuring that no material variations due to shipment timing

influenced the results of the two polishing procedures. The observed discrepancies can be attributed to several factors:

1. Testing Sample Preparation: Differences between aggregate coupons (BWT) and ring samples (TWPT).
2. Polishing Processes: Variations between the BWT and TWPT devices.
3. Device Sensitivity: Differences in the sensitivity of the BPT and DFT measurement techniques.

A noticeable disparity was also observed in the ranking of aggregates when sorted by descending polishing resistance values (e.g., PSV from BWT and DFT20 @ 100,000 from TWPT), as shown in Table 17. This discrepancy indicates that the measured polishing resistance values obtained using the two methods do not align. The order, also referred to as sequence, was not the same between the rank based on PSV results and the rank based on DFT20 results. Similar differences were observed in the ranking based on initial BPN and DFT20 values before polishing, as shown in Table 18.

**Table 17. Ranking based on PSV vs polished DFT20**

	Rank based on PSV (BWP)	Rank Based on DFT20 (TWPD)
1	Agg Source 2	Agg Source 1
2	Agg Source 1	Agg Source 4
3	Agg Source 3	Agg Source 2
4	Agg Source 4	Agg Source 3
5	Agg Source 5	Agg Source 5
6	Agg Source 7	Agg Source 6
7	Agg Source 6	Agg Source 7

**Table 18. Ranking based on unpolished BPN vs unpolished DFT20**

	Rank based on unpolished BPN	Rank based on unpolished DFT20
1	Agg Source 2	Agg Source 1
2	Agg Source 3	Agg Source 2
3	Agg Source 1	Agg Source 4
4	Agg Source 4	Agg Source 3
5	Agg Source 7	Agg Source 5
6	Agg Source 6	Agg Source 6
7	Agg Source 5	Agg Source 7

As shown in Table 5, the AGG SOURCE 1 aggregate tested in this study has the highest proportion of silicon dioxide, a hard mineral. This suggests that AGG SOURCE 1 should exhibit greater microtexture and polishing resistance compared to AGG SOURCE 2. However, the BPN does not accurately reflect this. While factors such as slip speed, rubber slider properties, temperature of the sample, and surface texture may influence the measured values, the primary source of variation between the BWT and TWPT is likely due to differences in testing sample preparation procedures and the polishing devices used.

Key differences between the BWT and TWPT include:

1. The TWPT uses a pneumatic wheel, while BWT employs solid wheels with carbide grits.
2. The TWPT is a dry test, while the BWT is conducted as a wet test.
3. The TWPT can polish field-cored samples, while the BWT cannot.
4. The speed range of the TWPD-based procedure with the DFT device is 10-90 km/hr, while the BWT measurements (BPNs) are maintained at a constant speed of 10 km/hr.
5. The AASHTO PP103-based sample is compatible with both DFT and BPT measurements.
6. The DFT device sliders cover more area than the BPT, thus reducing localized effect.

As shown in Table 19, the TWPT/DFT test results of the seven aggregates cover a much wider range of values than BWT/BPT. For this reason, it is considered a better tool for evaluating the frictional properties of the aggregates.

**Table 19. Range of DFT20 @ 100,000 vs PSV values**

<b>Range of DFT20 Values</b>	<b>Agg Source 7</b>	<b>Agg Source 2</b>	<b>Agg Source 3</b>	<b>Agg Source 6</b>	<b>Agg Source 1</b>	<b>Agg Source 4</b>	<b>Agg Source 5</b>
Max Value	0.26	0.48	0.45	0.28	0.54	0.48	0.35
Min Value	0.21	0.4	0.41	0.26	0.47	0.43	0.31
<b>Range of PSV Values</b>	<b>Agg Source 7</b>	<b>Agg Source 2</b>	<b>Agg Source 3</b>	<b>Agg Source 6</b>	<b>Agg Source 1</b>	<b>Agg Source 4</b>	<b>Agg Source 5</b>
Max Value	27	40	36	25	36	35	30
Min Value	21	35	33	20	30	28	23

### **Proposed New Aggregate Friction Rating Table**

Based on the aforementioned observations, it is recommended that DOTD adopt the TWPD/DFT testing procedure for initial aggregate source friction rating evaluations. Considering there is a need to update the current PSV-based friction rating table, this report proposes a new aggregate friction rating table based on the TWPT/DFT20 @ 100,000 aggregate polishing results obtained.

In this project, a total of 41 aggregate ring samples were prepared and tested using two TWPD devices. The summarized results of the DFT20 @ 100,000 polishing cycle are presented in Table 20. A one-way ANOVA test, conducted at a significance level of 0.05, was used to evaluate whether there were statistical differences in polished DFT20 values among the various aggregates and ring samples. Upon identifying statistical differences, two classification methods were employed: confidence intervals ( $\alpha = 0.05$ ) and data range analysis.

**Table 20. Summary of DFT20 @ 100,000 polishing cycle results for all TWPD ring samples**

Ranking Based on 100,000 DFT20				95% confidence Intervals		Range	
Aggregate Ring No.	Ranking Letter	Mean	STD	Upper Bound	Lower Bound	Max	Min
1	A	0.548	0.017	0.562	0.535	0.570	0.520
2	A/B	0.548	0.021	0.568	0.527	0.570	0.530
3	A/B/C	0.530	0.013	0.540	0.520	0.540	0.510
4	A/B/C/D	0.525	0.013	0.538	0.512	0.540	0.510
5	B/C/D/E	0.510	0.014	0.521	0.499	0.530	0.490
6	C/D/E	0.507	0.021	0.523	0.490	0.530	0.480
7	C/D/E	0.507	0.021	0.523	0.490	0.530	0.480
8	C/D/E	0.507	0.021	0.523	0.490	0.530	0.480
9	C/D/E/F	0.500	0.014	0.514	0.486	0.510	0.480
10	D/E/F/G	0.490	0.022	0.511	0.469	0.520	0.470
11	E/F/G/H	0.478	0.011	0.488	0.468	0.490	0.460
12	F/G/H/I	0.460	0.016	0.474	0.446	0.480	0.440
13	F/G/H/I/J	0.458	0.028	0.484	0.431	0.490	0.430
14	G/H/I/J/K	0.455	0.019	0.474	0.436	0.480	0.440
15	H/I/J/K	0.450	0.014	0.461	0.439	0.470	0.430
16	I/J/K/L	0.438	0.010	0.447	0.428	0.450	0.430
17	I/J/K/L	0.430	0.012	0.441	0.419	0.440	0.420
18	I/J/K/L	0.427	0.023	0.445	0.409	0.470	0.410
19	I/J/K/L/M	0.423	0.013	0.435	0.410	0.440	0.410
20	K/L/M	0.416	0.011	0.426	0.406	0.430	0.400
21	J/K/L/M	0.415	0.013	0.428	0.402	0.430	0.400
22	K/L/M/N	0.413	0.010	0.422	0.403	0.420	0.400
23	K/L/M/N	0.413	0.010	0.422	0.403	0.420	0.400
24	L/M/N/O	0.410	0.014	0.424	0.396	0.420	0.390
25	L/M/N/O	0.410	0.014	0.424	0.396	0.420	0.390
26	M/N/O/P	0.388	0.008	0.396	0.380	0.400	0.380
27	N/O/P	0.375	0.012	0.385	0.365	0.390	0.360
28	N/O/P	0.375	0.012	0.385	0.365	0.390	0.360
29	O/P/Q	0.372	0.012	0.381	0.362	0.390	0.360
30	O/P/Q	0.372	0.021	0.389	0.355	0.410	0.350
31	P/Q	0.362	0.012	0.371	0.352	0.380	0.350
32	Q/R	0.335	0.019	0.354	0.316	0.350	0.310
33	Q/R	0.335	0.019	0.354	0.316	0.350	0.310
34	R/S	0.315	0.006	0.321	0.309	0.320	0.310
35	R/S	0.315	0.006	0.321	0.309	0.320	0.310
36	S/T	0.273	0.005	0.277	0.268	0.280	0.270
37	T	0.268	0.005	0.272	0.263	0.270	0.260
38	T	0.268	0.005	0.272	0.263	0.270	0.260
39	T	0.262	0.015	0.273	0.250	0.290	0.250
40	T	0.243	0.013	0.255	0.230	0.260	0.230
41	T	0.233	0.010	0.242	0.223	0.240	0.220
<b>Overall Polished DFT20 Average (and STD)</b>					<b>0.409 (0.014)</b>		
<b>Overall Polished DFT20 Range</b>					<b>0.220 - 0.570</b>		

As shown in Table 20, the overall average polished DFT20 measurement was determined to be 0.409, with values ranging from 0.22 to 0.57. The ranking order revealed significant differences among the DFT20 results of the various ring samples. Based on the ranking order, along with the calculated confidence intervals and ranges, four distinct DFT20 measurement groups were identified, as highlighted in Table 20. Based on the analysis of the previously presented results, two ranking systems based on polished DFT20 can be proposed, as shown in Table 21(a) and 21(b). These proposed ranking systems present four and five levels, respectively.

**Table 21. (a) First proposal and (b) second proposal for new aggregate friction rating based on DFT20**

(a)

Rating	Polished DFT20x100
I	> 49
II	40 – 49
III	30 – 40
IV	< 30

(b)

Rating	Polished DFT20
I	> 48
II	38 - 48
III	30 - 38
IV	26 - 29
V	< 26

The updated Friction Rating (FR) table has a wider range, spanning from 49 to 30, compared to the existing table, which ranges from 37 to 30. This expanded range increases the tolerance for individual friction rating groups, making the ranking more accommodating to variations in friction measurements. By allowing for a broader spectrum of values, the new table can better account for the inherent variability in friction characteristics across different samples. This adjustment helps ensure that the friction ratings are more robust and reliable, providing a more accurate reflection of the actual performance of the materials being assessed. Consequently, this leads to improved decision-making in selecting materials for use in applications where friction properties are critical. Finally, Table 22 presents the new friction rating for the aggregates tested in this research.

**Table 22. Aggregates rated based on the new DFT20 based rating system**

Aggregate	Rating
Agg Source 1	I
Agg Source 2	II
Agg Source 3	II
Agg Source 4	II
Agg Source 5	III
Agg Source 6	IV
Agg Source 7	IV

### Results from In-Situ Pavement Friction Measurements

Tables 23 and 24 present the average in-situ pavement friction measurement results for the eight pavement projects selected for this project. Specifically, Table 23 lists the DFT20 and CTM (MPD) field results, while Table 24 shows LWST (SN40R & SN40S) and laser profiler (MPD) field results. Furthermore, the selection of these test sites was based on the following considerations:

1. The field projects have the same aggregates that were tested in the lab, or at least some of the aggregates studied in the lab, on their constitutions.
2. The selected roads have different levels of traffic (i.e., different T.I.).
3. The selected projects were incorporated with the Project 12-5P results so that the previous relationships could be updated.

**Table 23. Field DFT and MPD results**

Mixture	Route	Age (Years)	ADT (Two ways)	#Test	DFT20		CTM (MPD)	
					Avg	C.V. (%)	Avg	C.V. (%)
Superpave (SP) 12.5 mm	LA1107	2	1100	3	0.53	9.21	0.39	3.37
	LA92	4	475	3	0.41	5.28	0.52	10.01
	US90	2	33100	3	0.44	1.17	0.58	7.94
	LA113	2	900	3	0.49	11.03	0.46	11.64
	LA 959	3	1400	3	0.46	2.69	0.57	3.80
	LA88	1	22750	3	0.40	1.3	0.45	2.42
Superpave 12.5 mm Range					0.41~0.53		0.39~0.58	

Mixture	Route	Age (Years)	ADT (Two ways)	#Test	DFT20		CTM (MPD)	
					Avg	C.V. (%)	Avg	C.V. (%)
SMA	LA 415	3	25370	3	0.44	1.51	0.79	11.71
OGFC	I-10	1	45800	3	0.37	4.83	1.33	7.77

**Table 24. LWST and Laser Profile test results**

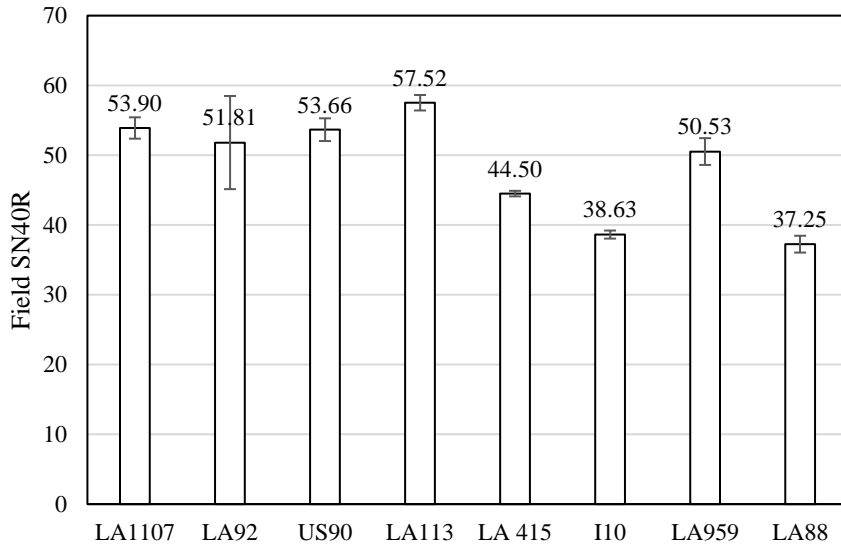
Mixture	Route	Age (Years)	ADT (two ways)	#Test	SN40R		SN40S		LASER PROFILER (MPD)	
					Avg	C.V. (%)	Avg	C.V. (%)	Avg	C.V. (%)
Superpave 12.5 mm	LA1107	2	1100	3	53.90	2.84	32.96	4.46	0.51	3.10
	LA92	4	475	3	51.81	12.88	40.52	1.53	0.63	7.36
	US90	2	33100	3	53.66	3.03	45.98	6.09	0.64	5.63
	LA113	2	900	3	57.52	1.93	45.36	13.29	0.59	2.61
	LA 959	3	1400	3	48.90	3.79	29.36	11.31	0.64	8.56
	LA88	1	22750	3	37.25	3.24	22.44	0.28	0.61	5.54
Superpave 12.5 mm Range					48.9 ~ 57.52		22.44 ~ 45.98		0.51 ~ 0.64	
SMA	LA 415	3	25370	3	44.50	0.89	35.42	10.10	0.73	9.58
OGFC	I-10	1	45800	3	38.63	1.50	39.83	0.38	1.20	2.85

### Lock Wheel Skid Trailer Test Results (LWST)

**SN40R Results.** Figure 20 displays the field results for SN40R. The roads that displayed the highest results for SN40R, which were primarily influenced by microtexture, were LA 113 and LA 1107. Furthermore, the roads with the lowest results were LA 415, I-10, and LA 88. Figure 20 shows that all of the roads built with 12.5 mm Superpave mixture outperformed those built with Stone Matrix Asphalt (SMA) mixture (e.g., LA 415) and Open Graded Friction Coarse (OGFC) mixture (e.g., I-10). LA 113 and LA 1107 were primarily composed of aggregate AGG SOURCE 6 and reclaimed asphalt pavement (RAP), which explains why they slightly outperformed LA 92, which was composed of AGG SOURCE 7. Furthermore, these three roads have a similar T.I., which demonstrates that under the same traffic conditions, the field microtexture of aggregate AGG SOURCE 6 is still superior to aggregate AGG SOURCE 7. These results are in accordance with the laboratory findings, which displayed the same behavior. On the other hand, US 90, LA 415, and I-10 underperformed the majority of the roads

with aggregates AGG SOURCE 6 and AGG SOURCE 7, although they had sandstones (i.e., AGG SOURCE 1 and AGG SOURCE 2) in their compositions. This result is explained by the fact that these roads were subjected to higher traffic conditions (i.e., higher T.I.); therefore, the SN40R results were lower. Furthermore, these roads had a different mixture type. A previous study performed by Wu and King revealed that OGFC mixtures tend to have a lower friction microtexture performance compared to other mixtures [9].

**Figure 20. SN40R field results**



**SN40S Results.** Figure 21 presents the SN40S results of the respective roads. US 90 and LA 113 displayed the best results, while LA 959 and LA 88 demonstrated the worst results. US 90 has sandstone on approximately 40% of its composition, which makes it a more friction-resistant road. LA 113 is primarily composed of limestone, like LA 959 and LA 88. However, its T.I. is lower; therefore, it has been subjected to a lower traffic amount. LA 415 and I-10 showed better performance. This is primarily attributed to the fact that LA 415 and I-10 had superior macrotextures compared to the rest on the roads, as shown in Figure 22, and that SN40S is influenced by both microtexture and macrotexture.

**Figure 21. SN40S field results**

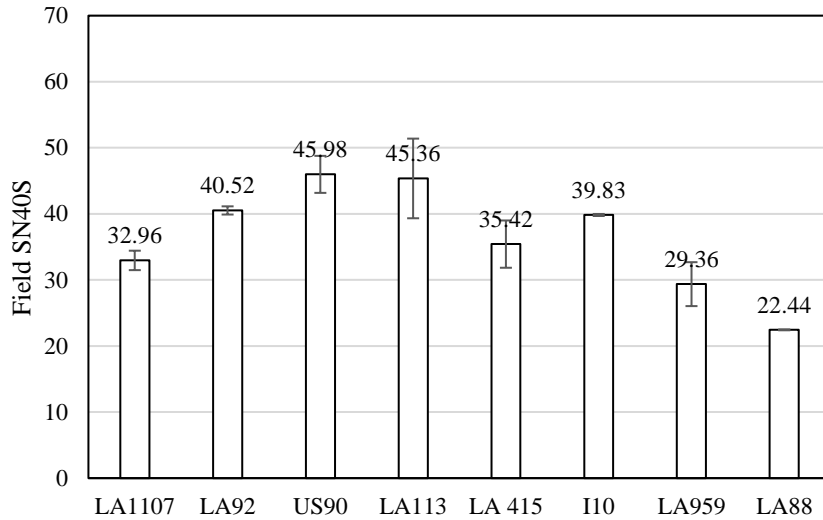
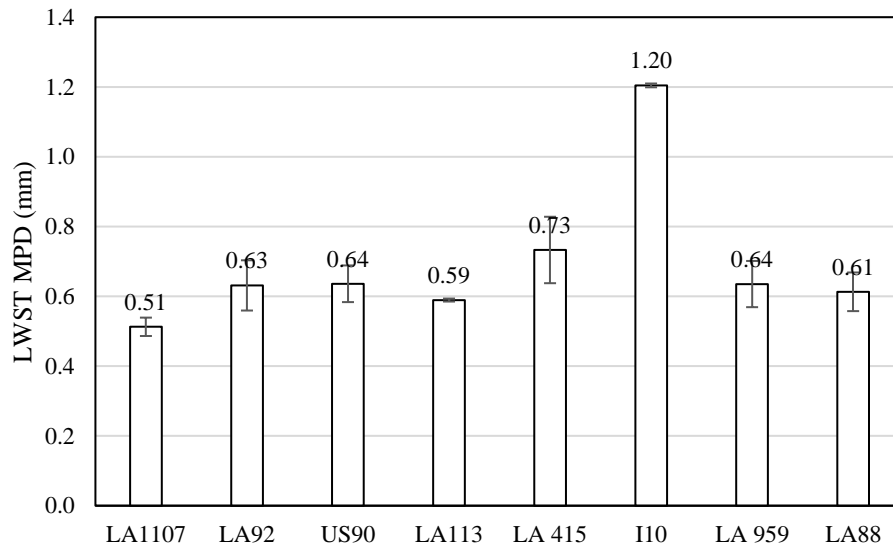


**Figure 22. LWST MPD field results**

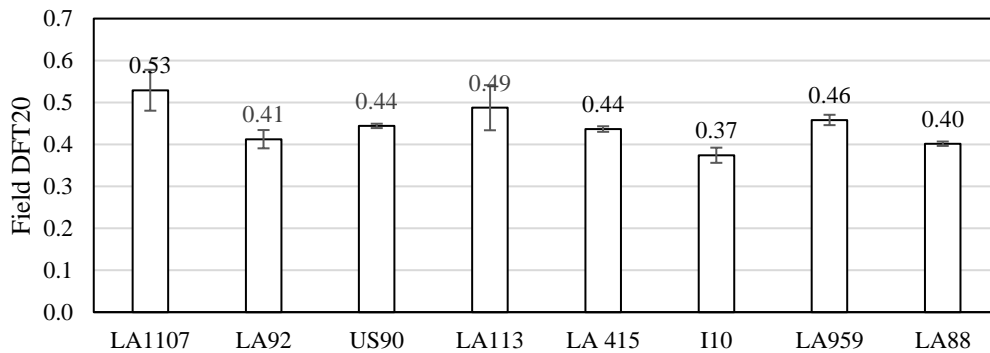


**DFT20, BPT and CTM Field Results.** Figure 23 shows the DFT20 field results of the different roads. These results are similar to those presented by SN40R in Figure 20, with the notable difference that LA 1107 displayed the highest results. The reason for this is that both DFT20 and SN40R are primarily influenced by microtexture. Furthermore, I-10 and LA 88 also displayed low DFT20 results, similar to the SN40R results. These low results are due to the fact that LA 88 has the worst performing limestone in terms of friction resistance and has been subjected to higher traffic compared to the other aggregates. I-10 has been subjected to

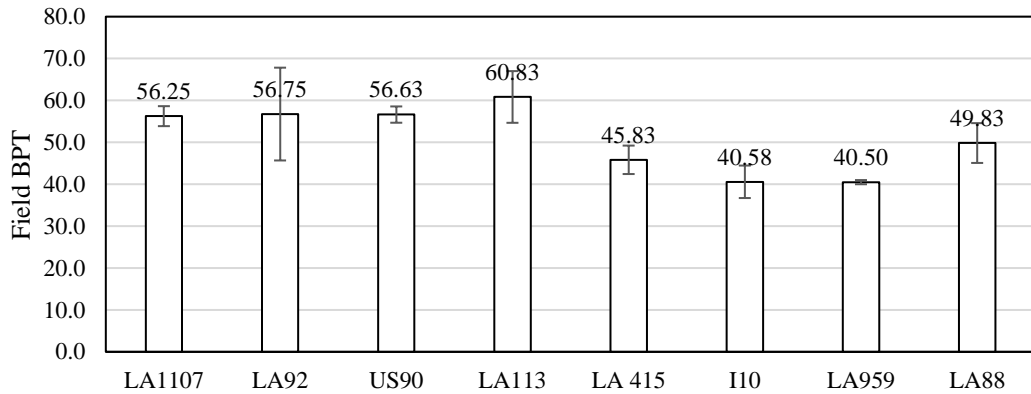
highest traffic level of all of the tested projects. Furthermore, the mixture type used for the I-10 was OGFC, which is known to have a lower DFT20 compared to the other mixes.

Figure 24 presents the BPT results of the tested roads. Figure 24 also shows that both LA 113 and LA 1107 have a high microtexture. However, its results indicate that LA 88 has a high microtexture, which is different than the DFT20 results in Figure 17. Nevertheless, I-10 continues to display the lowest friction performance among all of the tested roads. It is notable that the BPT results were not in agreement with the SN40R results, which was not the case for DFT20 field results. This finding is significant since it shows that DFT is more reliable in the field. Finally, Figure 25 presents the mean profile depth field results by means of CTM. These results are similar to those obtained using the LWST laser, showing that I-10 has the largest MPD of all the roads. I-10 was built using OGFC mixture design, which is known for its high macrotexture, as presented in previous studies [2]. Moreover, there were similar macrotexture results between the LWST and the CTM for LA 415, LA 92, US 90, LA 113, and LA 959. LA 88 and LA 1107 did not display the same results as the LWST laser profiler device.

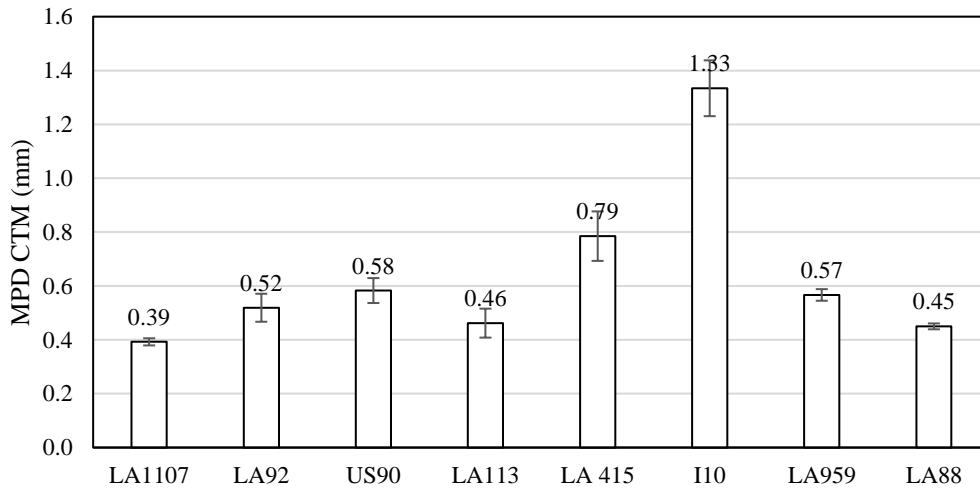
**Figure 23. DFT20 field results**



**Figure 24. BPT field results**



**Figure 25. CTM MPD**



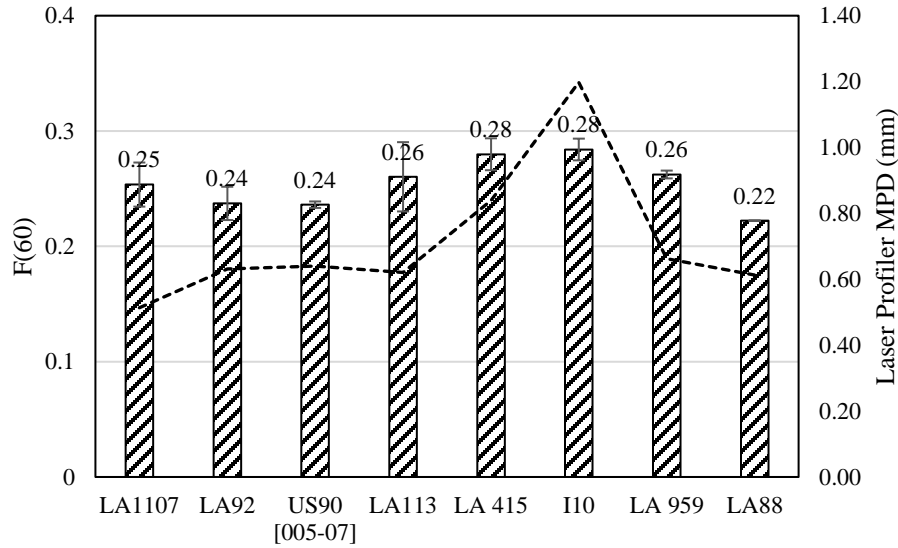
### **Discussion of Field Friction Measurements on Selected Asphalt Pavement Projects**

The F(60) value presented in Figure 26 was quantified for each field test using the relationships presented by ASTM E1960 by utilizing the measurements gathered by the DFT and CTM. This value is an indicator of the combined effect of both the microtexture and the macrotexture on the friction performance of the roads. The highest F(60) results were displayed by roads LA 415 and I-10. The reason behind this is the high macrotexture displayed by these roads, as shown on the second axis of Figure 26. This high macrotexture is due to the mixture type utilized for the construction of each road using stone mastic asphalt (SMA) on LA 415 and

Open Graded Friction Course (OGFC) on I-10. These two mixture types have shown higher macrotextures compared to the other mixes in previous studies [2] [9]. On the other hand, the lowest F(60) values were displayed by LA 92, US 90 and LA 88. The reason behind these low values is the lower macrotexture values in combination with the lower microtexture, which are presented by the DFT20 results in Figure 23. Furthermore, LA 88 had a very high T.I. (i.e., 4.15) compared to the rest of the projects. Moreover, it was primarily built with AGG SOURCE 7, which was the lowest friction-performing aggregate according to the laboratory results. This explains why this project underperformed the other roads in terms of F(60). It is also important to note that although LA 415 and I-10 displayed low DFT20 results, the combined action of both microtexture and macrotexture made a significant difference, causing these roads to achieve a superior F(60). Furthermore, no particular field friction correlation was found between the field friction and the microtexture and macrotexture indicators (i.e., DFT20 and MPD).

The aggregate constitution of the roads and the level of traffic to which they have been exposed play a key role in their overall friction performance. The roads utilizing AGG SOURCE 1 (i.e., LA 415 and I-10) displayed higher friction results than the rest of the roads. Furthermore, the roads containing AGG SOURCE 6 showed lower friction results; however, they had higher results than the roads containing aggregates AGG SOURCE 7. This trend is consistent with the DFT20 results shown in Figure 14, indicating that sandstones (i.e., AGG SOURCE 1) are superior in terms of friction performance to limestones (i.e., AGG SOURCE 6, AGG SOURCE 7). Nevertheless, it is important to note that US 90, which contained aggregate AGG SOURCE 2, had lower friction results than LA 1107, which contained AGG SOURCE 6. The reason for this result was related to traffic; US 90 had a higher T.I. and was therefore exposed to approximately 15 times more traffic than LA 1107.

**Figure 26. F(60) field results**



As mentioned before, in order to make a proper comparison, it is relevant to emphasize that not all roads were subjected to the same level of traffic. Some of the tested roads were located in rural areas (e.g., LA 1107, LA 92, and LA 959), and some had higher traffic (e.g., I-10). Therefore, in the interest of a more accurate discussion, the T.I. of the tested roads should be further explained. The project with the highest T.I. was LA 415, followed by US 90 and I-10. These three projects had sandstones in their constitution; LA 415 and I-10 had AGG SOURCE 1, while US 90 contained AGG SOURCE 2. It would be logical to assume that since these projects contained sandstones, their results would outperform the rest of the projects in every aspect. However, none of these projects excelled in terms of microtexture indicators such as DFT20, BPT, and SN40R. This is due to the higher T.I. to which they were exposed compared to the other roads. Nevertheless, when the macrotexture of these roads was incorporated into the analysis, they outperformed the rest of the projects. This behavior can be clearly seen in the F(60) calculations. The rest of the projects (e.g., LA 1107, LA 92, LA 113, and LA 959, which mainly contain limestones and RAP) had a low T.I., and LA 959, which primarily contained limestones and RAP) had a low T.I., indicating that they are in an early stage of their pavement friction life. Therefore, they have not been subjected to higher cycles of polishing, which translates to higher microtexture results. Nevertheless, considering the laboratory results, it is expected that in the future, these projects will display a lower microtexture due to polishing.

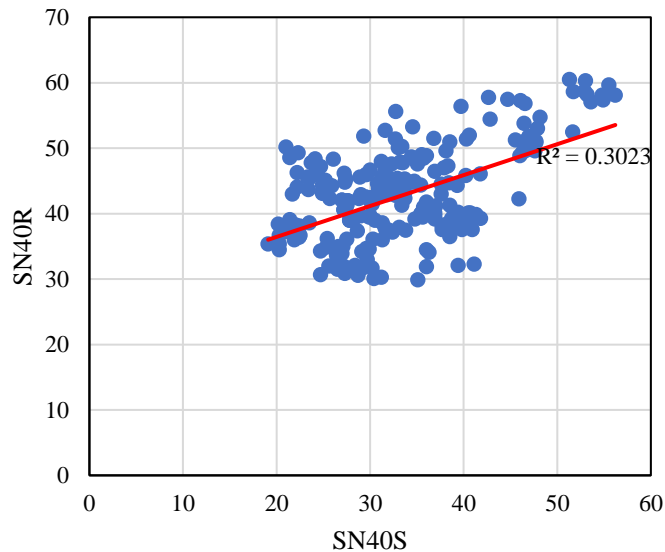
## Correlation Analysis Among Field Measurements

As outlined in the Methodology section, the correlations among various in-situ friction devices and measurements established in LTRC Project 12-5P [2] have been updated with the addition of new measurement results obtained in this study. The following sections present these updated relationships, which provide an enhanced basis for future field friction evaluations and analyses.

### SN40R vs SN40S

Figure 27 presents the LWST measurement results for all of the projects performed in this study, as well as those from Project 12-5P. In general, the LWST test results obtained by using a ribbed tire (i.e., SN40R) are higher than those from a smooth tire (i.e., SN40S). Furthermore, a poor linear correlation was found between SN40R and SN40S, with an  $R^2$  of 0.3. Nevertheless, the trend-up correlation also implies that an increase in SN40R would result in an increment of the SN40S.

Figure 27. SN40R vs SN40S

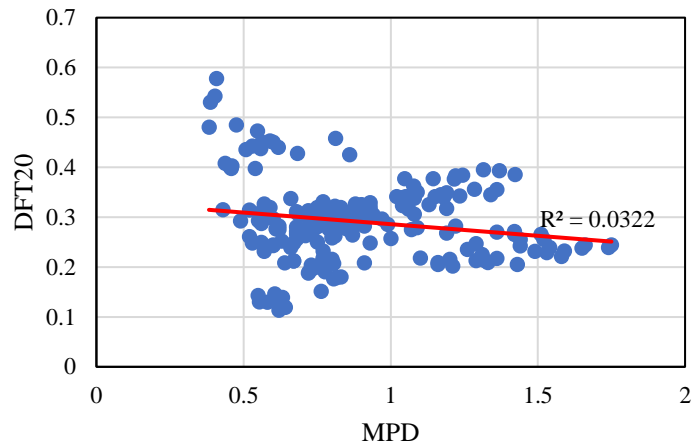


### DFT vs MPD

Figure 28 plots a potential correlation between the DFT20 field results measured for the projects and the mean profile depth (MPD) measured with the CTM device. Figure 28 shows

that there is no clear trend between these two results. Furthermore, Figure 28 indicates that macrotexture and microtexture are not necessary correlated. It is notable that this is not the case for the change in microtexture and macrotexture, as stated in the adjustment for macrotexture section.

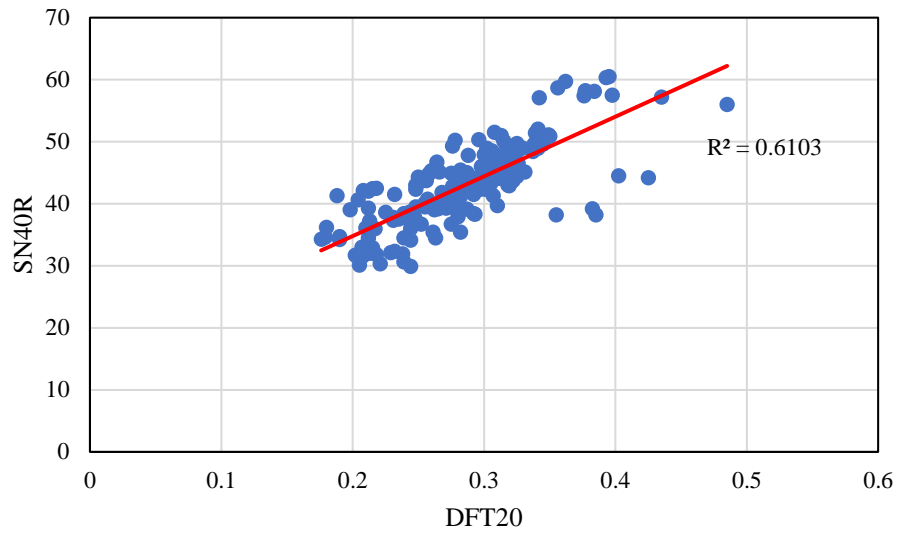
**Figure 28. DFT vs MPD**



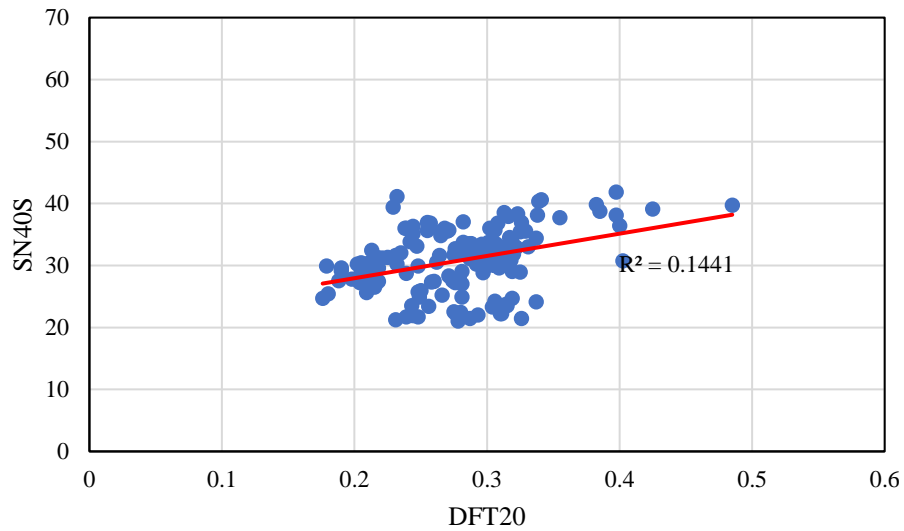
### **SN vs DFT**

Figures 29 and 30 present a potential relationship between the DFT20 vs SN40R and DFT20 vs SN40S results for the new field projects and previous 12-5P projects. A strong linear correlation was obtained for the DFT20 vs SN40R results, while the DFT20 vs SN40S results produced a poor correlation. These results confirm that the ribbed tire is more sensitive to microtexture than the smooth tire.

**Figure 29. SN40R vs DFT20**



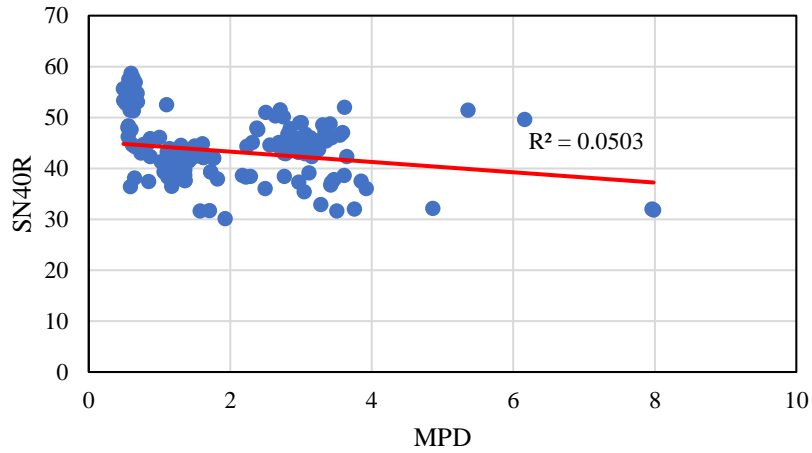
**Figure 30. SN40S vs DFT20**



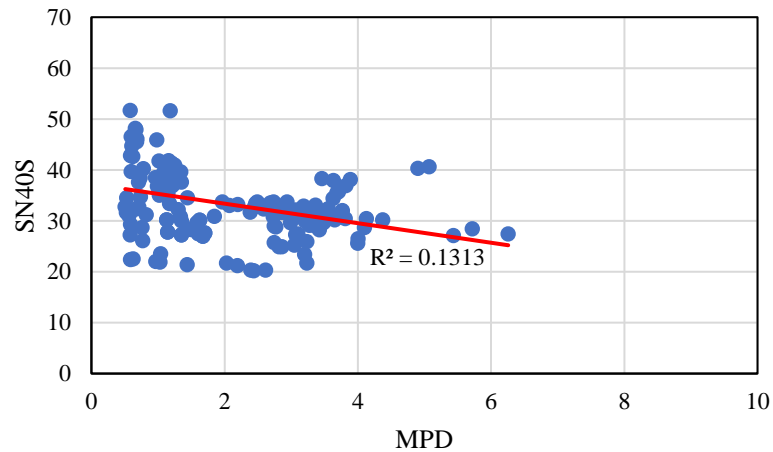
### **SN vs MPD**

Figure 31 presents the relationship between SN40R and MPD, while Figure 32 presents the correlation between SN40S and MPD. As expected, the correlation between SN40S and MPD is slightly better than that between SN40R and MPD. This is because MPD is an indicator of the macrotexture, which can be better detected by the smooth tire.

**Figure 31. SN40R vs MPD**



**Figure 32. SN40S vs MPD**



### **Laser Profiler MPDs CTM MPD**

A correlation between texture measuring devices was also updated based on the new data, as shown in Figure 33. A very good correlation was found between the MPD results from the CTM and laser profiler device ( $R^2=0.93$ ).

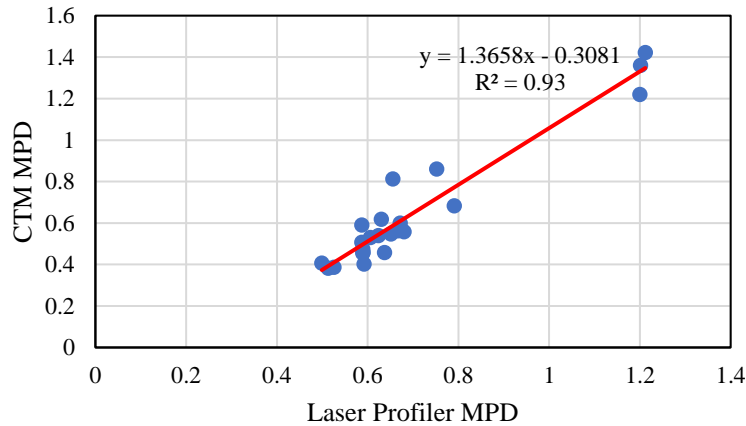
$$CTM(MPD) = 1.37 * Laser Profiler(MPD) - 0.31 \quad R^2=0.93 \quad (22)$$

Where,

CTM (MPD): Mean Profile Depth from Circular Texture Meter; and

Laser Profiler (MPD): Mean Profile Depth from LWST Laser Profiler.

**Figure 33. Laser Profiler (MPD) vs CTM (MPD)**



### SNR vs (SNS, MPD)

A multiple regression analysis was performed with data from the skid numbers using both ribbed (SN40R) and smooth tires (SN40S) along with the MPD from the laser profiler, obtaining a perfect fit.

$$SN40R = -1 * SN40S - 2 * MPD - 1.83 \times 10^{-5} \quad (R^2=1) \quad (23)$$

Where,

SN40R = Skid number at 40 mph with ribbed tire; and

SN40S = Skid number at 40 mph with smooth tire.

### SN vs (DFT, CTM)

A non-linear regression fitted on SN40S, DFT, and CTM data using both the new information and that obtained in Project 12-5P; this is shown in Equation 24. The presented relationship was fitted, obtaining an  $R^2$  of 0.45. Furthermore, a multilinear regression was fitted for the SN40R, DFT, and CTM information, obtaining an  $R^2$  of 0.49, as shown in Equation 25.

$$SN40S = 1.78 * DFT20 * e^{\left(\frac{-0.39}{MPD}\right)} \quad R^2 = 0.45 \quad (24)$$

$$SN40R = 0.642 * DFT20 - 0.0062 * MPD + 0.24 \quad R^2=0.49 \quad (25)$$

Where,

SN40R = Skid number at 40 mph with ribbed tire;

SN40S = Skid number at 40 mph with smooth tire;

DFT20 = DFT friction result at a speed of 20 km/hr; and

MPD = Mean Profile Depth from CTM (mm).

### Speed Gradient Correlations

It is important to be able to estimate the skid number at designated speed from different speeds, because there are times when speed constraints on roads prevent a desired speed from being achieved. Relationships for the speed gradients for SN40S have been developed by Fugro [61]; therefore, a relationship for SN40R is necessary. In order to address this issue, several skid numbers at different speeds (e.g., 30, 40, and 50 mph) were obtained along with their respective mean profile depth (MPD). A non-linear model was fitted with the gathered data, obtaining a good relationship.

$$SN40R = SNR_V x e^{\left(\frac{V-40}{73.26*MPD+68.86}\right)} \quad R^2=0.86 \quad (26)$$

Where,

SN40R = Skid number at 40 mph with ribbed tire;

SNR<sub>V</sub> = Skid number at any speed;

V = Velocity of testing in mph; and

MPD = Mean profile depth from laser profiler (mm).

### Development of F(60) Prediction Model

As described in the literature, the research team previously performed a friction study on lab-made asphalt slabs under LTRC Project 09-2B [9] and a field friction study under LTRC Project 12-5P [2]. Based on the data obtained from Projects 09-2B and 12-5P, as well as the TWPD aggregate results from the current project, a synthetic dataset was created. This dataset included each aggregate's DFT20, mixture's MPD, and polishing cycles. Next, an F(60) prediction model was developed, as shown in Equation 27. This can be used to predict the F(60) design of a pavement based on the design life traffic, mixture type, and blended aggregate's DFT20 of the TWPD test. For the development of the model, the F(60) was determined by utilizing the relationship presented by ASTM E1960 utilizing the MPD and DFT20 measurements gathered from the slab [33]. In the case of DFT20, it was calculated by using the information

regarding AGG SOURCE 1 and AGG SOURCE 6, which were utilized in the creation of the slabs in Project 09-2B.

The model has the following form:

$$F(60) = (0.1556 - 0.0995 * MPD + 0.1192 * DFTAgg + 0.4394 * MPD * DFTAgg * e^{-0.4612*10^{-6}*N} \quad (R^2 = 0.91) \quad (27)$$

Where,

DFTAgg = DFT of the Aggregate Ring Sample;

MPD = Mean Profile Depth depending on the mixture type; and

N = Polishing Cycles.

In terms of the MPD, this value was determined by fitting the Weibull distribution factors from the mixture design gradation (i.e.,  $\lambda$  (scale) and  $k$  (shape)) [2]. Once these factors are obtained, the MPD can be determined using Equation 28.

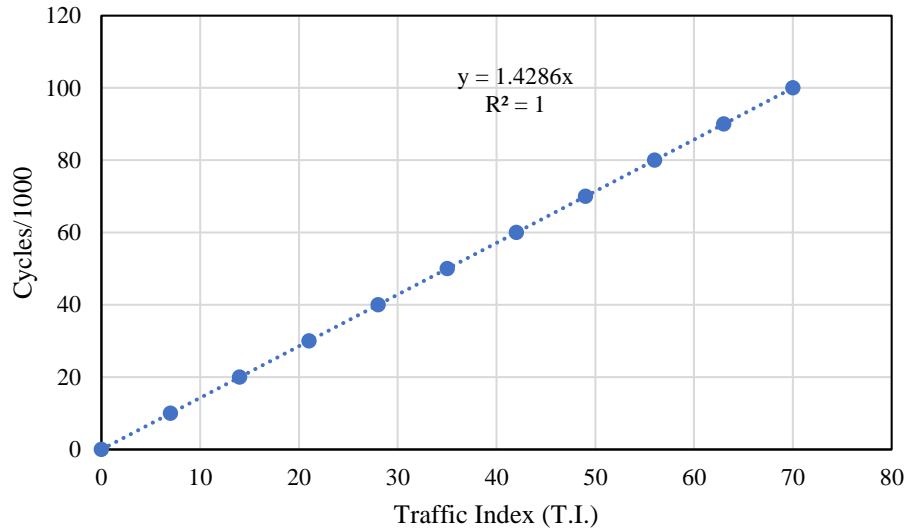
$$MPD = 0.0036 * \lambda + 0.3095 * k - \frac{0.0123}{k^4} \quad (R^2 = 0.80) \quad (28)$$

In case the mixture has more than one aggregate, a blended DFT value should be determined using Equation 29. This equation is based on the analysis that was performed on the TWPD section, presented in Figure 17. It is important to note that for the development of this model, DFT20 was quantified using 70% of AGG SOURCE 6 and 30% of AGG SOURCE 1 for the combined mixture types.

$$\text{Blend DFT agg} = \text{DFT agg1} * (\text{aggregate percentage}) + \text{DFT agg2} * (\text{aggregate percentage}) + \dots \quad (29)$$

A relationship between the number of cycles of the TWPD device and the traffic index (T.I.) was developed to correlate the laboratory cycles with actual road traffic, as shown in Figure 34. For this purpose the information from Project 12-5P report was used. The relationship was performed by equalizing the DFT20 results from the DFT20 vs Polishing Cycles curves with the DFT20 results from the DFT20 vs T.I. relationships (see Figures 33 and 34 from the Project 12-5P report) [2]. It was assumed that the DFT20 from the lab was equal to the DFT20 from the field for the same mixture type and aggregate.

Figure 34. Cycles vs T.I.



$$\text{Cycle} = 1428.6 * \text{T.I.}, \text{ when T.I.} \leq 70 \quad (30)$$

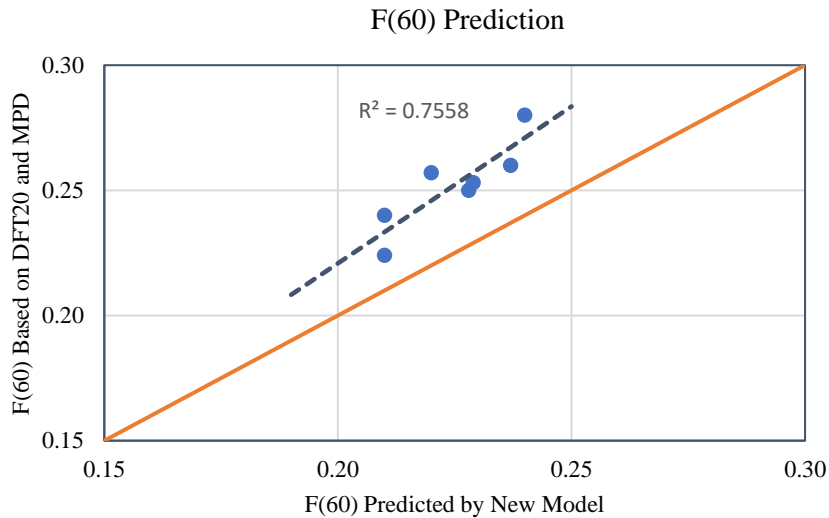
$$\text{Cycle} = 100,000, \text{ when T.I.} > 70 \quad (31)$$

To evaluate the developed F(60) model, Table 25 presents the prediction of the F(60) of the roads tested on this project. For this purpose, the T.I. was first quantified, then the parameters of  $\lambda$  and  $k$  were calculated based on the aggregate gradation of the field projects, as shown in Table 25. Once these two parameters were established, the MPD was determined based on Equation 28. Furthermore, the number of cycles was determined based on the T.I. using Equation 30. The blended DFT20 was obtained using Equation 29 with the percentage of each aggregate used on the road. Having determined the number of laboratory cycles, the MPD, and the blended DFT20, the predicted F(60) was quantified using Equation 27. Finally, the predicted F(60) was compared with the F(60) calculation using the field DFT20 and field MPD per ASTM E1960. Figure 35 presents the plot of the results of the F(60) predicted by the new model versus the results of the F(60) calculations based on the field DFT20 and MPD. The correlation between these two values was good, yielding an  $R^2$  of 0.76. This value shows that the predictions are in accordance with the field results. However, as shown in Figure 35, the predicted F(60) values are generally slightly lower than the field-measured results by approximately 0.02 to 0.04. This difference likely reflects variations in field conditions, including traffic loading and mixture characteristics. Additional field friction testing may be warranted to further validate and refine the developed model.

**Table 25. F(60) prediction results**

Road Name	T.I.	$\lambda$	k	MPD	Predicted Cycles	Blended DFT20 from Aggregate Ring Sample	Predicted F(60) Based on New Model	Field F(60) Based on DFT20 and CTM (MPD)
LA1107	0.40	4.25	1.20	0.38	580.18	0.39	0.23	0.25
LA92	0.35	4.30	1.21	0.38	502.85	0.33	0.21	0.24
US90	6.04	4.74	1.22	0.39	8698.85	0.45	0.24	0.26
LA113	0.33	4.39	1.23	0.39	471.64	0.39	0.23	0.25
LA 415	6.95	6.79	1.25	0.41	10021.23	0.46	0.24	0.28
LA959	0.77	4.12	1.08	0.34	1106.01	0.37	0.22	0.26
LA88	4.15	4.30	1.21	0.38	5931.37	0.33	0.21	0.22

**Figure 35. F(60) prediction**



Finally, a prediction was made for the aggregate DFT20 under different ADT per design lane and different mixture types. For this purpose, a terminal design F(60) of 0.18 was used. Furthermore, the T.I. was quantified by multiplying the ADT per lane by the number of years. For the ADT intervals, a middle value was used (e.g., for values between 1,000 and 3,000,

2,000 was used, and for values more than 10,000, 12,000 was used). Once the T.I. was determined, the cycles were quantified. Finally, the MPD was established depending on the mixture type. Once the F(60), cycles, and MPD were determined, the DFT20 was quantified. Table 26 presents the aggregate DFT 20 requirement depending on the ADT and mixture type used in a wearing course mix design.

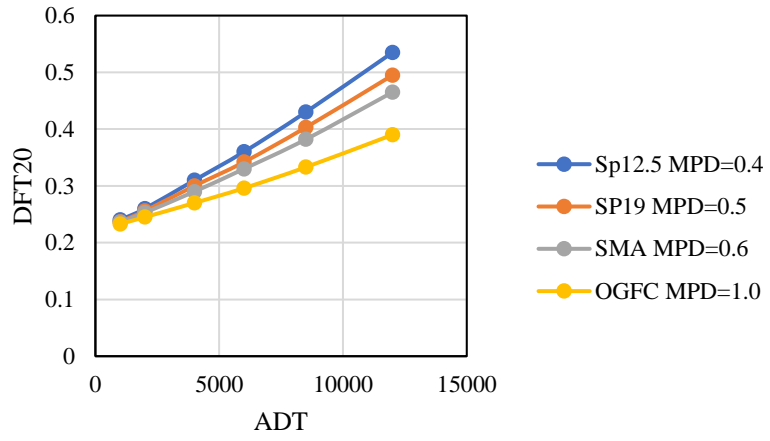
**Table 26. Aggregate DFT20 requirement depending on ADT and mixture type**

Mixture	DFTagg requirement at the end of 15-year pavement design life					
	ADT@design lane					
	<1000	>1000~3000	3000~5000	5000~7000	7000~10000	>10000
12.5-SP (MPD=0.4mm)	0.240	0.26	0.31	0.36	0.43	0.535
19-SP (MPD=0.5mm)	0.237	0.256	0.3	0.342	0.403	0.495
SMA (MPD=0.6mm)	0.236	0.253	0.29	0.33	0.382	0.465
OGFC (MPD=1.0mm)	0.233	0.245	0.27	0.296	0.333	0.39

Different curves can be found if different inputs of MPD are used to calculate the DFT20. Figure 36 presents the ADT vs DFT20 curve for different asphalt mixture types with varying MPD. The different ADTs were gathered from Table 26 and represent the different stages of the friction pavement life. An increasing trend can be observed in Figure 36 for every mixture type; this implies that at higher levels of traffic, a higher blended DFT20 is required for the road.

Figure 36. Cycles vs F(60)

ADT vs. DFT20 for Different Mixes



## Conclusions

In this study, two different test procedures—BPT in combination with BPW and DFT in combination with TWPD—were performed to assess the friction performance of seven different aggregates used in Louisiana. Through experimental data acquisition and statistical analysis, several valuable insights were obtained, leading to the following key findings:

- The results from the BWP polishing stone test before and after polishing yielded a variation beyond the allowed limits. Furthermore, the aggregate friction rating based on the PSV test results differs from the AML and the previous year's results, adding uncertainty and inconsistency to this testing procedure.
- The PSV-based DOTD aggregate friction rating variation was assessed by duplicate sample preparation, shipment source, and chemical analysis. The standard deviation of both sample duplicates was beyond the allowed limits. Furthermore, the results from the shipment source indicate a general decrease in their friction ratings compared to previous PSV results. Finally, the chemical variations from the aggregates obtained within the same quarry suggest that the different polishing resistance results for the PSV tests are linked to petrological differences within the quarry. Nevertheless, a general chemical trend was found, indicating that higher SiO<sub>2</sub> contents are associated with higher BPN and PSV values; conversely, high CaO contents are associated with low results.
- The DFT20 results gathered from the TWPD tests before and after polishing show a standard deviation below the allowable limits. This indicates that this test procedure is more reliable than the aforementioned one.
- The rankings obtained by the two test procedures differ. According to the DFT20 ranking, AGG SOURCE 1 was the best-performing aggregate in terms of both skid resistance potential and polishing resistance, while AGG SOURCE 2 was considered the best by the PSV ranking. Additionally, AGG SOURCE 6 was considered the worst-performing aggregate based on the PSV ranking. On the other hand, AGG SOURCE 7 was deemed the worst by the DFT20 ranking. This finding indicates inconsistency between the two test procedures.
- The variation of TWPD in combination with the DFT test procedure was analyzed based on aggregate, DFT speed, 90° rotation, sample duplicate, and operator. From all these analyses, it was found that the DFT20 does not display any significant statistical difference

among the different measurements. This finding implies that the DFT20 is a reliable measurement that does not change, considering the aforementioned variables.

- The results from the TWPD tests, in combination with the DFT device, followed the same order as the chemical analysis. Aggregates with higher percentages of SiO<sub>2</sub> and lower contents of CaO displayed better friction results. The exception to this trend was AGG SOURCE 5; however, this was due to its high MgO content. On the other hand, the BWP test, in combination with BPT, did not display the same order results as the chemical composition trend. This indicates that the TWPD in combination with the DFT is more reliable than the BWP in combination with the BPT.
- The macrotexture (MPD) did not display any significant change after the TWPD test was conducted on the samples. This finding indicates that this device can substantially alter the microtexture of the aggregates without significantly changing its macrotexture. Furthermore, it was found that the change in macrotexture within two sample duplicates is related to the change in DFT. Due to this finding, an adjustment for the DFT20 results was made based on the macrotexture variation.
- Field measurements were conducted on roads that utilized the tested aggregates. LWST, DFT, CTM, and BPT tests were conducted on these roads. The SN40R results indicated that roads with primarily limestones in their composition had a superior performance than the ones containing sandstones, namely LA 415 and I-10. Nevertheless, this is due to the fact that these roads have been subjected to higher traffic. In the future, at a higher T.I., it is expected that the other roads will underperform those containing sandstone. Moreover, the SN40S results indicated a superior performance for these roads. This is due to the fact that SN40S includes the macrotexture in the overall analysis. LA 415 and I-10 were built with SMA and OGFC mixture types, respectively, and are known for having a superior macrotexture compared to Superpave, the mixture type used on the other projects. Furthermore, the DFT20 results were in general accordance with the SN40R results, meaning that they are both primarily influenced by the microtexture. Nevertheless, the BPT results, although it is also a surrogate for microtexture, did not yield the same trend as SN40R and DFT20. This reinforces the fact that DFT is more reliable than BPT. Finally, the F(60) was determined per ASTM E1960, including DT20 and CTM (MPD) field results, indicating that LA 415 and I-10 display superior friction performance. Moreover, the lowest F(60) values were displayed by LA 92, US 90, and LA 88 due to their lower macrotexture values in combination with the lower microtexture results. In general, roads utilizing AGG SOURCE 1 (i.e., sandstone) displayed higher friction results than the rest of the roads. Furthermore, the roads containing AGG SOURCE 6 (i.e., limestone) showed

lower friction results; however, they had higher results than the roads containing aggregates AGG SOURCE 7 (i.e., limestone). This trend is consistent with the laboratory results gathered by the TWPD.

- Finally, a new prediction F(60) model was developed based on previous laboratory information. This model takes into account the effect of the mixture macrotexture, which was predicted by determining the  $\lambda$  and  $k$  parameters obtained after fitting a Weibull distribution on the mixture aggregate gradation, the blended DFT20 of the aggregate ring sample, and the laboratory cycles of the TWPD test.
- Finally, the information gathered from the field tests, namely aggregate gradation, field DFT20, and field MPD, were used to predict the field F(60). The results of the prediction model were in good correlation with the actual F(60) field results.

These findings indicate that the TWPD in combination with DFT is more accurate and reliable than BWP in combination with BPT test.

## Recommendations

- It is recommended that DOTD adopt and implement the AASHTO PP103 polishing test procedure, which combines the Three-Wheel Polishing Device (TWPD) with the Dynamic Friction Tester (DFT), as a replacement for the previous method utilizing the British Wheel Polisher (BWP) and British Pendulum Tester (BPT).
- The developed F(60) prediction model provides valuable guidance for asphalt engineers in determining the friction requirements of blended coarse aggregates during the design of wearing course mixtures.
- Given the limited number of aggregate sources tested in this project, it is recommended that additional aggregate sources be evaluated using the TWPD/DFT protocol. The results can then be utilized to establish new friction rating criteria based on DFT20 @ 100,000 for DOTD's initial aggregate source friction approval process.

## Acronyms, Abbreviations, and Symbols

<b>Term</b>	<b>Description</b>
AASHTO	American Association of State Highway and Transportation Officials
AML	Approved Materials List
ASTM	American Society for Testing and Materials
BPT	British Pendulum Tester
BPN	British Pendulum Number
BWP	British Wheel Polisher
cm	centimeter(s)
CTM	Circular Track Meter
DFT	Dynamic Friction Tester
DOTD	Louisiana Department of Transportation and Development
F(60)	Friction Number at 60 km/hr
FHWA	Federal Highway Administration
FR	Friction Rating
ft.	foot (feet)
HMA	Hot Mix Asphalt
in.	inch(es)
IFI	International Frictional Index
JMF	Job Mix Formula
lb.	pounds
LTRC	Louisiana Transportation Research Center
LWST	Locked Wheel Skid Tester
MPD	Mean Profile Depth
MTD	Mean Texture Depth
m	meter(s)
NCAT	National Center for Asphalt Technology
NCHRP	National Cooperative Highway Research Program
OGFC	Open Graded Friction Course
PSV	Polished Stone Value
SMA	Stone Matrix Aggregate
SN	Skid Number
Superpave	Superior Performing Pavement
TWPD	Three-Wheel Polishing Device

## References

- [1] J. J. Henry, *Evaluation of pavement friction characteristics*, vol. 291. Transportation Research Board, 2000.
- [2] Z. Wu, K. Bill, and Subedi, “Evaluation of LADOTD Aggregate Friction Rating Table by Field Measurements,” no. 225, 2016, [Online]. Available: [www.ltrc.lsu.edu](http://www.ltrc.lsu.edu)
- [3] J. W. Hall and K. L. Smith, *Guide for Pavement Friction*. 2009. doi: 10.17226/23038.
- [4] J. Jewett Henry, H. Abe, S. Kameyama, A. Tamai, A. Kasahara, and K. Saito, “Determination of the International Friction Index (IFI) using the Circular Texture Meter (CTM) and the Dynamic Friction Tester (DFT),” 2000.
- [5] R. L. Rizenberg., J. L. Burchett, and C. T. Napier, “Skid Resistance of Pavements,” no. September 1972, 1972, doi: 10.1515/9783112518069.
- [6] S. Najafi, G. Flintsch, and A. Medina, “Case Study on the Evaluation of the Effect of Tire-Pavement,” *Transp. Res. Board 93rd Annu. Meet. January 12-16, Washington, D.C.*, 2014.
- [7] G. Flintsch, K. McGhee, E. D. L. Izeppi, and S. Najafi, “The Little Book of Tire Pavement Friction,” *Apps. Vtti. Vt. Edu*, no. September, pp. 0–22, 2012.
- [8] H. W. Kummer and W. E. Meyer, “Rubber and Tire Friction,” *Autom. Saf. Proj. Dep. Mech. Eng.*, 1960.
- [9] Z. Wu and B. King, “Development of Surface Friction Guidelines for LADOTD LTRC Project Number : 09-2B SIO Number : 30000119 Department of Civil and Environmental Engineering Louisiana State University Baton Rouge , LA 70803 Louisiana Department of Transportation and Developm,” no. 1, 2012.
- [10] R. Davis, “Comparison of Surface Characteristics of Hot-Mix Asphalt Pavement Surfaces at the Virginia Smart Road,” *Texture*, 2001.
- [11] R. S. McDaniel and B. J. Coree, *Identification of Laboratory Techniques to Optimize Super pave HMA Surface Friction Characterization*, vol. Phase I: F, no. April 2010. 2003.
- [12] B. D. Prowell and D. I. Hanson, “Evaluation of circular texture meter for measuring surface texture of pavements,” *Transp. Res. Rec.*, vol. 965, no. 1929, pp. 88–96, 2005, doi: 10.3141/1929-11.
- [13] D. Wilson and R. Dunn, “Polishing Aggregates to Equilibrium Skid Resistance,” vol. 14, 2005.

- [14] S. N. Goodman, Y. Hassan, and A. O. Abd El Halim, “Preliminary estimation of asphalt pavement frictional properties from superpave gyratory specimens and mix parameters,” *Transp. Res. Rec.*, no. 1949, pp. 173–180, 2006, doi: 10.3141/1949-16.
- [15] J. Henry, *NCHRP SYNTHESIS 291 Evaluation of Pavement Friction Characteristics A Synthesis of Highway Practice*. 2000.
- [16] Y. Zong *et al.*, “Effect of aggregate type and polishing level on the long-term skid resistance of thin friction course,” *Constr. Build. Mater.*, vol. 282, p. 122730, 2021, doi: 10.1016/j.conbuildmat.2021.122730.
- [17] M. Saghafi, I. N. Abdallah, M. Ahmad, S. Nazarian, and C. Herrera, “Correlating Aggregate Friction Test Results Under Accelerated Laboratory Polishing and Aggregate Crushing,” *Int. J. Pavement Res. Technol.*, vol. 17, no. 2, pp. 423–434, 2024, doi: 10.1007/s42947-022-00245-z.
- [18] B. Ergin, İ. Gökalp, and V. E. Uz, “Effect of Aggregate Microtexture Losses on Skid Resistance: Laboratory-Based Assessment on Chip Seals,” *J. Mater. Civ. Eng.*, vol. 32, no. 4, pp. 1–12, 2020, doi: 10.1061/(asce)mt.1943-5533.0003096.
- [19] C. Chen, F. Gu, M. Heitzman, B. Powell, and K. Kowalski, “Influences of alternative friction aggregates on texture and friction characteristics of high friction surface treatment,” *Constr. Build. Mater.*, vol. 314, no. PB, p. 125643, 2022, doi: 10.1016/j.conbuildmat.2021.125643.
- [20] M. Saghafi *et al.*, “Practical Specimen Preparation and Testing Protocol for Evaluation of Friction Performance of Asphalt Pavement Aggregates with Three-Wheel Polishing Device,” *J. Mater. Civ. Eng.*, vol. 34, no. 1, pp. 1–14, 2022, doi: 10.1061/(asce)mt.1943-5533.0004018.
- [21] A. S. El-Ashwah, K. Broaddus, and M. Abdelrahman, “Predicting the Friction Coefficient of High-Friction Surface Treatment Application Aggregates Using the Aggregates’ Characteristics,” *J. Mater. Civ. Eng.*, vol. 35, no. 5, pp. 1–15, 2023, doi: 10.1061/(asce)mt.1943-5533.0004739.
- [22] G. S. Reddy, M. A. Montoya, I. N. Abdallah, S. Nazarian, and R. Izzo, “Alternative Approaches for Rapid Evaluation of Frictional Resistance of Aggregates,” *Transp. Res. Rec.*, 2024, doi: 10.1177/03611981241239961.
- [23] B. N. J. Persson, “Theory of rubber friction and contact mechanics,” *J. Chem. Phys.*, vol. 115, no. 8, pp. 3840–3861, 2001, doi: 10.1063/1.1388626.
- [24] J. J. Henry and J. C. Wambold, “Use of Smooth-Treaded Test Tire in Evaluating Skid Resistance,” *Transp. Res. Board*, no. 1348, pp. 35–42, 1992.
- [25] F. Copple and P. T. Luce, “Determination and Improvements of Relevant Pavement Skid Coefficients.” 1977.

- [26] J. J. Henry and K. Saito, “Skid-Resistance Measurements With Blank and Ribbed Test Tires and Their Relationship To Pavement Texture.,” *Transp. Res. Rec.*, no. 9, pp. 38–43, 1983.
- [27] W. H. Parcells, T. M. Metheny, and R. G. Maaq, “Predicting Surface Friction From Laboratory Tests.,” *Transp. Res. Rec.*, no. c, pp. 33–40, 1982.
- [28] K. T. Diringer and R. T. Barros, “Predicting the skid resistance of bituminous pavements through accelerated laboratory testing of aggregates,” *ASTM Spec. Tech. Publ.*, no. 1031, pp. 61–76, 1990, doi: 10.1520/stp23353s.
- [29] B. M. Gallaway, J. Epps, and H. Tomita, “Effects of pavement surface characteristics and textures on skid resistance,” no. March, pp. 1–44, 1971.
- [30] M. C. Leu and J. J. Henry, “Prediction of Skid Resistance As a Function of Speed From Pavement Texture Measurements.,” *Transp. Res. Rec.*, vol. 1, no. 666, pp. 7–13, 1978.
- [31] G. G. Balmer and R. R. Hegmon, “Recent Developments in Pavement Texture Research.,” *Transp. Res. Rec.*, pp. 29–33, 1980.
- [32] J. J. Henry, “Use of Blank and Ribbed Test Tires for Evaluating Wet-Pavement Friction.,” *Transp. Res. Rec.*, no. 2, pp. 1–6, 1980.
- [33] ASTM International, “ASTM E1960 Standard Practice for Calculating International Friction Index of a Pavement,” vol. 07, no. Reapproved, pp. 1–5, 2015, doi: 10.1520/E1960-07R15.2.
- [34] M. Jackson, “Harmonization of Texture and Skid-Resistance Measurements,” vol. 32224, no. 904, 2008.
- [35] ASTM, “ASTM E1960 - Standard Practice for Calculating International Friction Index of a Pavement,” vol. 07, no. Reapproved, pp. 1–5, 2023, doi: 10.1520/E1960-07R23.2.
- [36] J. Wambold, C. Antle, J. Henry, and Z. Rado, “International PIARC: Experiment to compare and harmonize texture and skid resistance measurements Technical Committee 1 Surface Characteristics,” 1995.
- [37] B. . Sullivan, “Development of a Fundamental Skid Resistance Asphalt Mix Design Procedure,” *Pavement Manag. Serv.*, pp. 1–15, 2005.
- [38] R. Liang, “Continuing Investigation of Polishing and Friction Characteristics of Limestone Aggregate in Ohio,” 2009.
- [39] L. G. Fuentes and M. Gunaratne, “Evaluation of the speed constant and its effect on the calibration of friction-measuring devices,” *Transp. Res. Rec.*, no. 2155, pp. 134–144, 2010, doi: 10.3141/2155-15.

- [40] K. J. Kowalski, R. S. McDaniel, and J. Olek, *Identification of laboratory techniques to optimize superpave HMA surface friction characteristics*. 2010. doi: 10.5703/1288284314265.This.
- [41] S. Erukulla, “Refining a Laboratory Procedure to Characterize Change in Hot-Mix-Asphalt Surface Friction,” vol. 11, no. 2, pp. 10–14, 2011.
- [42] D. I. H. Timothy W.Vollor, “Development of Laboratory Procedure for Measuring Friction of Hma Mixtures – Phase I,” *NCAT Rep. 06-06*, no. December, 2006.
- [43] E. Masad, A. Rezaei, A. Chowdhury, and P. Harris, “Predicting Asphalt Mixture Skid Resistance,” no. 2, p. 226, 2009.
- [44] E. Masad, A. Rezaei, A. Chowdhury, and T. Freeman, “Field Evaluation of Asphalt Mixture Skid Resistance and its Relationship to Aggregate Characteristics,” vol. 7, no. 2, p. 128, 2010.
- [45] S. Hu, F. Zhou, T. Scullion, E. Fernando, and M. Souliman, “Develop Surface Aggregate Classification of Reclaimed Asphalt Pavement: Technical Report,” 2022.
- [46] J. Groeger, A. Simpson, and K. Pokkuluri, “Evaluation of Laboratory Tests to Quantify Frictional Properties of Aggregates,” *State Highw. Adm.*, no. Md, 2010.
- [47] L. DOTD, “Standard Specifications for Roads and Bridges,” 2016.
- [48] State of Louisiana Department of Transportation and Development, “Qualified Product List, LADOTD,” pp. 1–58, 2024.
- [49] AASHTO T 278-90 (2017), “Standard Method of Test for Surface Frictional Properties Using the British Pendulum Tester,” 2017.
- [50] AASHTO T 279-18, “Standard Method of Test for Accelerated Polishing of Aggregates Using the British Wheel,” *AASHTO provisional Stand. Washington, D.C.*, vol. 04, no. 2022, pp. 4–7, 2018.
- [51] ASTM, “ASTM D3319 Standard Practice for the Accelerated Polishing of Aggregates Using the British Wheel,” pp. 1–5, 2023, doi: 10.1520/D3319-23.2.
- [52] ASTM International, “ASTM E1911-19 Standard Test Method for Measuring Surface Frictional Properties Using the British,” vol. 93, no. Reapproved 2013, pp. 1–5, 2014, doi: 10.1520/E0303-93R13.2.
- [53] AASHTO, “Standard Practice for Sample Preparation and Polishing of Unbound Aggregates for Dynamic Friction Testing - AASHTO PP 103,” vol. 21, no. 2022, 2020.

- [54] Y. P. Subedi, "Evaluation of Louisiana Friction Rating Table by Field Measurements," *M.Sc. Thesis, Louisiana State Univ. Louisiana, USA*, 2015.
- [55] J. Ashby, "Blended Aggregate Study," *Louisiana Dep. Transp. Dev.*, 1980.
- [56] ASTM, "ASTM E303 Standard Test Method for Measuring Surface Frictional Properties Using the British," vol. 93, no. 2018, pp. 1–7, 2022, doi: 10.1520/E0303-22.Copyright.
- [57] ASTM, "Standard Practice for the Accelerated Polishing of Aggregates Using the British Wheel," pp. 1–5, 2023, doi: 10.1520/D3319-23.2.
- [58] X. L. Xu, X. Lu, Z. X. Qin, and D. L. Yang, "Influence of silica as an abrasive on friction performance of polyimide-matrix composites," *Polym. Polym. Compos.*, vol. 25, no. 1, pp. 43–48, 2017, doi: 10.1177/096739111702500107.
- [59] M. Cao, X. Ming, K. He, L. Li, and S. Shen, "Effect of macro-, micro- and nano-calcium carbonate on properties of cementitious composites-A review," *Materials (Basel)*, vol. 12, no. 5, 2019, doi: 10.3390/ma12050781.
- [60] D. Kumar, J. Jain, and N. N. Gosvami, "Macroscale to Nanoscale Tribology of Magnesium-Based Alloys: A Review," *Tribol. Lett.*, vol. 70, no. 1, pp. 1–29, 2022, doi: 10.1007/s11249-022-01568-5.
- [61] FUGRO, "LTRC Multi-Section Skid and Laser Profile Testing Final Report," 2023.
- [62] M. S. M. of Tests, "Laboratory method of polishing aggregates using the Circular Track Polishing Machine," pp. 4–9, 2012.

# Appendix A

## Laboratory Method of Polishing Aggregates Using the Three Wheel Polisher Machine along with Dynamic Friction Tester (DFT) and Circular Texture Meter (CTM)

### Scope

This procedure is used to prepare and test aggregate ring samples using the Three-Wheel Polisher Machine along with the Dynamic Friction Tester (DFT) and Circular Texture Meter (CTM).

### Materials and Equipment

1. Three Wheel Polisher Machine
2. Three patterned pneumatic tires type 2.80/2.50 with a cold tire pressure of  $240 \pm 34$  kPa ( $35 \pm 5$  psi)
3. Circular stainless steel casting mold with an outside diameter of 355.6 mm (14 in.), inside diameter of 209.55 mm (8 1/4 in.) and 25.4 mm (1 in.) height
4. Square stainless steel mold with dimensions of 508 mm x 508 mm x 76 mm (20.0 x 20.0 in. x 3.0 in.) for holding the prepared sample during polishing and testing.
5. Resin—bonding agent
6. Wollastonite—NYAD 400 Extender Pigment
7. Oven
8. Silica—Amorphous Fumed, 150 grit size
9. Mold release agent—#2 Green Wax or Equivalent
10. Miscellaneous supplies, including disposable cups, spatula, and stirring rods
11. 7 lbs. of -1/2 to 3/8 in. aggregate
12. Dynamic Friction Tester (DFT)
13. Synthetic Rubber Sliders
14. Tank with Water Supply

15. DFT Data Record Sheet
16. Computer
17. Circular Texture Meter (CTM)

### **Sample Preparation**

The aggregate ring sample preparation process followed the guidelines of the Maryland Department of Transportation and AASHTO PP103 and consisted of the following steps [53] [62]:

1. Initially, the aggregates were sieved to obtain the desired size passing through 1/2 in. (12.7 mm) sieve and being retained on the 3/8 in. (9.5 mm) sieve. The next step corresponded to the washing of the aggregate to remove debris and dust.
2. Subsequently, the aggregates were subjected to oven drying for a duration of 24 hours at a temperature of 50°C to make sure all the moisture was eliminated.
3. Wax (i.e., a releasing agent) was placed on the molds to prevent the attachment of the aggregate ring sample after it sets.
4. Later, appropriately shaped aggregates were selected and placed in the mold with the flat side facing down in the ring sample mold. Eye judgment was used to select flat and angular aggregates. The ring sample mold has an inner diameter of 7.75 in. (196.8 mm) and an outer ring with a width of 2.87 in. (73 mm) per specifications [53].
5. Once the aggregates were placed, a polyester resin was prepared to cover the corresponding aggregates. The preparation of this resin consisted of adding 1,332 grams (2.94 lb) of resin to a container. Next, 49.5 grams of aerosol were added and blended thoroughly. Subsequently, 540 grams (1.19 lbs.) of Wollastonite were added and mixed again. The process was finalized with the addition of 18 grams of Ketone to finalize the resin preparation process.
6. After the resin was poured, the sample was left to cure for 24 hours before being removed from the mold. It is important to note that two aggregate ring samples were prepared per aggregate type. Figure 37 provides a graphical representation of the entire ring sample preparation process.

**Figure 37. Aggregate ring sample preparation process**



## Testing Procedure

### Equipment Setup

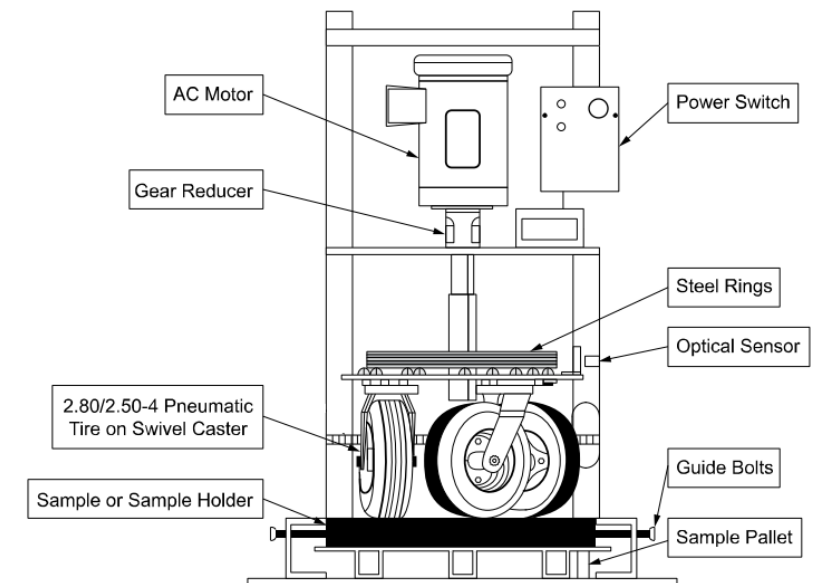
Check the following equipment before starting the polishing procedure:

1. The ambient temperature should be  $68 \pm 4^{\circ}\text{F}$  ( $20 \pm 2^{\circ}\text{C}$ ).
2. No water should be introduced during polishing.
3. The tire tread should be free of any visible contamination.
4. Clean the tires if necessary.
5. Replace the tires if they are cut.
6. Replace the tires if the tread is worn. Tire replacement due to wear is recommended when the tread depth is at least 2 mm or at approximately 1.5 million revolutions, whichever happens first.
7. Ensure that all three wheels have the proper tire pressure of  $240 \pm 34 \text{ kPa}$  ( $35 \pm 5 \text{ psi}$ ).

The testing procedure was conducted according to AASHTO PP103 [53]. The following steps were performed:

1. The ring sample was placed on a stainless steel sample holder. The dimensions of the sample holder were 20 in. x 20 in. x 20 in. (508 mm x 508 mm x 508 mm). This holder had two small gaps of 0.5 in. (25 mm) that allowed easy removal of the specimen after testing.
2. The sample holder, along with the aggregate ring sample, was placed inside a Three-Wheel Polisher Device. This device consisted of an AC motor attached to a gear reducer that was connected to different steel rings that make three 2.80/2.50-4 pneumatic tires rotate. The pressure of the tires was  $240 \pm 34$  kPa ( $35 \pm 5$  psi). Furthermore, the tires had a tread with a ribbed pattern and a depth of no less than 2 mm (0.1 in). It is relevant to state that the wheel path of the tires was approximately 208 mm. Figure 38 presents the parts of the Three-Wheel Polisher Device used for testing.

**Figure 38. Composition of Three-Wheel Polisher Device [53]**



3. Before initializing the polishing cycles, the initial dynamic friction measurement was taken through means of the Dynamic Friction Tester (DFT), and the macrotexture was assessed through means of Circular Texture Meter (CTM).
4. The CTM device must be connected to a 12V DC power supply to ensure proper functioning. The places where the device is placed must be marked so they are consistent

with the places where the DFT device is positioned. It is important to note that the CTM readings must be performed before the DFT measurements. The reason is that the laser should operate in dry conditions to avoid the water film produced by the DFT.

5. The DFT device must be operated according to the guidelines presented by ASTM E1911 [52]. The DFT tank must be filled with water and placed at least two feet above the DFT device to ensure proper flow. Furthermore, the hose must be lifted two feet above the water tank to remove air bubbles.
6. The DFT device must be connected to a 12V DC power supply battery to ensure proper functioning. Once the DFT tests start, proceed to record the readings at 20, 40, and 60 km/hr.
7. Be sure to review the rubber sliders prior to each test since the thickness of the rubber pads and the steel packing must always be greater than 5.5 mm.
8. The samples were subjected to polishing cycles through means of the tires, which were rotating on top of them at a speed of  $60 \pm 5$  revolutions per minute (rpm).
9. DFT testing was conducted at 0, 50,000, and 100,000 polishing cycles while CTM testing at 0 and 100,000 polishing cycles. Furthermore, the devices were rotated  $90^\circ$  for every measurement to assess if the placement of the testing devices had an effect on the results.

### Reporting Data

Proceed to record the mean profile depth (MPD) measurements in Table 27 and the DFT measurements in Table 28.

**Table 27. Data collection format for MPD**

MPD at 0 Cycles	MPD at 100,000 Cycles
MPD I:	MPD I:
MPD II:	MPD II:
MPD III:	MPD III:
MPD IV:	MPD IV:
Average:	Average:

**Table 28. Data collection format for DFT**

DFT at 0 Cycles			DFT at 50,000 Cycles			DFT at 100,000 Cycles					
	DFT20	DFT40	DFT60		DFT20	DFT40	DFT60		DFT20	DFT40	DFT60
DFT I:				DFT I:				DFT I:			
DFT II:				DFT II:				DFT II:			
DFT III:				DFT III:				DFT III:			
DFT IV:				DFT IV:				DFT IV:			
Average:				Average:				Average:			

### Blended DFT

Often, the ring sample may have several aggregates in its composition. Therefore, a prediction of the composed DFT may be needed. The calculation of the blended DFT value can be determined using the present equations. To determine the DFT of an aggregate ring sample of two aggregate sources:

$$DFT_{Blended} = \frac{(DFT_1)(X_1)}{100} + \frac{(DFT_2)(X_2)}{100} \quad (32)$$

To determine the blended DFT of three or more aggregate sources:

$$DFT_{Blended} = \frac{(DFT_1)(X_1)}{100} + \frac{(DFT_2)(X_2)}{100} + \dots + \frac{(DFT_n)(X_n)}{100} \quad (33)$$

Where,

$DFT_{Blended}$  : Combined DFT Result of different aggregates;

DFT1: DFT results of the first aggregate;

DFT2: DFT results of the second aggregate;

DFTn: DFT results of any number of used aggregates in the ring sample;

X1: Percentage of aggregate one of the total aggregate composition;

X2: Percentage of aggregate two of the total aggregate composition;

Xn: Percentage of any number of aggregates of the total ring sample composition.

### Adjustment by Macrotecture

The results from this test indicated that statistically significant differences in MPD were related to statistically significant differences in DFT20. This finding indicates that MPD can be used

as a surrogate for aggregate ring sample variation. Based on this data, an adjustment factor was developed, as shown in Equation 34 below.  $\Delta DFT20$  corresponds to the variation between two different aggregate ring samples, while  $\Delta MPD$  corresponds to the variation due to macrotexture within two different aggregate ring samples.

$$\Delta DFT20 = 0.2 * \Delta MPD + 0.01 \quad (34)$$

Where,

$\Delta DFT20$ : Change in DFT20 measurements; and

$\Delta MPD$ : Change in MPD (mm).

# Appendix B

## DFT Data Analysis

### Effect of Static Measurements

One of the goals of this investigation was to determine if the DFT device was reliable to be used as a replacement for the British Pendulum Tester (BPT). The first step in achieving this goal was to plot the different DFT results at different speeds (km/hr). Different measurements at 10, 20, 30, 40, 50, 60, 70, and 80 km/hr were taken. As shown in Figure 39, there were many fluctuations in the results beyond 60 km/hr. Therefore, only measurements between 10 and 60 km/hr were used for this analysis. Furthermore, Figure 40 presents the friction results at different speeds. Moreover, after conducting an ANOVA test, a statistical difference was found. Therefore, a Tukey statistical analysis at a confidence level of 0.05 was performed to determine the statistical difference among the samples. This analysis revealed that the DFT results at the speeds of 20 km/hr, 30 km/hr, and 40 km/hr do not have any statistical difference between each other. Nevertheless, the DFT results at the speeds of 60 km/hr, 50 km/hr, and 10 km/hr present statistical differences compared to the results, as shown in Figure 40 (note that different letters on top of the bars represent statistical differences, while the same letters represent no statistical differences). Furthermore, all of the analyzed measurements yielded results below the reliability limit per ASTM E1911, meaning that the DFT measurements are reliable. Moreover, Table 29 presents the DFT results at 60, 40 and 20 km/hr at different voltages for 30 different measurements.

Figure 39. DFT data at different speeds

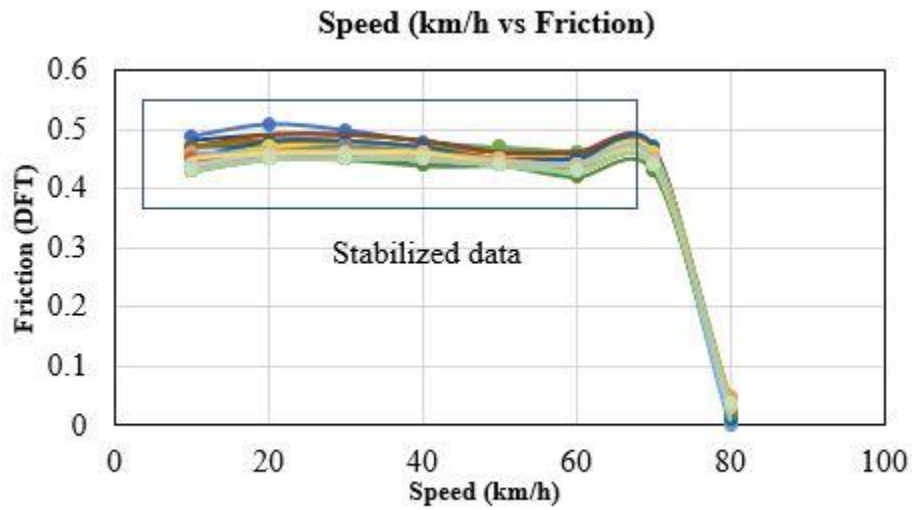


Figure 40. Reliability analysis

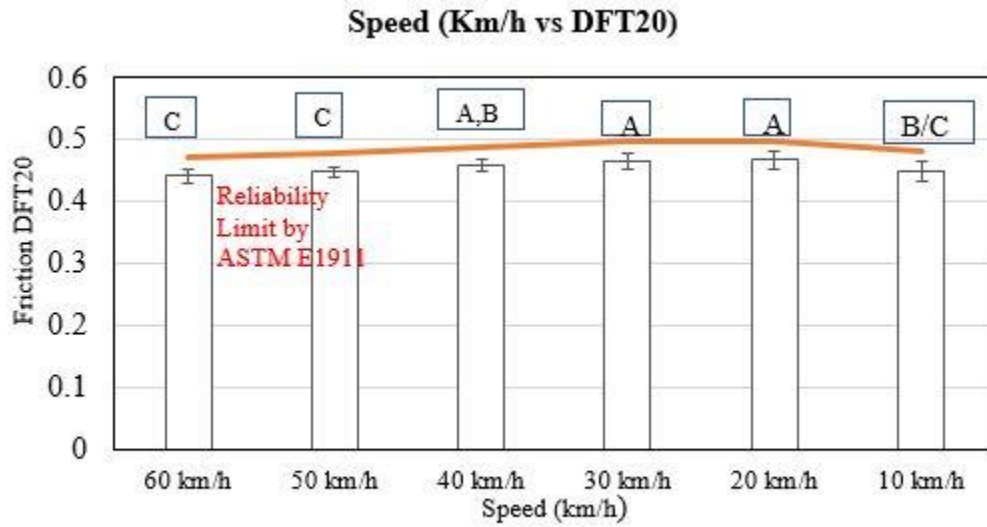


Table 29. 30 DFT20 measurements at same position with voltages

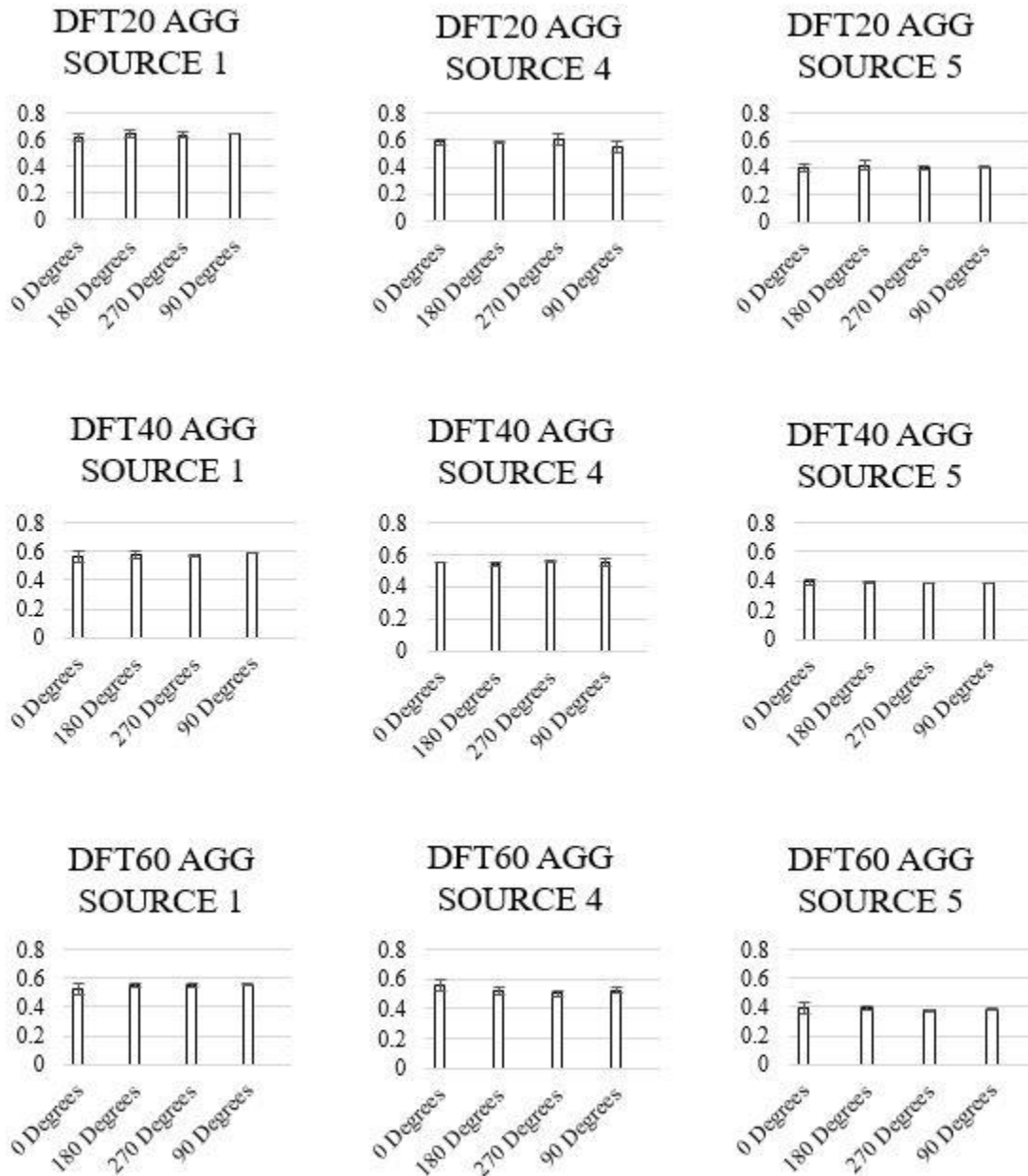
#Test	DFT60	DFT40	DFT20	Voltage
1	0.46	0.48	0.51	12.10
2	0.46	0.47	0.48	12.07

#Test	DFT60	DFT40	DFT20	Voltage
3	0.45	0.45	0.47	12.06
4	0.45	0.46	0.47	12.04
5	0.43	0.45	0.46	12.50
6	0.46	0.47	0.48	12.51
7	0.46	0.48	0.49	12.26
8	0.46	0.48	0.49	12.21
9	0.45	0.46	0.47	12.14
10	0.44	0.46	0.48	12.10
11	0.45	0.47	0.48	12.06
12	0.44	0.46	0.47	12.04
13	0.44	0.46	0.47	12.35
14	0.44	0.46	0.46	12.27
15	0.44	0.46	0.47	12.19
16	0.44	0.46	0.47	12.09
17	0.44	0.46	0.46	12.02
18	0.43	0.45	0.46	12.50
19	0.44	0.44	0.46	12.35
20	0.43	0.45	0.46	12.29
21	0.43	0.46	0.46	12.24
22	0.44	0.46	0.46	12.21
23	0.43	0.45	0.46	12.18
24	0.42	0.44	0.45	12.15
25	0.43	0.45	0.45	12.40
26	0.44	0.46	0.46	12.28
27	0.43	0.45	0.46	12.20
28	0.44	0.46	0.46	12.12
29	0.44	0.45	0.45	12.09
30	0.43	0.45	0.45	12.05
<b>Avg</b>	<b>0.44</b>	<b>0.46</b>	<b>0.47</b>	<b>12.20</b>
<b>SD</b>	<b>0.01</b>	<b>0.01</b>	<b>0.01</b>	<b>0.14</b>
<b>CV</b>	<b>0.03</b>	<b>0.02</b>	<b>0.03</b>	<b>0.01</b>

### Effect of 90° Rotation on DFT

Figure 41 presents the DFT20 results at different rotations and speeds. No Tukey letters were added to the bars, since no statistical difference was found among the test results

Figure 41. DFT Results at 90° rotation



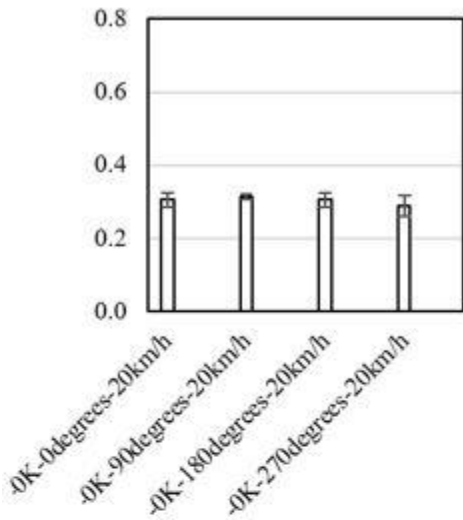
### Effect of 90° Rotations and Two Samples Simultaneously

The next objective of the test was to determine if the aggregate ring sample, combined with 90° rotations, had any effect on the DFT results. For this purpose, two different aggregate ring samples were studied per sample at three different speeds: 20, 40, and 60 km/hr, considering 90° rotations. It is also important to note that this analysis was conducted at zero polishing

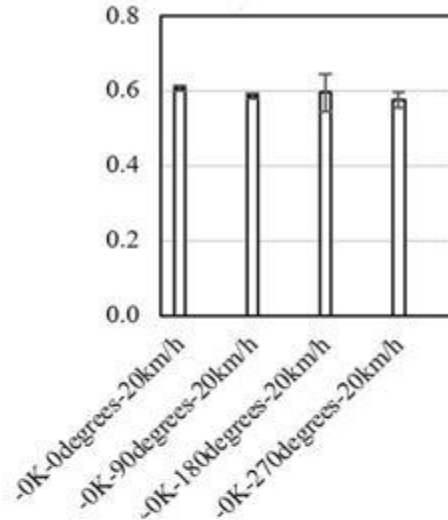
cycles. This was performed to minimize the effect of ring aggregate samples since different aggregates have different polishing rates.

Figure 42 presents the DFT20 results per aggregate ring type (i.e., AGG SOURCE 7, AGG SOURCE 2, AGG SOURCE 3, AGG SOURCE 6, AGG SOURCE 1, AGG SOURCE 4, AGG SOURCE 5). A Tukey HSD test at a confidence level of 0.05 was conducted, and no statistical difference was found within the aggregate sample type considering the effect of the 90° rotation. Furthermore, Figure 43 presents the DFT40 results per aggregate ring type (i.e., AGG SOURCE 7, AGG SOURCE 2, AGG SOURCE 3, AGG SOURCE 6, AGG SOURCE 1, AGG SOURCE 4, AGG SOURCE 5). A Tukey HSD test was conducted for the DFT results at 40 km/hr. The DFT results among each sample revealed that there was no statistical difference within each sample, except for sample AGG SOURCE 4, as shown in Figure 13. Finally, Figure 44 presents the DFT at 60 km/hr results of the different aggregate ring samples. A Tukey HSD test was also conducted at this speed, and it was found that two samples (i.e., AGG SOURCE 1 and AGG SOURCE 4) presented significant statistical differences. From the overall analysis at different speeds, it can be said that only DFT20 did not display any type of statistical difference while including variations due to the sample effect and 90° rotation. Since DFT20 did not present any kind of variation related to the 90° rotation and to the sample effect, it was chosen as the surrogate for microtexture for this research. Furthermore, Table 30 presents the results of the DFT20 unpolished at 0 polishing cycles and polished after 100,000 polishing cycles.

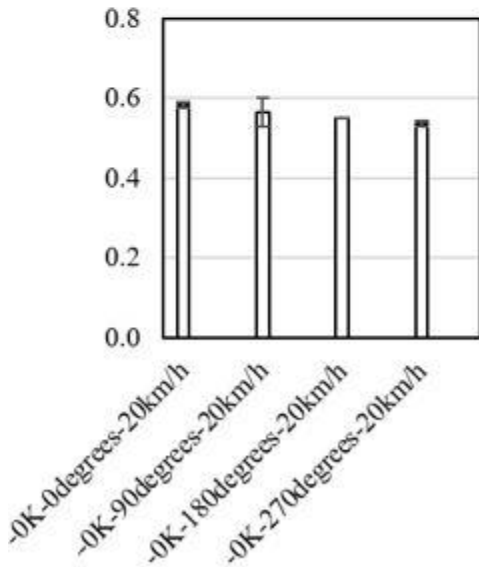
Figure 42. DFT20 results considering sample effect and 90° rotation



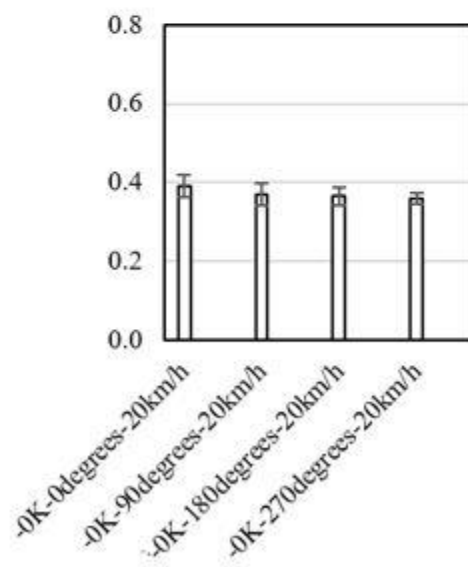
AGG SOURCE 7



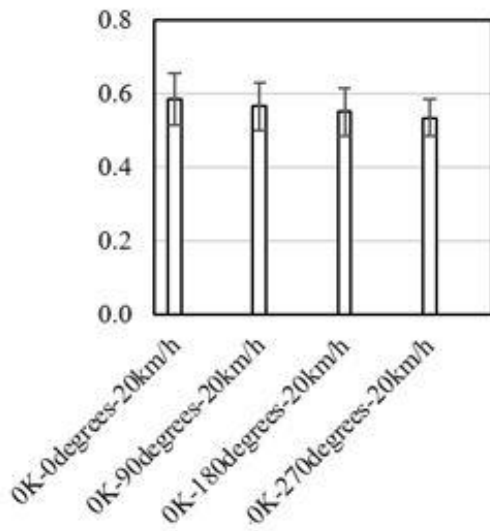
AGG SOURCE 2



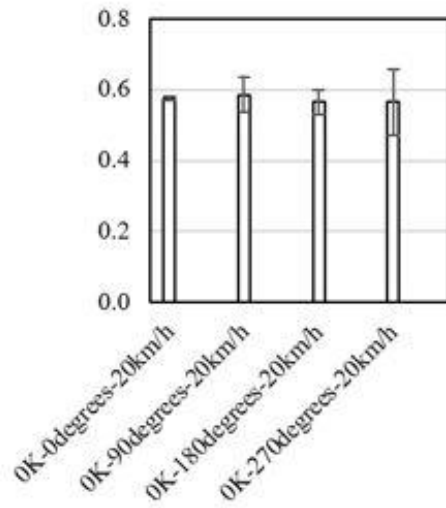
AGG SOURCE 3



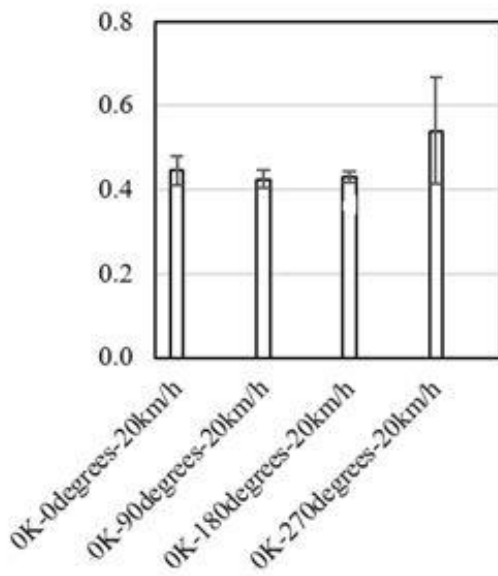
AGG SOURCE 6



AGG SOURCE 1

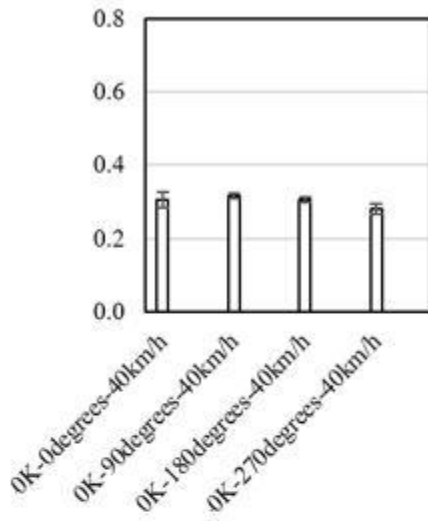


AGG SOURCE 4

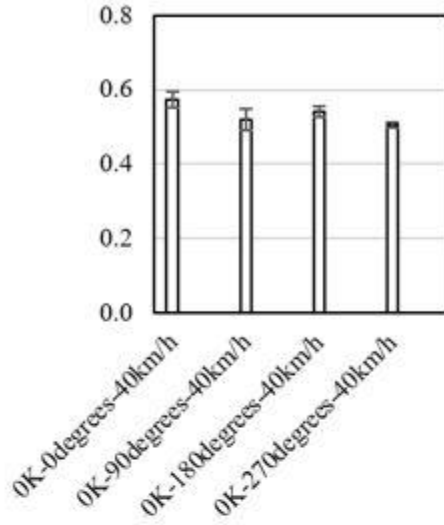


AGG SOURCE 5

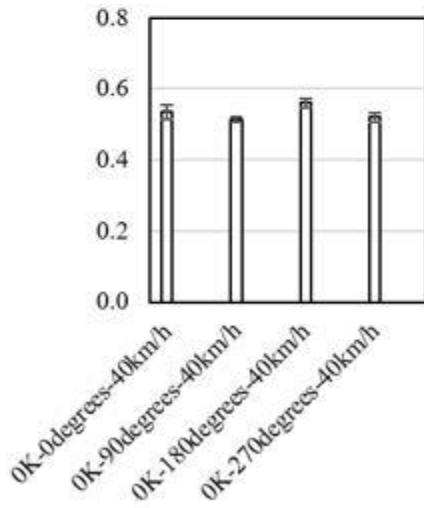
Figure 43. DFT40 results considering sample effect and 90° rotation



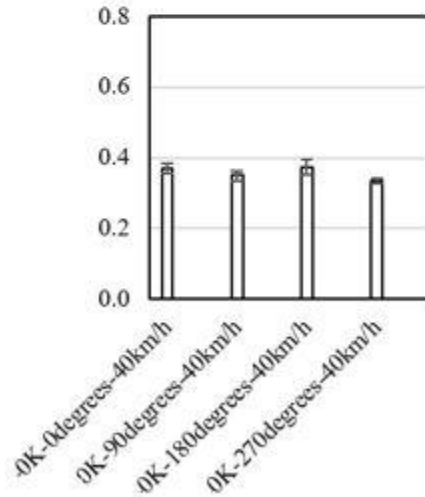
AGG SOURCE 7



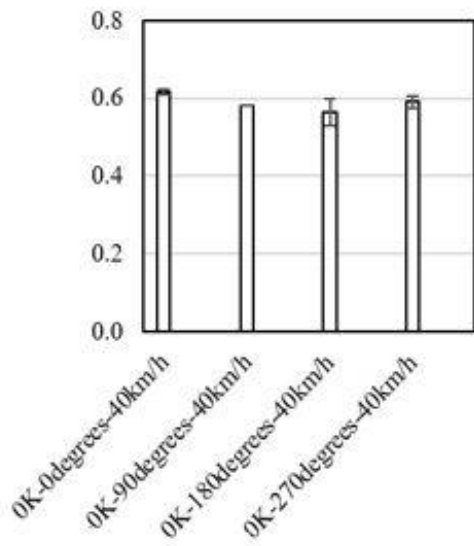
AGG SOURCE 2



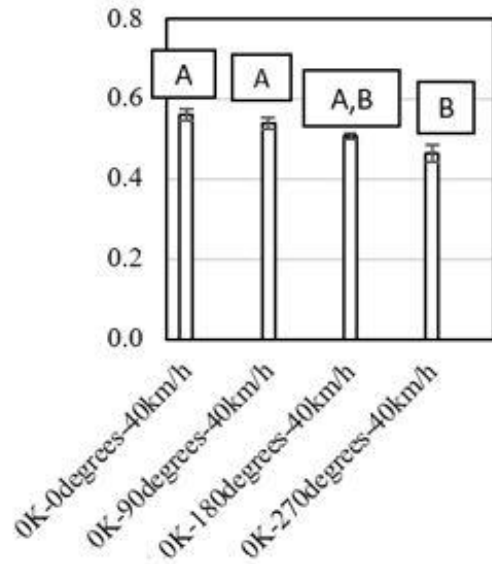
AGG SOURCE 3



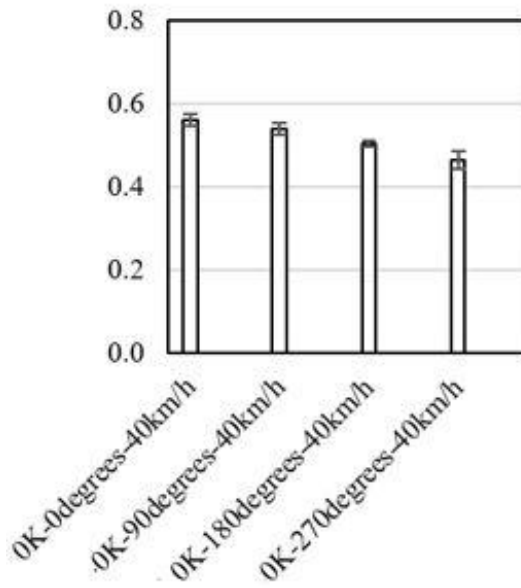
AGG SOURCE 6



AGG SOURCE 1

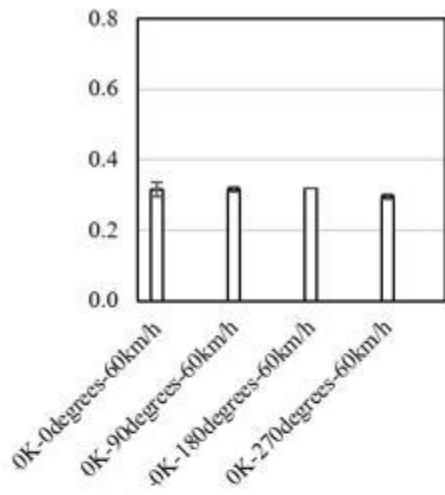


AGG SOURCE 4

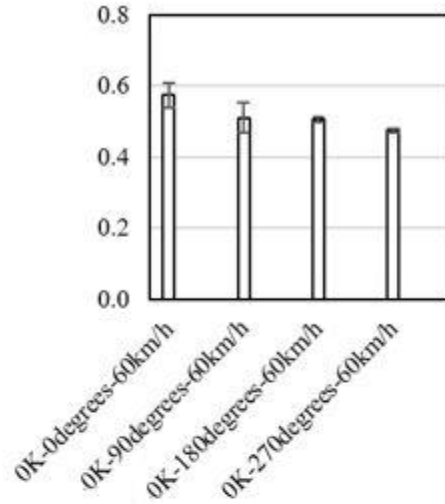


AGG SOURCE 5

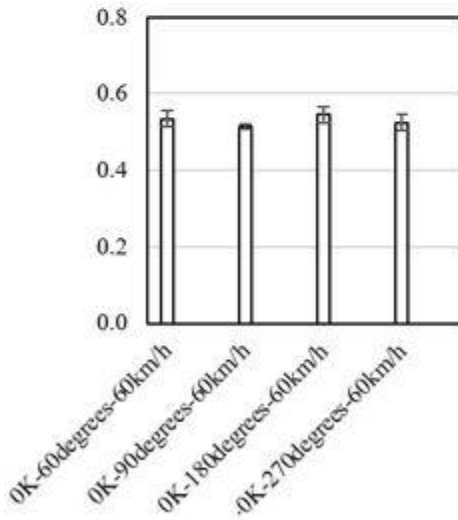
Figure 44. DFT60 results considering sample effect and 90° rotation



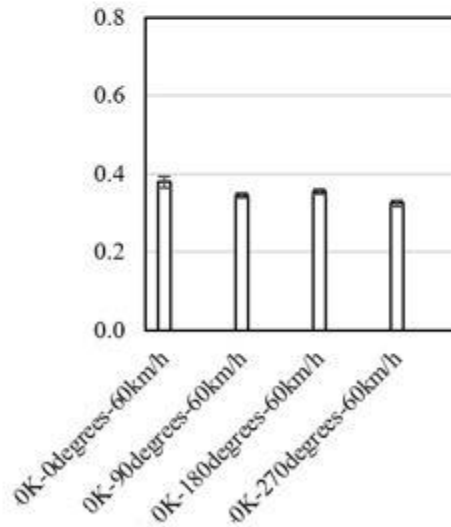
AGG SOURCE 7



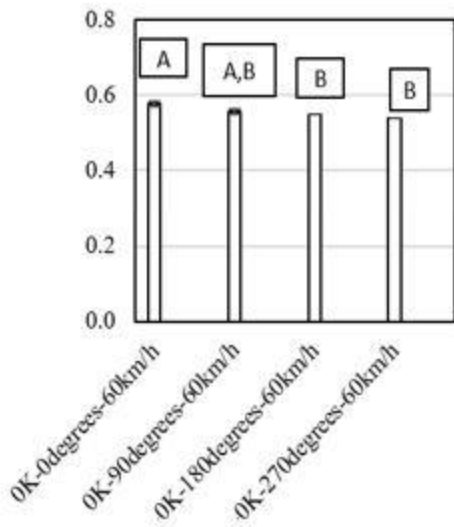
AGG SOURCE 2



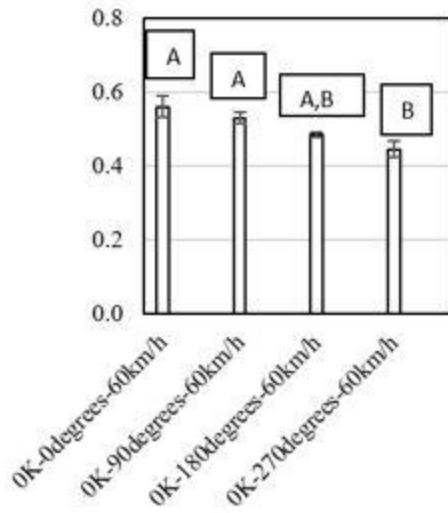
AGG SOURCE 3



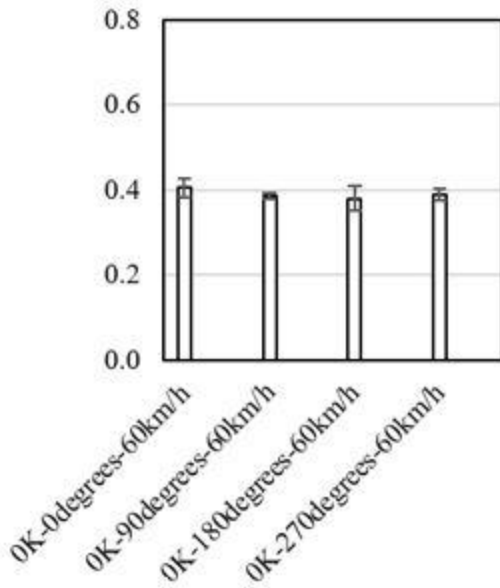
AGG SOURCE 6



AGG SOURCE 1

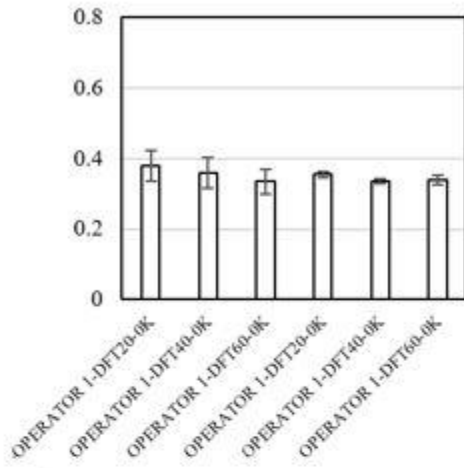


AGG SOURCE 4

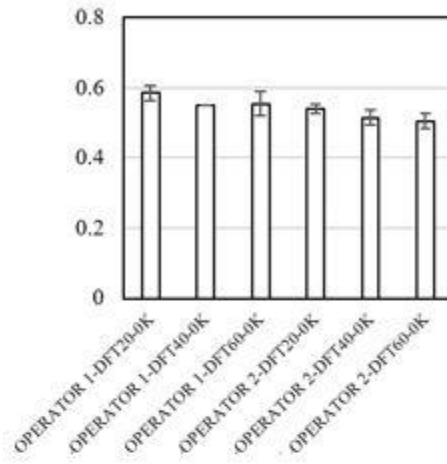


AGG SOURCE 5

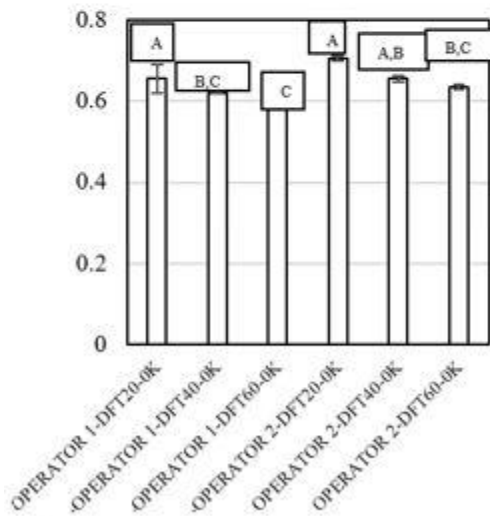
Figure 45. DFT difference based on time and operator



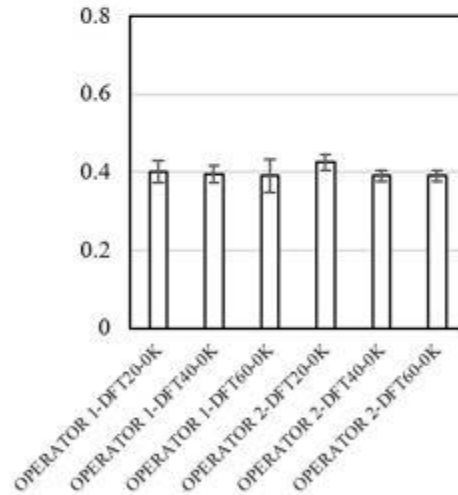
AGG SOURCE 6



AGG SOURCE 4



AGG SOURCE 1



AGG SOURCE 5

**Table 30. DFT and CTM test results per tested aggregate ring sample**

Aggregate	Sample	DFT Unpolished	DFT Polished	MPD Unpolished	MPD Polished
AGG SOURCE 7	S1	0.32	0.22	1.45	1.54
		0.29	0.22	1.42	1.4
		0.32	0.21	1.19	1.52
		0.31	0.23	1.19	1.54
	S2	0.29	0.26	1.09	1.16
		0.3	0.24	1.14	1.25
		0.29	0.24	1.16	1.18
		0.27	0.23	1.15	1.12
AGG SOURCE 2	S1	0.6	0.44	1.02	1
		0.59	0.46	0.97	0.98
		0.63	0.48	1	1.04
		0.59	0.44	1.05	1.01
	S2	0.61	0.43	0.87	0.82
		0.58	0.42	1.18	0.87
		0.56	0.4	0.82	0.91
		0.56	0.41	0.95	0.82
AGG SOURCE 3	S1	0.58	0.42	1.37	1.33
		0.54	0.44	1.44	1.32
		0.55	0.42	1.4	1.41
		0.53	0.41	1.58	1.34
	S2	0.59	0.45	1.32	1.34
		0.59	0.44	0.92	1.37
		0.55	0.43	1.14	1.26
		0.54	0.43	1.48	1.47
AGG SOURCE 6	S1	0.41	0.27	1.03	0.98
		0.39	0.27	1.01	1
		0.38	0.27	0.99	1.05
		0.37	0.26	1	0.98
	S2	0.37	0.28	1.06	1.05
		0.35	0.27	0.98	0.97
		0.35	0.27	0.99	0.97
		0.35	0.27	1.06	0.92
AGG SOURCE 1	S1	0.63	0.51	1.16	1.08
		0.62	0.54	1.13	1.16
		0.63	0.53	1.25	1.15
		0.62	0.52	1.13	1.21

Aggregate	Sample	DFT Unpolished	DFT Polished	MPD Unpolished	MPD Polished
	S2	0.65	0.47	1.19	1.06
		0.62	0.52	1.03	0.96
		0.62	0.49	1.03	1.12
		0.63	0.48	0.99	0.95
AGG SOURCE 4	S1	0.58	0.48	1.21	1.06
		0.55	0.47	1.07	1.18
		0.52	0.48	1.16	1.04
		0.54	0.46	1.12	1.18
	S2	0.5	0.43	1.01	1.04
		0.5	0.44	1.04	0.96
		0.48	0.45	1.01	1.04
		0.51	0.44	1.02	1.06
AGG SOURCE 5	S1	0.38	0.35	1.47	1.59
		0.4	0.35	1.43	1.4
		0.39	0.33	1.42	1.27
		0.39	0.31	1.45	1.42
	S2	0.47	0.32	1.3	1.32
		0.44	0.32	1.22	1.28
		0.42	0.31	1.22	1.44
		0.45	0.31	1.31	1.42